University of Massachusetts Medical School
eScholarship@UMMS

GSBS Dissertations and Theses | Graduate School of Biomedical Sciences

2013-06-13

Dynamic Regulation at the Neuronal Plasma Membrane: Novel Endocytic Mechanisms Control Anesthetic-Activated Potassium Channels and Amphetamine-Sensitive Dopamine Transporters: A Dissertation

Luke R. Gabriel
University of Massachusetts Medical School Worcester

Let us know how access to this document benefits you.
Follow this and additional works at: https://escholarship.umassmed.edu/gsbs_diss

 Part of the Amino Acids, Peptides, and Proteins Commons, and the Molecular and Cellular Neuroscience Commons

Repository Citation
Gabriel LR. (2013). Dynamic Regulation at the Neuronal Plasma Membrane: Novel Endocytic Mechanisms Control Anesthetic-Activated Potassium Channels and Amphetamine-Sensitive Dopamine Transporters: A Dissertation. GSBS Dissertations and Theses. https://doi.org/10.13028/M22K5H. Retrieved from https://escholarship.umassmed.edu/gsbs_diss/725

This material is brought to you by eScholarship@UMMS. It has been accepted for inclusion in GSBS Dissertations and Theses by an authorized administrator of eScholarship@UMMS. For more information, please contact Lisa.Palmer@umassmed.edu.

DYNAMIC REGULATION AT THE NEURONAL PLASMA MEMBRANE: NOVEL ENDOCYTIC MECHANISMS CONTROL ANESTHETIC-ACTIVATED POTASSIUM CHANNELS AND AMPHETAMINE-SENSITIVE DOPAMINE TRANSPORTERS

A Dissertation Presented

By

LUKE ROBERT GABRIEL

Submitted to the Faculty of the
University of Massachusetts Graduate School of Biomedical Sciences, Worcester
in partial fulfillment of the requirements for the degree of

DOCTOR of PHILOSOPHY

JUNE 13, 2013

NEUROSCIENCE

DYNAMIC REGULATION AT THE NEURONAL PLASMA MEMBRANE: NOVEL ENDOCYTIC MECHANISMS CONTROL ANESTHETIC-ACTIVATED POTASSIUM CHANNELS AND AMPHETAMINE-SENSITIVE DOPAMINE TRANSPORTERS

A Dissertation Presented
By

LUKE ROBERT GABRIEL

The signatures of the Dissertation Defense Committee signify completion and approval as to style and content of the Dissertation

Haley Melikian, Ph.D.,Thesis Advisor

William Kobertz, Ph.D., Member of Committee

Ann Rittenhouse, Ph.D., Member of Committee

Reid Gilmore, Ph.D., Member of Committee

Michael Robinson, Ph.D., Member of Committee

The signature of the Chair of the Committee signifies that the written dissertation meets the requirements of the Dissertation Committee

Andrew Tapper, Ph.D., Chair of Committee

The signature of the Dean of the Graduate School of Biomedical Sciences signifies that the student has met all graduation requirements of the school.

Anthony Carruthers, Ph.D.,
Dean of the Graduate School of Biomedical Sciences

Program in Neuroscience

June 13, 2013

Dedication

This dissertation is dedicated to my loving partner Kathryn Devaney without whom I would not have been able to accomplish this feat.

Moreover, I would like to dedicate this, my academic career's culmination to my mother, Janet Gabriel, who read Chicken Little every night for two years, kindling my love for understanding the unknown.

Acknowledgments

I would like to acknowledge my mentor, Haley Melikian, for her patient guidance during my graduate school matriculation. I would like to thank Bill Kobertz and Ann Rittenhouse for collaboration and help during my foray into potassium channel biology.

I would have been unable to complete this work without my co-workers, past and present, specifically Zachary Stevens, Demetra Orthodoxou, Patrick Kearney, and Sijia Wu. Special thanks to Anatoli Lvov for designing and executing experiments for the KCNK3 portion of my dissertation and Liwang Lu for training in mouse brain sectioning.

I would like to acknowledge my funding agencies during my graduate studies: the National Institutes of Health and the UMass Medical School Center for AIDS Research.

Abstract

Endocytic trafficking dynamically regulates neuronal plasma membrane protein presentation and activity, and plays a central role in excitability and plasticity. Over the course of my dissertation research I investigated endocytic mechanisms regulating two neuronal membrane proteins: the anesthetic-activated potassium leak channel, KCNK3, as well as the psychostimulant-sensitive dopamine transporter (DAT). My results indicate that KCNK3 internalizes in response to Protein Kinase C (PKC) activation, using a novel pathway that requires the phosphoserine binding protein, 14-3-3β, and demonstrates for the first time regulated KCNK3 channel trafficking in neurons. Additionally, PKC-mediated KCNK3 trafficking requires a non-canonical endocytic motif, which is shared exclusively between KCNK3 and sodium-dependent neurotransmitter transporters, such as DAT. DAT trafficking studies in intact *ex vivo* adult striatal slices indicate that DAT endocytic trafficking has both dynamin-dependent and –independent components. Moreover, DAT segregates into two populations at the neuronal plasma membrane: trafficking-competent and -incompetent. Taken together, these results demonstrate that novel, non-classical endocytic mechanisms dynamically control the plasma membrane presentation of these two important neuronal proteins.

Table of Contents

List of Figures

List of Abbreviations

14-3-3β	Phosphoserine binding protein
ACSF	Artificial cerebrospinal fluid
AMPA	2-amino-3-(3-hydroxy-5-methyl-isoxazol-4-yl)propanoic acid
AMPH	Amphetamine
BCA	Bicinchonoic acid assay
BIM	Bis-(indole)maleimide
CCD	Charge-coupled device
CGN	Cerebellar granule neurons
CV	Column volume
CytoD	Cytochalasin D
DA	Dopamine
DAPI	4',6-diamidino-2-phenylindole
DAT	Dopamine transporter
DHPG	(S)-3,5-dihydroxyphenylglycine
DMEM	Dulbecco's Modification of Eagle's Medium
EGFR	Epidermal growth factor receptor
ENaC	Epithelial sodium channel
GABA	γ-Aminobutyric acid
GFP	Green flourescent protein
GLUT4	Glucose transporter type 4
KCNK3	Potassium channel subfamily K member 3
KCNK9	Potassium channel subfamily K member 9
mGluR	Metabotropic glutamate receptor
NMDA	N-methyl-D-aspartate
NHS	N-hydroxy-succinimide

PKA	Protein Kinase A
PKC	Protein Kinase C
PMA	Phorbol 12-myristate 13-acetate
RIPA	Radio-Immunoprecipitation Assay
TBS-T	Tris-buffered saline, pH 7.4 and 0.1% Tween-20
TCEP	Tris (2-carboxyethyl)phosphine
TEA	Tetraethylammonium
TfR	Transferrin receptor
TH	Tyrosine hydroxylase
TMB	3,3',5,5'-tetramethylbenzidine
Tris	2-Amino-2-hydroxymethyl-propane-1,3-diol
TTX	Tetrodotoxin

Preface

Parts of this dissertation have appeared in the following:

Gabriel, L., Lvov, A., Orthodoxou, D., Rittenhouse, A. R., Kobertz, W. R., & Melikian, H. E. (2012). The Acid-sensitive, Anesthetic-activated Potassium Leak Channel, KCNK3, Is Regulated by 14-3-3β-dependent, Protein Kinase C (PKC)-mediated Endocytic Trafficking. *Journal of Biological Chemistry*, *287*(39), 32354-32366.

Gabriel, L., Stevens, Z., & Melikian, H. (2009). Measuring plasma membrane protein endocytic rates by reversible biotinylation. *Journal of visualized experiments: JoVE*, (34)

CHAPTER I

INTRODUCTION

Neurotransmission and neuronal endocytic trafficking

The brain is the center of the nervous system and the most complex biological structure known. This complexity enables the simple ability to process visual stimuli to the more complicated and subtle social cue interpretation required in modern human society. The human brain consists of more than 100 billion neurons, which process and transmit information in the form of electrical action potentials that are converted to chemical signals, in the form of small molecule neurotransmitters at the terminal bouton (Albright, Jessell, Kandel, & Posner, 2000). Dysfunctional neuronal communication is the underlying cause of many psychiatric and neurological diseases, such as schizophrenia (Lisman, 2012), Parkinson's disease (Michel, Toulorge, Guerreiro, & Hirsch, 2013), and autism (Roussignol et al., 2005).

Intrinsic neuronal activity is regulated by the ion flow across the plasma membrane, which establishes an electrochemical gradient that provides the thermodynamic energy source for numerous cellular processes, such as action potential propagation and small molecule transport. Under resting conditions, the membrane potential is hyperpolarized to -70mV. When the membrane is depolarized to a threshold value, -40mV, voltage-gated sodium channels activate

and allow sodium ions to flow inward, activating an action potential. The action potential propagates from the cell soma down the axon to the axon terminal. Following their activation, sodium channels rapidly inactivate and voltage-gated potassium channels open and repolarize the membrane back to the negatively polarized membrane resting potential. Once the action potential arrives at and depolarizes the axon terminal, it drives voltage-gated calcium channel activation, which initiates synaptic vesicle fusion and, consequently, neurotransmitter release. The synaptic vesicle contents (neurotransmitters) then act at pre- and post-synaptic receptors to activate or inhibit ion channels, or activate receptors that initiate signal cascades on the pre- or post-synaptic neuron. The neurotransmitter signal is then terminated either by presynaptic reuptake that is facilitated by neurotransmitter transporters, or by enzymatic degradation.

This multi-step process enables neurons to regulate their excitability and action potential frequency. The importance of ion channels in normal neuronal activity is best illustrated by instances where channels dysfunction. For example, a mutation in the sodium channel SCN1A causes increased action potential frequency leading to epileptic seizure (Escayg et al., 2000; Lossin, Wang, Rhodes, Vanoye, & George, 2002). Action potential termination is equally important as a mutation in the voltage-gated potassium channel Kv1.1 causes a longer polarization rectification step and leads to episodic ataxia (Browne et al., 1994; D'Adamo, Liu, Adelman, Maylie, & Pessia, 1998). In addition to the action potential's importance,

dysfunctional neurosecretion can also have a profound effect on homeostasis. For example, mutations in the vesicle biogenesis protein dysbindin cause decreased neurotransmitter levels in synaptic vesicles, leading to decreased neurotransmitter release and is correlated with schizophrenia susceptibility (Murotani et al., 2007; Straub et al., 2002). Furthermore, mutations in dopamine β-hydroxylase (DBH) prevents norepinephrine (NE) synthesis and, accordingly, noradrenergic neurotransmission and results in profound orthostatic hypotension (Robertson et al., 1991). Consequently, mechanisms that control both neuronal excitability and chemical transmission have important impact on behavior.

Regulated membrane trafficking (endo– and exocytosis) specifically alters protein surface expression in response to cellular cues and plays a pivotal role in neuronal function. For example, the ionotropic glutamate receptor GluR2 in CA1 hippocampal post-synaptic termini, upon phosphorylation by src family kinases, internalizes into endosomal compartments consequently muting neuronal response to excitatory glutamate signaling ultimately leading to long-term depression (Scholz et al., 2010). Conversely, the ionotropic glutamate receptor GluR1 in CA1 hippocampal post-synaptic termini, upon phosphorylation by protein kinase A (PKA), re-inserts into the plasma membrane, leading to long-term potentiation (Ehlers, 2000). Additionally, the $GABA_A$ receptor inserts into the plasma membrane from intracellular compartments following insulin signaling and thereby enhances inhibitory GABA neurotransmission (Wan et al., 1997).

Moreover, mutations in the $GABA_A$ receptor intracellular loop result in decreased endocytosis and leads to deficits in spatial memory because of elevated inhibitory neurotransmission in CA3 hippocampal neurons (Kittler et al., 2008). This acute redistribution phenomenon is not restricted to ligand-gated channels as the voltage–gated Kv1.2 channel internalizes following M1 muscarinic receptor activation and subsequent phosphorylation in the channel's C-terminus, which leads to dissociation from the actin-binding protein, cortactin, and increased neuronal excitability (Hattan, Nesti, Cachero, & Morielli, 2002). Consequently, understanding the mechanisms that regulate neuronal membrane trafficking is likely to significantly enhance our understanding of the mechanisms that impact neuronal excitability and neurotransmission. This thesis will examine how endocytosis regulates two neuronal proteins that significantly influence excitability and neurotransmission: the acid-sensitive potassium leak channel KCNK3 and the amphetamine- and cocaine-sensitive dopamine transporter (DAT).

Mechanisms governing endocytic trafficking

Cells rely upon multiple trafficking mechanisms to regulate surface protein expression. These mechanisms are defined by the constituent proteins necessary to mediate trafficking and can be divided into clathrin-dependent and –independent mechanisms. Clathrin-mediated endocytosis (CME) is the major means by which the majority of plasma membrane proteins internalize. Membrane cargo proteins, such as the low-density lipoprotein receptor (LDLR; (Mello, Brown, Goldstein, &

Anderson, 1980)) and the transferrin receptor (TfR; (Draper, Goda, Brodsky, & Pfeffer, 1990)). These cargo proteins are sequestered to clathrin-coated pits (CCPs) via interactions between intrinsic endocytic signals encoded on the cargo and the clathrin adaptor protein, AP-2 (Keyel et al., 2006). After cargo is targeted to CCPs, the membrane invaginates and pinches off from the plasma membrane, giving rise to clathrin-coated vesicles. This process requires the GTPase dynamin for the ultimate scission step, by which the endocytic vesicle is 'pinched' off the plasma membrane citation. The clathrin coat subsequently dissociates from the vesicle, and the vesicle progresses to endosomal compartments.

Two endocytic signals for clathrin-mediated endocytosis have been extensively characterized: the dileucine and tyrosine–containing motifs (Bonifacino & Traub, 2003). The dileucine motif, in the degenerate form [DE]XXXL[LI] uses the clathrin adaptor protein AP–2 to sort into vesicles for endoyctosis. [DE]XXXL[LI] and is encoded by a variety of divergent proteins, such as the vesicular monoamine transporter VMAT2 (Tan, Waites, Liu, Krantz, & Edwards, 1998), the glucose transporter GLUT4 (Verhey, Yeh, & Birnbaum, 1995), and tyrosinase, (Honing, Sandoval, & von Figura, 1998), and is recognized both at the plasma membrane and in internal membranes. In these cases, the signal ~~serves to~~ targets and sequesters these proteins to endosomal compartments specific to their respective functions, For example, tyrosinase is targeted to the melanosome by its dileucine endocytic signal. The tyrosine-containing motif consists of the amino acid

sequences NPXY or YXXØ. The NPXY signal is found on Type I membrane proteins, such as the LDL receptor, and is involved in rapid internalization. The YXXØ signal is found on a wide variety of proteins, like the transferrin receptor (Jing, Spencer, Miller, Hopkins, & Trowbridge, 1990) and furin, (Schafer et al., 1995) and is responsible for rapid internalization from the plasma membrane as well as playing a role in membrane protein steady–state distribution. The discovery and characterization of signals that are responsible for endocytic sorting and cellular distribution is ongoing in the field of membrane trafficking.

As work progresses in understanding membrane trafficking determinants, so–called "non–canonical" signals are being discovered. The neuron-specific potassium-chloride cotransporter 2 (KCC2) contains a non-canonical di-leucine motif (LLXXEE) that regulates its rapid internalization through CME (Zhao et al., 2008). Another example is the purinoreceptor P2X4, which contains a non-canonical tyrosine-based motif (YXXGΦ) that also internalizes through CME (Royle, Bobanovic, & Murrell-Lagnado, 2002). Whether all non-canonical endocytic signals use clathrin is an area of ongoing study. The further discovery and study of these non-canonical endocytic signals can further expand on the understanding on the molecules involved in protein surface expression regulation.

In addition to CME there are many clathrin-independent mechanisms that mediate endocytosis. Lipid-rich domains, termed rafts, are the site of other mechanisms

beyond CME that are used to internalize surface proteins. These can be further subdivided in to dynamin-dependent and –independent mechanisms. Caveolin, a membrane-associated protein, is required for a form of clathrin-independent, dynamin-dependent trafficking that occurs at these rafts. Caveolin has been shown to be mediate internalization for the SV40 virion, GM1 ganglioside, and GPI-linked proteins (Balasubramanian, Scott, Castle, Casanova, & Schwartz, 2007; Kirkham et al., 2005; Tagawa et al., 2005). Moreover, caveolin is required to sequester GPCRs to lipid-rich domains whereupon they undergo internalization (Burgueno et al., 2003; Veyrat-Durebex, Pomerleau, Langlois, & Gaudreau, 2005). There is no clearly defined endocytic signal that targets cargo proteins to caveolae, nor are the molecules required, beyond caveolin, for caveolae formation known. However, experimentally disrupting the plasma membrane lipid composition has been demonstrated to block caveolin-dependent endocytosis.

Lipid raft-mediated internalization that is independent of clathrin, dynamin and caveolin has also been reported for many membrane proteins. Flotillins appear to play a role in many of these cases. Flotillins are caveolin-related membrane-associated proteins that are enriched in membrane raft microdomains and have been shown to mediate internalization for proteoglycans and the GPI-linked CD59 molecule (Ait-Slimane, Galmes, Trugnan, & Maurice, 2009; Payne, Jones, Chen, & Zhuang, 2007). Flotillin-mediated endocytosis is mediated by an actin-dependent mechanism (Langhorst, Solis, Hannbeck, Plattner, & Stuermer, 2007).

Furthermore, flotillin also regulates endosomal sorting following endocytosis, as shRNA-mediated flotillin depletion targeted Shiga toxin to lysosomes instead of the *trans*-Golgi network (Pust, Dyve, Torgersen, van Deurs, & Sandvig, 2010). Flotillin also can act as an activator of CME. For example, flotillin can divert Nieman-Pick C1-like 1 protein (NPC1L1) to target to lipid rafts, which are then internalized via CME (Zhang et al., 2011). The identification of adaptor molecules, endocytic signals, and cargoes in flotillin-dependent trafficking is an emerging field.

Other trafficking mechanisms at lipid rafts require the GTPases Arf6 or RhoA, which traffic MHCI and interleukin 2 receptor (IL2-R), respectively (Lamaze et al., 2001; Naslavsky, Weigert, & Donaldson, 2003). These endocytic mechanisms do not require clathrin, caveolin, or dynamin and represent wholly different cellular processes that can also act to regulate cell surface protein expression. Given the myriad of mechanisms regulating cellular surface protein trafficking, this process offers dynamic regulation at the plasma membrane for any number of critical molecules.

K^+ Leak Channels and neuronal excitability

The electrochemical gradient is constantly in flux by tonic ion flow through membrane-bound K^+ 'leak' channels. Unlike voltage gated K^+ channels, which rely on membrane potential to open, leak channels are constitutively open and allow

potassium to flow down its concentration gradient (Talley, Sirois, Lei, & Bayliss, 2003). Although described in the literature for decades and their activity subtracted as background (Hodgkin & Huxley, 1952), the proteins responsible for leak current were largely unknown until the cloning and characterization of the *Drosophila melanogaster* K^+ channel KCNKØ (Goldstein, Price, Rosenthal, & Pausch, 1996). Subsequently, the cloning and initial characterization found 15 genes encoding KCNK channels in humans (Goldstein, Bockenhauer, O'Kelly, & Zilberberg, 2001). Most potassium channels contain a single pore per channel monomer and require 4 pore-forming domains (tetrameric) to assemble a functional channel. KCNK channels are marked by containing two potassium-conducting pore helices per monomeric subunit, and consequently are named the tandem pore family, KCNK or K_2P. Thus, only two channel monomers are required to form a dimeric multimer with four pore-forming domains.

There is a wide diversity to the general stimuli that K^+ leak channels respond to for their activation. These are mainly voltage-independent with some having weak voltage dependence (TWIK-1; (Lesage et al., 1996)) whereas others respond to small molecules (TRESK-1 inhibition in response to arachidonic acid; (Sano et al., 2003)). Ultimately, the membrane localization and overall activity of leak K^+ channels is the steady-state determinant of both excitable and non-excitable resting membrane potential in cells. The total current elicited by a particular channel is determined, in large part, by its cellular distribution, specifically its

presence on the plasma membrane. Despite their critical importance in setting the resting membrane potential, studies focused on the mechanisms underlying their regulation are still in their infancy.

The two–pore K^+ leak channel KCNK3 (TASK–1 or $K_2P3.1$) channel is expressed in a wide variety of tissues including the liver, heart, kidney, and brain (Duprat et al., 1997; Lopes, Gallagher, Buck, Butler, & Goldstein, 2000). KCNK3 is the target for volatile anesthetics, such as isofluorane and halothane (Lopes, Zilberberg, & Goldstein, 2001). These agents increase channel activity and are believed to be responsible for the respiratory depression found in patients under general anesthesia, as well as playing a role in somnolence. Conversely, channel activity is decreased by treatment with local anesthetics, like (Kindler, Yost, & Gray, 1999). This channel's alternate name (TASK: TWIK-related acid sensitive K^+ channel) indicates its sensitivity to extracellular pH. ~~as~~, At physiological pH, the channel is active with an open probability of p=0.5, whereas at acidic pH the channel does not open ($p<0.001$) (Y. Kim, Bang, & Kim, 1999). The channel functions as a homo-dimer but, interestingly, can hetero-oligomerize with a closely related two-pore channel, KCNK9. This KCNK3-KCNK9 heterodimer exhibits an increase in pH sensitivity as compared to KCNK3 and is expressed at high levels in hypoglossal motor neurons (Berg, Talley, Manger, & Bayliss, 2004). Whether the KCNK3-KCNK9 heterodimer and the KCNK3 homodimer undergo the same small molecule regulation has not been fully explored.

KCNK3 has a prominent role in a variety of physiological functions, both in the CNS and periphery. Extracellular hypoxia in the brain results in KCNK3 inactivation (Buckler, Williams, & Honore, 2000), which is believed contribute to excitotoxicity during oxygen deprivation. In cultured cerebellar granule neurons, hypoxia inhibits channel activity and depolarizes the neurons, which ultimately facilitates neuronal death (Plant, Kemp, Peers, Henderson, & Pearson, 2002). KCNK3 also plays a central role in carotid body control of respiration in response to changes in blood oxygen levels. This is best illustrated in KCNK3$^{(-/-)}$ mice, which do not exhibit enhanced respiration rates in response to low blood oxygen (Trapp, Aller, Wisden, & Gourine, 2008). Additionally, KCNK3 -/- mice display malformed adrenal cortex and primary hypoaldosteronism, suggesting that KCNK3 plays a critical role in adrenal gland development (Davies et al., 2008).

KCNK3 has also been implicated in multiple sclerosis and HIV progression. Pharmacological channel inhibition slows multiple sclerosis progression by deactivating T-cells responsible for the autoimmune response mediating myelin destruction (Bittner et al., 2012). Additionally, KCNK3 activity is correlated with Type I HIV particle budding (Hsu, Seharaseyon, Dong, Bour, & Marban, 2004). Mechanistically, the HIV protein Vpu associates with the channel and leads to decreased current. This KCNK3-associated current downregulation is a requirement for viral maturation and cellular egress. KCNK3 is also as KCNK3 is

the molecular target for the Szechuan spicy peppercorn agent, specifically the *sanshool* compound, and mediates the numbed tongue sensation induced by eating this seasoning through direct channel inhibition and subsequent hypoglossal sensory neuron activation (Bautista et al., 2008). Surface expression regulation could, in part, be responsible for these functional effects.

At the cellular level, there are several signaling pathways that have been shown to regulate KCNK3 activity. Specifically, both protein kinase C (PKC) and adenylate cyclase activity decrease KCNK3-associated currents (Lopes et al., 2000).. Furthermore, upstream of PKC, phospholipase C activation also decreases KCNK3 activity (X. Chen et al., 2006; Schiekel et al., 2013). The endothelin-1 receptor, which signals via Gq activation of PKC, also decreases KCNK3-associated currents (Tang et al., 2009). PKC regulation of KCNK3 activity is likely to have profound physiological impact, as PKC-mediated KCNK3 downregulation was recently reported to cause arrythmia following heart surgery (Harleton et al., 2013). Protein kinase G-mediated phosphorylation also modulates KCNK3 intrinsic channel by decreasing proton sensitivity and thus causing overall greater activity at physiological pH (Toyoda et al., 2010). To date, it is unclear whether membrane trafficking is involved in KCNK3 regulation.

Although KCNK3 plasma membrane trafficking has not been studied, molecules required for biosynthetic KCNK3 trafficking have been reported. The channel is

held in the endoplasmic reticulum by COPI and p11 binding (Girard et al., 2002). Following PKA phosphorylation at the KCNK3 carboxy terminus, the phosphoprotein binding protein 14-3-3β displaces these binding partners and is required for efficient endoplasmic reticulum exit (Mant, Elliott, Eyers, & O'Kelly, 2011; O'Kelly, Butler, Zilberberg, & Goldstein, 2002). Due to its wide distribution of expression and its high activity at physiological pH, KCNK3 is an important, yet poorly understood, molecule that contributes to maintaining the potassium gradient. Whether the regulation previously observed depends on plasma membrane channel trafficking is still an open question.

The dopamine transporter

Work done by Julius Axelrod and colleagues in the early 1960s demonstrated that radiolabeled norepinephrine, when introduced systemically, would accumulate in tissue heavily innervated by sympathetic nerves (Whitby, Axelrod, & Weil-Malherbe, 1961). Further work in dennervated rodents, discovered that presynaptic boutons are the uptake site (Birmingham & Iversen, 1969). This observation was the basis for the hypothesis that there is a process that transported monoamines across the plasma membrane into these tissues. In the central nervous system, it was discovered that brain regions did not transport norepinephrine equally, with areas innervated by dopaminergic neurons (i.e. dorsal striatum) transporting both D- and L-stereoisomers with equal affinity, whereas noradrenergic areas (i.e. locus coeruleus) showing specificity for the L-

isomer (Snyder & Coyle, 1969). Consequently dopamine, thought to only be a precursor in the norepinephrine synthesis pathway, was observed to preferentially accumulate in the striatum, leading to the hypothesis that dopamine (DA) was a neurotransmitter and that a specific reuptake mechanism existed to limited its extracellular half-life.

Following this discovery, requirements for DA transport were further characterized. Transport was found to be both sodium- and chloride- dependent in synaptosomes (Bogdanski, Blaszkowski, & Tissari, 1970; Iversen, 1974; Kuhar & Zarbin, 1978). DA transport in synaptosomes was potently inhibited by amphetamine (AMPH) and cocaine treatment (Horn, Coyle, & Snyder, 1971). Later, the DA transporter was identified as being the 'cocaine receptor' described as the site for cocaine's reinforcing effects (Calligaro & Eldefrawi, 1987). The anti-Parkinson drug benztropine blocked DA uptake, indicating the importance for DA in movement (Coyle & Snyder, 1969). Consequently, the DA transporter is an important protein to discover fully its identity and function.

The DA transporter (DAT) belongs to the SLC6 gene family of solute carriers, whose members include the GABA transporter and norepinephrine and serotonin transporters. The identification of specific gene products in the SLC6 family was first shown in 1988 when brain-derived RNA pools were expressed in *Xenopus* oocytes, which conferred neurotransmitter uptake intracellular neurotransmitter

accumulation (Blakely, Robinson, & Amara, 1988). This was followed by the independent expression cloning of the GABA (Guastella et al., 1990) and NE (Pacholczyk, Blakely, & Amara, 1991) transporters. Sequence comparison of these two neurotransmitter transporters revealed ~50% homology, suggesting that they were members of a larger transporter gene family. Based on sequence similarities, homology cloning strategies successfully identified cDNA clones for the serotonin and DA transported were found (Blakely et al., 1991; Kilty, Lorang, & Amara, 1991). The ability to specifically express these proteins opened new methods to study the transporters.

While DAT primarily clears DA from the synapse via a sodium- and chloride-dependent mechanism, other functions have also been attributed to DAT. DAT mediates a transport-independent chloride current, whose cellular importance is still being investigated (Ingram, Prasad, & Amara, 2002). Interestingly, DAT can also operate in a voltage- and calcium-dependent “reverse transport” mode that effluxes DA through DAT (Khoshbouei, Wang, Lechleiter, Javitch, & Galli, 2003; Raiteri, Cerrito, Cervoni, & Levi, 1979). However, free cytosolic DA levels are low, due to efficient packaging ~~dopamine~~ into vesicles, whether this activity is important has yet to be attributed to any particular neuronal function.

DAT’s importance in movement and as a psychostimulant target is demonstrated in $DAT^{(-/-)}$ mice, which are hyperlocomotive and do not exhibit psychostimulant-

induced hyperlocomotion (Giros, Jaber, Jones, Wightman, & Caron, 1996). Furthermore, there is a DA dearth in dopaminergic terminals and the DA clearance from synapses is slowed, demonstrating the critical importance of DAT not only for re-uptake, but also for maintaining synaptic DA levels. Cocaine has been shown to competitively bind the transporter although the reinforcing effects of the drug still occur in $DAT^{(-/-)}$ mice (Giros et al., 1996). Due to confounding developmental expression alterations in other cocaine-binding transporters, such as the norepinephrine transporter, an elegant experiment was performed to specifically assay DAT's importance in mediating cocaine reinforcement. A DAT knock-in mouse expressing a cocaine-insensitive DAT point mutant lacks cocaine-mediated conditioned place preference (R. Chen et al., 2006) and does not self administer cocaine demonstrating that DAT is required for cocaine reinforcement in a minimally perturbed neurological system (Thomsen, Han, Gu, & Caine, 2009).

In addition to being the primary target for cocaine, DAT is also the main locus for AMPH's reinforcing properties. In contrast with cocaine, which is a competititve DAT antagonist, AMPH is a competitive DAT substrate that is transported into the cytoplasm. Following transport into the cytoplasm, AMPH increases intracellular DA levels by reversing VMAT2 transport and initiates a kinase cascade to begin the transporter to run in reverse, leading to efflux of this newly released free intracellular DA (Kahlig et al., 2006). Methylphenidate, a pharmaceutical prescribed for attention deficit hyperactivity disorder (ADHD) patients, also targets

the transporter (Schweri et al., 1985). As a target for addictive and therapeutic psychostimulants, DAT is a critically important neurological molecule and understanding its regulation has wide physiological importance.

Dopaminergic Neurotransmission

Dopaminergic neurotransmission is critical for movement initiation, motivation and reward pathways, as well as mood stabilization. Dopaminergic signaling arises from a finite subset of brain nuclei: the substantia nigra and the ventral tegmental area (VTA). Furthermore, dopaminergic neurons have two firing patterns: tonic and phasic (Floresco, West, Ash, Moore, & Grace, 2003; Grace & Bunney, 1983). Tonic firing is constant low frequency DA release whereas a short, high frequency burst of DA release, marks phasic firing. These two firing patterns emit significantly different synaptic DA levels and post-synaptic effects. Both firing forms are required for dopaminergic neurotransmission. For example, tonic dopaminergic transmission in the nigrostriatal pathway is required in the striatum to inhibit spastic movement (Hauber, 1998). Alteration in the nigrostriatal tonic dopaminergic firing leads to disinhibition and allows for movement initiation. Phasic firing in the mesolimbic pathway is induced during behavioral reinforcement (Schultz, 2013). Furthermore, switching from tonic to phasic firing in mesocorticolimbic dopaminergic neurotransmission has been shown to be required for depression resistance, as mice unable to switch their firing patterns are more susceptible to socially-induced depression (Chaudhury et al., 2013). As dopaminergic signaling

is critical for these behaviors, signal latency must be regulated. The plasma membrane dopamine transporter (DAT) is primarily responsible for synaptic DA clearance and controlling dopaminergic signal latency and consequently regulation for this important protein would be important for these physiological activities.

DAT has been implicated in neurological disease. Aberrant dopaminergic signaling is observed in schizophrenic patients and although DAT levels are not measurably different in these patients, altered protein-protein interactions have been reported in the transporter, specifically a reduced association with the D2 receptor (Brunelin, Fecteau, & Suaud-Chagny, 2013). Depressed patients have greater DAT expression and transporter levels are decreased when chronically treated with bupropion, a dopamine and norepinephrine transporter inhibitor (Argyelan et al., 2005). Moreover, dopaminergic signaling is perturbed in mouse socially-induced depression models (Chaudhury et al., 2013). Recent work has shown that DAT mutations correlate with attention deficit hyperactivity disorder (ADHD) and that the ADHD-correlated R615C DAT mutant has an increased endocytic rate (Sakrikar et al., 2012). Consequently, DAT function and regulation are important to maintaining neurological function and communication.

Dopamine Transporter Trafficking

Regulated trafficking from the surface is an important aspect to functional control. In electron micrographs of the mouse striatum, DAT was reported to be localized

both at the cell surface in perisynaptic sites as well as in internal membrane-bound compartments (Nirenberg et al., 1997). Work by Melikian and Buckley demonstrated, that under basal conditions there is a significant endosomal DAT pool in PC12 cells. Further, PKC activation drives DAT from the plasma membrane to recycling endosomes, demonstrating for the first time that DAT surface expression is acutely regulated by membrane trafficking. Consequently, DAT internalization and recycling has since been a target for extensive studies for DAT.

Internalized DAT colocalizes with the small GTPases Rab-5 (early endosome marker) and -11 (recycling endosome marker) demonstrating that DAT internalizes into recycling endosomes (Melikian & Buckley, 1999; Sorkina, Doolen, Galperin, Zahniser, & Sorkin, 2003). Rab11 has been shown to be required for constitutive DAT recycling (Furman, Lo, Stokes, Esteban, & Gnegy, 2009). Constitutively active Rab11 mutant co-expression with DAT resulted in increased surface DAT expression, whereas the dominant-negative Rab11 mutant led to reduced surface DAT expression. These results are consistent with DAT following an endocytic-recycling pathway akin to that seen for the transferrin receptor (Ren et al., 1998).

At the cell surface, DAT is in both lipid-raft and non-lipid-raft membrane domains, suggesting that DAT surface trafficking may be facilitated by at least two distinct endocytic mechanisms (Foster, Adkins, Lever, & Vaughan, 2008). DAT undergoes

constitutive internalization and recycling to the surface, with a surface half-life of approximately 13 min when measured in heterologous systems. DAT constitutively internalized into vesicular structures and partially co-localized with transferrin (Loder & Melikian, 2003). Clathrin mediated endocytosis has been implicated for constitutive DAT endocytosis in heterologous cell systems using either overexpression of a dominant-negative dynamin I mutant (K44A) or knockdown of clathrin heavy chain, which block internalization (Sorkina, Hoover, Zahniser, & Sorkin, 2005).

DAT trafficking is acutely regulated by PKC activation, resulting in a rapid loss of surface DAT. PKC activation by phorbol 12-myristate 13-acetate (PMA) in rat pheochromacytoma PC-12 cells stably expressing hDAT increases the DAT endocytic rate and decreases the transporter recycling rate, thus reducing DAT surface levels (Loder & Melikian, 2003). Among all PKC isoforms, PKCβ is potentially important in constitutive maintenance of the surface DAT. Compared with wild-type mice, PKCβ$^{(-/-)}$ mice have a reduced surface DAT expression level and reduced DA uptake with no difference in the total DAT expression in the striatum (Chen et al., 2009). Recently, work in the Gnegy lab showed that PKCβ promotes DAT recycling to the plasma membrane in response to D2 receptor activation (Chen et al., 2013).

PKC-dependent regulation of DAT trafficking is readily apparent in various heterologous cell types, as well as in striatal dopaminergic nerve endings. In addition to PKC, basal DAT surface expression is also modulated by Akt, a protein kinase in the insulin pathway immediately downstream of PI3K. Akt activity correlates with increased DAT surface levels and overexpression of a dominant-negative mutant of Akt (K179R) or treatment with Akt inhibitors reduces DAT surface ~~DAT~~ expression (Garcia et al., 2005). PKC-dependent DAT internalization is also dependent upon ubiquitylation of three lysine groups in the N-terminus of DAT; mutation of these lysines resulted in a diminished internalization of DAT to PKC activation (Miranda, Wu, Sorkina, Korstjens, & Sorkin, 2005). The NEDD4–2 (neural precursor cell expressed, developmentally downregulated 4–2) protein was demonstrated to be a requisite component of PKC-dependent DAT ubiquitination and internalization (Vina-Vilaseca & Sorkin, 2010).

In addition to PKC-stimulated DAT trafficking, DAT surface expression is regulated by carboxy terminal palmitoylation at residue C580. DAT palmitoylation is required to maintain basal DAT surface levels and a DAT C580A mutant lacks palmitoylation and exhibits cell decreased surface expression (Foster & Vaughan, 2011). The physiological purpose for DAT's palmitoylation is still being studied, as the transporter is an integral membrane protein that would not require the modification to target to the membrane. Whether this plays a role in microdomain

targeting at the plasma membrane, or as a locus to recruit DAT binding partners remains to be seen.

In addition to their actions as competitive DAT inhibitors, both AMPH and cocaine acutely impact DAT trafficking. AMPH has a biphasic effect on DAT trafficking in heterologous expression systems and *ex vivo* striatal synaptosomes where the psychostimulant increases DAT surface expression over seconds of exposure, and then decreases DAT surface levels over minutes (Johnson, Furman, Zhang, Guptaroy, & Gnegy, 2005). It has been shown that AMPH treatment results in DAT internalization or reduced DA uptake in cultured cell lines stably expressing DAT or in striatal synaptosomes. Studies using the K44A dynamin mutant demonstrated that AMPH-induced DAT internalization is dynamin-dependent and is blocked by DAT inhibitors, such as cocaine and mazindol, indicating that AMPH must bind to the transporter to elicit internalization (Saunders et al., 2000). Other DAT substrates, such as DA and methamphetamine, also significantly reduce surface DAT expression or DA uptake (Chi & Reith, 2003). Cocaine will increase DAT surface expression in heterologous cells and anesthetized rats (Daws et al., 2002). Ca^{2+}/calmodulin-dependent protein kinase II (CaMKII) has been implicated in AMPH-induced DAT internalization (Fog et al., 2006). AMPH increases intracellular Ca^{2+} and activates CaMKII activity in striatal synaptosomes and in heterologous cells. The AMPH-induced internalization mechanism requires Akt inhibition via activation of CaMKII. However, the role of CaMKII in constitutive DAT

internalization is unclear as CaMKII inhibitors blocked AMPH-induced DAT internalization, but CaMKII inhibitors on do not alter basal DAT levels.

Our lab has uncovered a non–canonical endocytic signal in the dopamine transporter's carboxy terminus and is comprised of ten amino acids (FREKLAYAIA) that regulate both constitutive endocytosis as well as endocytosis elicited by PKC activation (Holton, Loder, & Melikian, 2005; Navaroli et al., 2011). In those studies, a gain-of-funcition assay in which the DAT C-terminus was fused to the non-internalizing membrane protein Tac demonstrated that DAT contains an endocytic signal. Using alanine–scanning mutagenesis, we determined that the hydrophobic residues L, Y, and I are responsible for the constitutive endocytosis, whereas the charged residues R, E, and K are the amino acids that confer sensitivity to PKC activation. Further mutagenesis studies revealed that mutations in the F, R, and E residues increase the constitutive DAT endocytic rate (Boudanova, Navaroli, Stevens, & Melikian, 2008b), N-terminal DAT truncations also result in an increased constitutive endocytic rate (Sorkina, Richards, Rao, Zahniser, & Sorkin, 2009). These results support the hypothesis that DAT surface expression may be regulated by an endocytic braking mechanism mediated by N- and C-terminal domains.

The endocytic sorting machinery that FREKLAYAIA requires is currently unknown. However, a yeast two-hybrid screen using FREKLAYAIA as bait revealed that the

small neuronal GTPase Rin, interacts with the DAT carboxy terminus and is required for PKC-stimulated DAT internalization. Rin cellular role is not well understood but it has been shown to interact with the PAR6/Cdc42/aPKC complex, which is involved in cell polarization via actin remodeling. Interestingly, a genomic screen in *Caenorhabditis elegans* has recently implicated the PAR6 complex in endocytosis and membrane recycling (Balklava, Pant, Fares, & Grant, 2007; Georgiou, Marinari, Burden, & Baum, 2008). FREKLAYAIA's discovery and initial characterization has elicited a search for other proteins that could potentially use this signal to regulate its surface presentation.

Many of the studies characterizing factors affecting constitutive or substrate-induced trafficking of DAT have relied heavily on the use of heterologous cells, and caution should be used in interpretation of the data. Our lab has found that PKC-stimulated DAT internalization was sensitive to DAT expression levels, suggesting that studies in overexpression systems may not accurately reflect relevant DAT trafficking mechanisms. of DAT was insensitive to PKC in cells expressing high basal levels of DAT. In addition to the effect of expression levels, the use of cell types that do not contain the normal contingent of proteins available in the DA terminal could also affect trafficking results. Therefore, findings from heterologous cells should be replicated in animal models. Moreover, previous studies describing molecular requirements for DAT trafficking relied on chronic depletion of trafficking molecules or shRNA-mediated depletion of trafficking proteins. Molecules such as

clathrin and dynamin are required during multiple membrane trafficking steps and their chronic perturbation may disrupt cellular trafficking globally, overstating their direct role in DAT trafficking.

CHAPTER II

MATERIALS AND METHODS

Materials: Anti-HA antibody (3F10) was from Roche Applied Science. Mouse anti-transferrin receptor antibody (H68.4) and fluorophore-conjugated secondary antibodies were from Invitrogen (Grand Island, NY). Mouse anti-actin antibodies and HRP-conjugated secondary antibodies were from Santa Cruz Biotechnology (Santa Cruz, CA). Rabbit anti-turboGFP antibodies were from Evrogen (Moscow, Russia). Rat anti-DAT (MAB369) and mouse anti-tyrosine hyrdroxylase antibodies were from Millipore (Billerica, MA). Dynasore, dynole, and phorbol 12-myristate 13-acetate (PMA) for KCNK3 experiments were from Tocris (Minneapolis, MN). PMA for DAT experiments was from Calbiochem. Sulfo-NHS-SS-biotin, streptavidin agarose, AminoLink Coupling Kit, and 3,3',5,5'-tetramethylbenzidine (TMB) substrate were from Pierce Biotechnology (Rockford, Il). Dihydroxyphenylethylamine, 3, 4-[Ring-2, 5, 6-^{3}H]- (Dopamine) was from Perkin-Elmer (Waltham, MA). Monensin and reagents used for ACSF were from SigmaAldrich (St. Louis, MO). All other reagents were from Fisher Scientific (Waltham, MA) or Sigma Aldrich and were of highest quality possible.

cDNA constructs: Rat HA3-KCNK3 pcDNA3.1(+) cDNA was the generous gift of Dr. Doug Bayliss (Mass. General Hospital, Boston, MA). Human 14-3-3β-GFP-C1

cDNA was the gift of Dr. Mitsuo Ikebe (UMass Medical School, Worcester, MA). KCNK3 point mutants were generated using the QuikChange Mutagenesis kit (Stratagene), and mutant cDNA regions were subcloned back into the wild type KCNK3 plasmids at XcmI/XbaI sites. All mutations were confirmed by dideoxynucleotide cycle sequencing (GeneWiz, New Jersey). shRNA constructs were purchased from Origene (Rockville, MD).

Cell culture and Transfections:

HEK 293T cells were cultured at 37°C, 5% CO_2 in Dulbecco's Modification of Eagle's Medium (DMEM) supplemented with 10% fetal bovine serum, 2 mM L–glutamine, and penicillin/streptomycin. For transfections, HEK cells were seeded in 6 well cultureware 24 hours prior to transfection, were transiently transfected with Lipofectamine 2000 according to the manufacturer's instructions (Invitrogen), and were assayed 48 hours post-transfection. For wide-field microscopy, cells were replated onto poly-D-lysine coated glass coverslips 24 hours post transfection. For knockdown experiments, KCNK3 cDNA and shRNA plasmids were co-transfected into HEK cells and assayed 48 or 72 hours post-transfection.

The human neuroblastoma cell line SK-N-MC stably expressing hDAT (DAT-SK-N-MC) was maintained in MEM supplemented with 10% fetal bovine serum, 2 mM L-glutamine and 100 Units/mL penicillin/streptomycin at 37°C in 5% CO_2. DAT-SK-N-MC cells were plated on 6-well cultureware (1.6 x 10^6 cells/well) or on #1.5

glass coverslips (2.0×10^5 cells/well) in 24-well cultureware and assayed 24 hours later for biochemistry and microscopy, respectively.

PC12 cells stably expressing hDAT (Loder & Melikian, 2003; Melikian & Buckley, 1999) were cultured at 37°C, 10% CO_2 in DMEM supplemented with 5% calf serum, 5% horse serum, 2 mM L-glutamine, 100 Units/mL penicillin/streptomycin, 0.2 mg/ml geneticin. For biochemical assays, DAT PC12 cells were plated on 6-well cultureware (1.5 x 10^6 cells/well) and assayed 24 hours later.

Cerebellar granule neuron preparation: Cerebellar granule neurons were isolated from P6 Sprague-Dawley rat pups. Animals were sacrificed and their cerebelli were surgically removed, minced and incubated in 0.05% Trypsin for 10 minutes under $C0_2$-balanced O_2 at 37°C. Following trypsinization, tissue was washed three times in CTPM (α-MEM supplemented with B27, 10% horse serum, 2 mM L-glutamine, 10 Units/mL penicillin/streptomycin, 100 kunitz/mL DNAse I, 25 mM KCl, 6 mg/mL glucose) and was dissociated by triturating progressively through 21G-26G needle holes in flame-sealed P1000 pipette tips. Cells were collected by centrifugation (1000x*g*, 5 min), re-suspended in CTPM and plated on poly-D-lysine coated glass coverslips (4 x 10^4 cells/well) or in 12 well cultureware (7.5 x 10^5 cells/well) for electrophysiological and biochemical assays, respectively. Cells were grown at 37°C, 5% CO_2 for 5 hours and the media was changed to Neurobasal media [Invitrogen] supplemented with B27, 10 Units/mL penicillin/streptomycin, 2 mM L-glutamine, and 25 mM KCl. Neurons were assayed at 4-13 DIV.

Striatal Slice Preparation: P30-38 male C57/B6 mice were sacrificed by cervical dislocation and decapitated. The brains were immediately chilled in sucrose-supplemented artificial cerebrospinal fluid (SACSF [2.5 mM KCl, 1.2 mM NaH_2PO_4, 1.2 mM $MgCl_2$, 2.4 mM $CaCl_2$, 26 mM $NaHCO_3$, 11 mM glucose, and 250 mM sucrose]) with 95% O_2/ 5% CO_2. Brains were mounted on a Vibratome 1500 sectioning system and 300 µm coronal sections were made. Sections corresponding to the striatum were kept. Following sectioning, striatal slices were incubated in ACSF (125 mM NaCl, 2.5 mM KCl, 1.2 mM NaH_2PO_4, 1.2 mM $MgCl_2$, 2.4 mM $CaCl_2$, 26 mM $NaHCO_3$, and 11 mM glucose) at 31°C for 40 min with 95% O_2/ 5% CO_2, then immediately used for trafficking studies.

Electrophysiological recordings: HEK Cells: Cells were transiently transfected with recombinant cDNA clones of the KCNK3 or KCNK9 channel (0.2 µg), green fluorescent protein (pEGFP-C1; 0.25 µg), and empty plasmid (pcDNA3.1(-), 0.55 µg) using 4 µl of Lipofectamine and 6 µl of PLUS™ reagent (Invitrogen). For shRNA experiments, 2 µg of DNA (1 µg of shRNA, 0.2 µg of channel, 0.8 µg of pcDNA3.1) and 4 µl of Lipofectamine were used. After terminating the transfections (4 h), cells were reseeded onto 8-mm round coverglasses (Warner Instruments) and incubated for an additional 24–48 h. K^+ currents were recorded at room temperature (24 ± 2°C) from voltage-clamped cells. The recording chamber was continuously perfused with extracellular (bath) solution that contained 160 mM

NaCl, 2.5 mM KCl, 2 mM $CaCl_2$, 1 mM $MgCl_2$, 8 mM glucose, and 10 mM HEPES (pH 7.5 with NaOH). Patch electrode tip resistance was 1–3 megaohms when filled with intracellular (electrode) solution that contained 126 mM KCl, 20 mM NaCl, 0.5 mM $MgCl_2$, 0.1 mM EGTA, 0.5 mM ATP-Na_2, 0.3 mM GTP-Na_3, 10 mM HEPES (pH 7.5 with KOH). Transfected (pEGFP-expressing) cells were identified using a GFP filter set of the Axiovert 40 CFL inverted light microscope (Zeiss). Currents were assayed for native-like function using a "family" of traces protocol, in which a cell held at −80 mV was stepped for 50 ms every 15 s to potentials between −120 and +45 mV in 15-mV increments, followed by a 20-ms command to −120 mV. The effect of PKC activation on the current was studied using phorbol 12-myristate 13-acetate, which was dissolved in ethanol and diluted in bath solution to 1 μM (0.006% final ethanol concentration). Current amplitude versus time was monitored by holding cells at −80 mV and recording the current during a 50-ms test depolarization (40 mV) every 30 s.

CGNs: Leak current from 5–14-day *in vitro* CGNs was recorded at room temperature (22–24°C) using the whole-cell configuration of an Axopatch 200B patch clamp amplifier (Axon Instruments, Foster City, CA). Electrodes were pulled from borosilicate glass capillaries (Drummond Scientific Co., Broomall, PA) and fire-polished to a tip diameter of ∼1 μm. The total pipette access resistance ranged from 2.0 to 2.5 megaohms. Cells were held at −20 mV to inactive voltage-activated Ca^{2+}, Na^+, and K^+ channels. Currents were elicited every 10 s by stepping from

−20 mV to various test potentials for 50 ms using the CED Signal software suite, version 2.15 (Cambridge Electronic Design, Cambridge, UK). Currents were filtered at 5 kHz using the amplifier's four-pole, low pass Bessel filter, digitized at 20 kHz with a micro1401 interface (CED), and stored on a personal computer. Electrodes were filled with internal solution containing 140 mM KCl, 4 mM NaCl, 10 mM HEPES, 10 mM EGTA, 5 mM $MgCl_2$, 4 mM ATP, 0.4 mM GTP, pH 7.5. Cells were patched in calcium Tyrode's solution containing 145 mM NaCl, 5.4 mM KCl, 5 mM $CaCl_2$, 10 mM HEPES with the pH adjusted to 7.5. After rupturing the cell membrane, the bath solution was exchanged by a gravity-fed perfusion system. The external solution contained 140 mM NaCl, 3 mM KCl, 10 mM HEPES, 10 mM glucose, 2 mM $MgCl_2$, 2 mM $CaCl_2$, 10 mM TEA, 0.0005 mM tetrodotoxin (TTX), pH 7.5. TEA and TTX were included in the bath solution to inhibit K_{Ca} current and any residual Na_v current, respectively. To activate PKC, PMA (1 μM) or (S)-3,5-dihydroxyphenylglycine (DHPG) (1 μM) was added to the bath after 2 min of measuring stable currents.

KCNK3 Antibody Preparation and Purification: An antigenic peptide corresponding to residues 311-327 in the KCNK3 C-terminus was synthesized and HPLC purified. Antigen was linked to a proprietary immune carrier used to immunize New Zealand rabbits according to standard 90-day protocols for antisera production (21st Century Biochemicals; Marlboro, MA). Antigen was cross-linked to agarose beads with the AminoLink Immobilization Kit according to the

manufacturer's instructions. Antigen (1 mg) was diluted in an equal volume of 100 mM sodium phosphate, pH 7.0 and incubated in activated agarose resin for 20 minutes at room temperature. The cross-linking reaction was quenched in 1 M Tris-HCl, pH 7.4 for 20 min at room temperature. Antigen-beads were poured into a 2 mL column and washed in 10 column volumes (CV) of 1 M NaCl. Column was equlibrated in PBS and chilled to 4°C. Antiserum (bleed 3) was applied to the antigen column, washed in PBS (10 CV), and eluted in 100 mM glycine, pH 2.5. Protein content was measured by A280 absorbance.

Enzyme-linked Immunosorbent Assay: Peptides corresponding to residues 311-327 in the KCNK3 C-terminus were cross-linked to 96 well plates with 1 M Na_2CO_3, pH 9.0 at room temperature for 60 minutes. Wells were washed three times in Tris-buffered saline, pH 7.4 and 0.1% Tween-20 (TBS-T) at room temperature. Antisera (bleed 3) and purified antibody were diluted at 1:16000 to 1:250 and incubated in antigen-coated wells for 2 h at room temperature. Wells were washed three times in TBS-T at room temperature. Anti-rabbit secondary antibodies linked to alkaline phosphatase (1:5000) were incubated in all wells for 60 minutes at room temperature. Wells were washed three times in TBS-T at room temperature. Antibody binding was visualized by TMB addition. The colorimetric reaction was quenched by equal volume addition of 2 M H_2SO_4. Antibody reactivity was measured by A450 absorbance.

Cell surface biotinylation for adherent cells: Cells were treated as described and chilled to 4°C in an ice bath. Cells were washed three times in ice-cold PBS^{++}. Surface proteins were covalently labeled with 1.0 mg/mL sulfo-NHS-SS-biotin in ice-cold PBS^{++} twice for 15 min at 4°C. Following biotinylation, cells were washed three times in PBS^{++} with 100 mM glycine (Quench) and incubated in Quench twice for 15 min at 4°C. Cells were washed three times in ice-cold PBS^{++}, then lysed as described for each protein and protein concentrations were determined using the BCA protein assay (Pierce). Biotinylated proteins were isolated by batch streptavidin chromatography (overnight, 4°C) and bound proteins were eluted in SDS-PAGE sample buffer. Samples were resolved by SDS-PAGE as described below.

Striatal slice biotinylation: Striatal slices were prepared as described. Surface proteins were covalently labeled with 1.0 mg/mL sulfo-NHS-SS-biotin in ice-cold ACSF for 45 min at 4°C, with bubbling 95% O_2/ 5% CO_2. Following biotinylation, slices were washed twice in ice-cold ACSF followed by 3 washes in ice-cold ACSF supplemented with 100 mM glycine. Slices were incubated twice in ice-cold ACSF supplemented with glycine for 20 min at 4°C, with bubbling 95% O_2/ 5% CO_2. Slices were washed four times with ice-cold ACSF and lysed as described below. Protein concentrations were determined using the BCA protein assay (Pierce). Biotinylated proteins were isolated by batch chromatography (overnight, 4°C) and

bound proteins were eluted in SDS-PAGE sample buffer. Samples were resolved by SDS-PAGE as described below.

SDS-PAGE and Immunoblotting: KCNK3: HEK293T cells transfected with HA3-KCNK3 or rat cerebellar granule neurons were surface biotinylated and lysed in 3.2 mM dodecyl maltoside, 50 mM Tris, pH 7.4, 150 mM NaCl, 2 mM EDTA, 1 µg/mL leupeptin, 1 µg/mL pepstatin, 1 µg/mL aprotinin, and 1 mM phenylmethyl sulfonyl fluoride for 20 min at 4°C. Biotinylated protein and ¼ total cellular lysate were resolved on 10% SDS-PAGE, transferred to nitrocellulose and KCNK3 was detected by immunoblotting using rat anti-HA antibody (Roche). Immunoreactive bands were detected using a VersaDoc CCD-camera system and non-saturating bands were quantified using Quantity One software (Biorad).

SDS-PAGE and Immunoblotting: DAT: DAT-PC12, DAT-SK-N-MC and mouse striatal slices were lysed in RIPA (50 mM Tris pH 7.4, 150 mM NaCl, 2 mM EDTA, 1% Triton X-100, 1% sodium deoxycholate, and 0.1% sodium dodecyl sulfate) with 1 µg/mL leupeptin, 1 µg/mL pepstatin, 1 µg/mL aprotinin, and 1 mM phenylmethyl sulfonyl fluoride for 20 min at 4°C. For SK-N-MC experiments, surface proteins and ¼ total cellular lysate were resolved on 10% SDS-PAGE, transferred to nitrocellulose and DAT was detected by immunoblotting using rat anti-DAT antibody (Millipore). For striatal slice experiments, surface proteins and 100% cellular lysate were resolved on 18% SDS-PAGE, transferred to nitrocellulose and

DAT was detected by immunoblotting using rat anti-DAT antibody (Millipore). Immunoreactive bands were detected using a VersaDoc CCD-camera system and non-saturating bands were quantified using Quantity One software (Biorad).

Immunocytochemistry and Wide-field microscopy: Cells were transfected in 6-well dishes and 24 h post-transfection were trypsinized and re-plated on poly-D-lysine-coated plates. 48 hours post-transfection, cells were treated as indicated, rinsed in PBS and fixed in 4% paraformaldehyde prepared in PBS for 10 min at room temperature. For transferrin (Tf) co-localization experiments, cells were loaded with 20 ng/μL Alexa594-Tf during drug treatments. Cells were blocked and permeabilized in blocking solution (PBS, 1% IgG/Protease-free BSA, 5% goat serum, 0.2% Triton X-100) for 30 min at room temperature, followed by incubation with the indicated primary antibodies for 45 min at room temperature. Cells were washed with PBS and incubated with Alexa^{594}- or Alexa^{488}-conjugated secondary antibodies (Invitrogen) for 45 minutes at room temperature. Cells were washed with PBS, dried and mounted on glass slides with ProLong Gold Mounting Medium with DAPI (Invitrogen). Immunoreactive cells were visualized with a Zeiss Axiovert 200M microscope using a 63X, 1.4 N.A. oil immersion objective and 0.4 μm optical sections were captured through the *z*-axis with a Retiga-1300R cooled CCD camera (Qimaging) using Slidebook 5.0 software (Intelligent Imaging Innovations). *Z*-stacks were deconvolved with a constrained iterative algorithm using measured

point spread functions for each fluorescent channel. All images shown are single 0.4 μm planes through the center of each cell.

[^{3}H]Dopamine Uptake Assay: Stably transfected DAT SK-N-MC cells were seeded onto 24-well plates, and [^{3}H]DA uptake was measured 24 h after transfection. Cells were rinsed and incubated in KRH buffer (120mM NaCl, 4.7 mM KCl, 2.2 mM $CaCl_2$, 1.2 mM $MgSO_4$, 1.2 mM KH_2PO_4, 0.18% glucose, and 10 mM HEPES, pH 7.4) at 37°C for indicated times with the indicated drugs. Uptake was initiated by adding [^{3}H]DA with indicated concentrations containing the monoamine oxidase inhibitor pargyline and ascorbic acid. Assays proceeded for 10 min (37°C) and were terminated by rapidly washing cells with ice-cold KRH buffer. Cells were solubilized in scintillation fluid, and accumulated radioactivity was determined by liquid scintillation counting in a Wallac Microbeta scintillation plate counter. Nonspecific uptake was defined in the presence of 10 μM GBR12909 and all samples included 100 nM desipramine to block uptake contribution by endogenously expressed norepinephrine transporters.

Internalization Assay: DAT SK-N-MC cells were seeded onto 6-well plates and internalization rates were measured 24 hours later. Cells were incubated in 10 μM dynole (an inhibitor for dynamin I and II) for 20 min at 37°C. Cells were rapidly chilled and biotinylated twice for 15 min at 4°C with 2.0 mg/mL sulfo-NHS-SS-biotin in PBS^{++} and were quenched twice for 15 min at 4°C in Quench. Cells were rapidly

warmed to 37°C, and incubated in 1 μM PMA for 10 min at 37°C, followed by rapidly cooling to 4°C to stop internalization. Residual surface biotin was stripped by reducing twice with 50 mM TCEP in Buffer NT (20 mM Tris, pH 8.6, 150 mM NaCl, 1 mM EDTA, and 0.2% BSA) for 15 min at 4°C. Cells were lysed in RIPA with protease inhibitors (1 μM leupeptin, 1 μM pepstatin, 1 μM aprotinin, and 1 μM phenylmethyl sulfonyl fluoride) and protein concentrations were determined using the BCA protein assay (Pierce). Equal protein masses were incubated with streptavidin beads (overnight, 4°C) to separate internalized biotinylated protein and bound proteins were eluted in 35 μL 2X SDS-PAGE sample buffer for 15 min at room temperature. Internalized protein was resolved with 10% SDS-PAGE and immunoblotted for DAT, as described previously.

Transferrin Uptake Assay: DAT-PC12 and DAT-SK-N-MC cells were treated as described followed by incubation in 1 μg/mL transferrin-Alexa^{594} (Tf^{594}) for 5 min at 37°C. For monensin experiments (an inhibitor of endosomal recycling), cells were incubated in 50 μg/mL transferrin for 10 min at 37°C. Cells were immediately chilled by washing three times in ice-cold PBS^{++} followed by incubation in stripping solution (500 mM NaCl and 500 mM acetic acid) for 15 min at 4°C. Cells were washed three times in room temperature PBS followed by incubation in 4% paraformaldehyde for 10 minutes while shaking at room temperature. Cells were washed three times with PBS followed by complete aspiration. Plates were

inverted and dried for 30 min at 37°C. Coverslips were mounted in ProLong Gold Mounting Medium with DAPI (Invitrogen) and imaged with wide-field microscopy.

CHAPTER III

TRAFFICKING OF THE pH-SENSITIVE K^+ LEAK CHANNEL KCNK3

INTRODUCTION

Potassium (K^+) leak channels are major determinants of neuronal membrane potential and excitability ((Dodson & Forsythe, 2004; Johnston, Forsythe, & Kopp-Scheinpflug, 2010). "2P" K^+channels are composed of two monomers, each with two pore-forming domains (Bayliss, Sirois, & Talley, 2003; Buckingham, Kidd, Law, Franks, & Sattelle, 2005; Enyedi & Czirjak, 2010; Goldstein, Wang, Ilan, & Pausch, 1998; Mathie, Al-Moubarak, & Veale, 2010), as opposed to tetrameric K^+channels, with each monomer contributing two pores (Ahern & Kobertz, 2009; Gouaux & Mackinnon, 2005). KCNK3 (TASK-1) channels are widely expressed, with enriched expression reported in motor neurons (Talley, Solorzano, Lei, Kim, & Bayliss, 2001), cerebellar granule neurons (Millar et al., 2000), and the carotid body (Bayliss, Talley, Sirois, & Lei, 2001). KCNK3 assembles as a functional homo- or heterodimer with its homolog KCNK9. Both KCNK3 homo- and heterodimers are acid-sensitive (Czirjak & Enyedi, 2002) and are activated by volatile anesthetics (Gruss et al., 2004), which decrease spontaneous neuronal firing rates (Putzke et al., 2007; Talley & Bayliss, 2002). KCNK3 is also inhibited by sanshool (Bautista et al., 2008), the Szechuan peppercorn component that induces a numbing sensation. Studies with KCNK3$^{(-/-)}$ mice demonstrated that

KCNK3 is critical for neuroprotection during stroke (Meuth et al., 2009); for chemosensory control of breathing (Trapp et al., 2008); and for adrenal cortex development, aldosterone production, and response to increased dietary sodium intake (Davies et al., 2008). Taken together, KCNK3 plays a major role in a number of physiological functions throughout the CNS and periphery, and mechanisms that alter KCNK3 function and availability are likely to have a significant systemic impact.

Multiple regulatory proteins control KCNK3 maturation and surface expression. *In vitro* studies demonstrate C-terminal KNCK3 phosphorylation by PKA correlated to enhanced KCNK3 surface expression, presumably by increased forward trafficking from the ER (Mant et al., 2011). In contrast, βCOP binds to the KCNK3 N terminus and prevents egress from the ER and Golgi to the plasma membrane (O'Kelly et al., 2002). The KCNK3/βCOP protein-protein interaction can be mitigated by p11 and 14-3-3β, both of which bind to the KCNK3 C terminus and increase KCNK3 forward trafficking (Girard et al., 2002; Renigunta et al., 2006).

Mounting evidence demonstrates that KCNK3 activity is acutely regulated, via either protein kinase C (PKC) (Lopes et al., 2000) or G_q-coupled receptor activation (X. Chen et al., 2006; Mathie, 2007; Veale et al., 2007). However, the mechanisms mediating KCNK3 regulation are completely unknown. In the current study, we show that PKC-regulated endocytic trafficking acutely modulates KCNK3. KCNK3

C-terminal residues are critical for KCNK3 endocytosis and define a novel K^+ channel endocytic signal. Moreover, we demonstrate that 14-3-3β is absolutely required for KCNK3 internalization, a role heretofore not described for a 14-3-3 protein. These results demonstrate that KCNK3 is not static in the plasma membrane but is dynamically trafficked, enabling potassium leak channels to acutely modulate neuronal excitability and potentially contribute to synaptic plasticity.

RESULTS

KCNK3 currents are downregulated by PKC activation

Previous studies reported PKC-dependent losses in KCNK3 currents in heterologous expression systems (Lopes et al., 2000) and cardiac myocytes (Besana et al., 2004). Given that the KCNK3 C terminus encodes SREKLQYSIP, a sequence homologous to the dopamine transporter (DAT) PKC-regulated endocytic signal, FREKLAYAIA, we hypothesized that KCNK3 may undergo PKC-mediated endocytic trafficking as a means to acutely regulate KCNK3 function. To test this possibility, we first asked whether PKC-mediated KCNK3 down-regulation occurred in neurons, by measuring whole cell leak current in CGNs, in which KCNK3 is endogenously expressed. Upon blocking Na_v currents with TTX and K_{ca} currents with TEA, we detected acid-sensitive (Fig. 3.1), indicating native KCNK3 and KCNK9 expression as observed previously in CGNs (Kang, Han, Talley, Bayliss, & Kim, 2004). The individual traces shown in Fig. 3.1 illustrate the

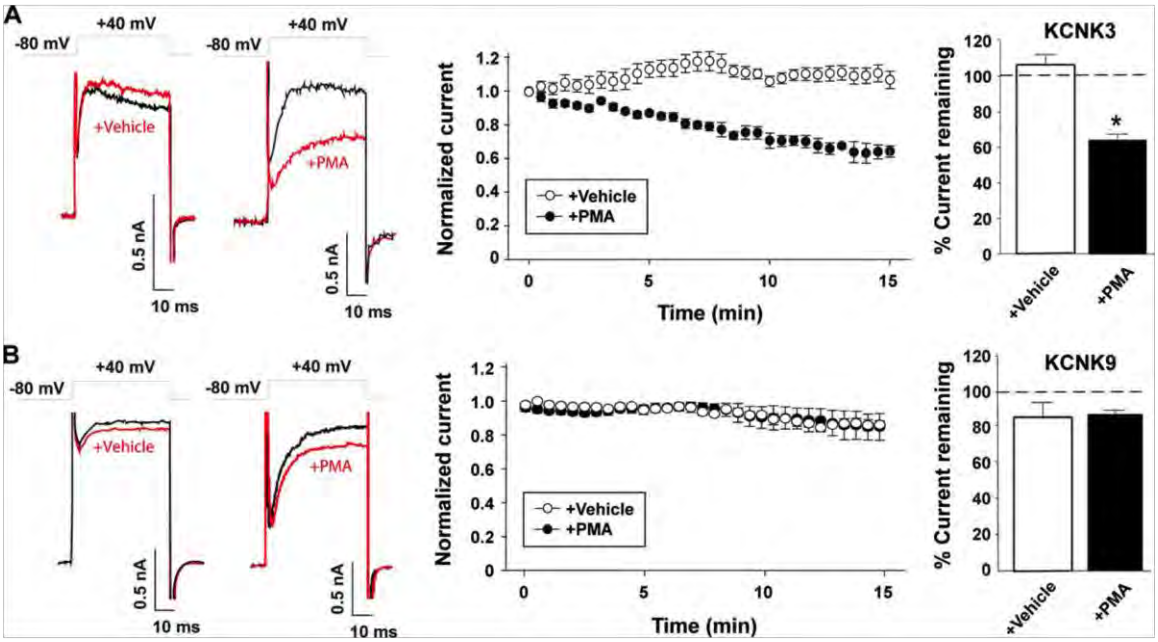

FIGURE 3.1: KCNK3 Currents are Specifically Downregulated by PKC Activation in HEK 293T Cells: Whole-cell K^+ leak currents from cells expressing either KCNK3 (A) or KCNK9 (B) channels were induced using depolarizing voltage steps from −80 to +40 mV every 30 s. For the each channel, representative traces taken before (black) and at the end of 15 min treatment (red) with either vehicle (ethanol) or 1 μM PMA are shown on the left. Average normalized time courses of currents recorded during this treatment are shown in the middle. Mean ± S.E.M. (error bars) of normalized current inhibition (after a 15-min exposure to PMA) from several identical experiments is shown on the right. *, $p < 0.001$; Student's t test; n = 3–5

decrease in leak current amplitude of CGNs following 15 min of treatment with 1 μM PMA. The average decrease in current amplitude over time can be observed and contrasted with currents recorded in the presence of vehicle, which remained stable over 15 min (Fig. 3.1). Consequently, after 15 min of PMA, 63 ± 10% (Fig 3.1) of the leak current remained, and this decrease in amplitude was significantly different from that in vehicle-treated cells (99 ± 13%) as shown in the summary "*bar graph"* in Fig. 3.1 ($p < 0.05$; two-way Student's *t* test for two means; $n = 8–9$/group).

Because CGNs express both KCNK3 and KCNK9 subunits, we next determined whether the PKC-mediated inhibition of the acid-sensitive leak current in neurons was specific for one of the KCNK subunits. Native acid-sensitive leak currents are generated by homo- and heterodimers composed of KCNK3 and its homolog, KCNK9. KCNK9 is 82% identical to KCNK3; however, their C termini are highly divergent, and KCNK9 does not encode a SREKLQYSIP endocytic motif. Treatment with 1 μM PMA decreased KCNK3 currents to 64.1 ± 3.4% of base-line levels by 15 min (Fig. 3.2), which was significantly lower than currents measured in vehicle-treated cells (101.6 ± 5.2% base line; $p < 0.001$; Student's *t* test; $n = 3–5$). In contrast, PMA had no effect on KCNK9 currents (vehicle = 84.8 ± 7.8% base line; PMA = 82.9 ± 3.6% base line; $p = 0.89$; Student's *t* test; $n = 3$) (Fig 3.2). These results suggested that the PMA-induced losses in acid-sensitive leak current in CGNs were specific for channels containing the KCNK3 subunit.

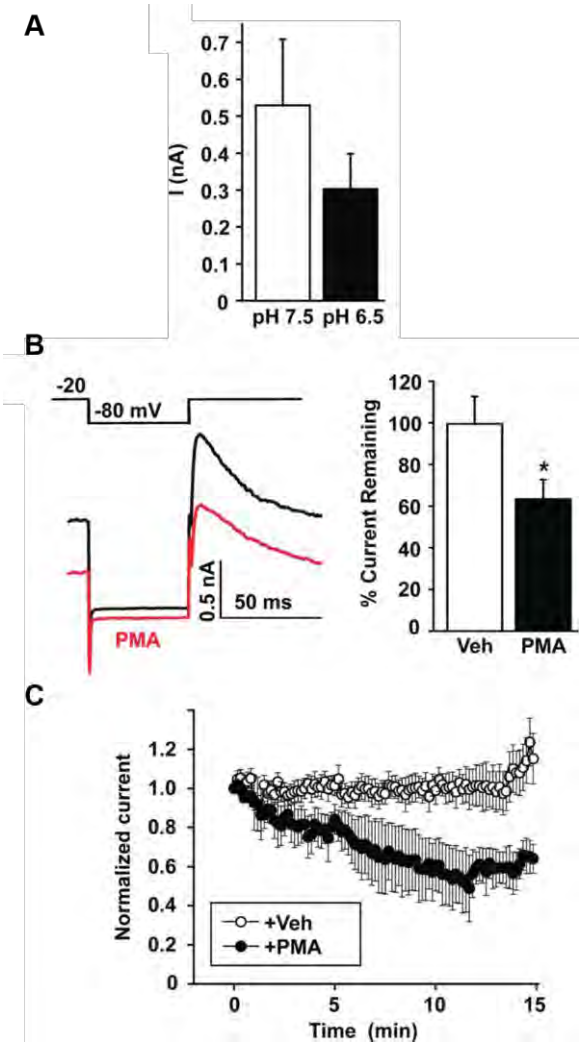

FIGURE 3.2: KCNK3 Currents are Specifically Downregulated by PKC Activation in Cerebellar Granule Neurons: Shown are whole-cell recordings of K^+ leak current in the presence of 0.5 μM TTX and 10 mM TEA. (A) average decrease in current amplitude following bath solution exchange from pH 7.5 to 6.5 (n = 7). (B) zinc sensitivity following introduction of 100 μM zinc (Zn^{2+}) (n = 5). (C) representative traces of leak current at time 0 min (black line) and 15 min following 1 μM PMA (red line). (D) average percentage of current remaining after 15 min with 1 μM PMA is significantly different from that with an equal volume of vehicle (Veh) added to the bath solution. *, $p < 0.05$; Student's t test; n = 8–9/group. (E) average normalized time courses of leak current following introduction of either vehicle (○) or 1 μM PMA (●) into the bath at time 0. Currents were sampled every 10 s (n = 8–9/group). Error bars, S.E.M.

KCNK3 requires a special solubilization protocol

Due to their high hydrophobic content, membrane proteins are often resistant to solubilization or prone to aggregation when dissolved in detergents. Consequently, detergent selection and optimization is required to maintain membrane proteins in solution in order to perform biochemical studies. KCNK3 contains 4 transmembrane domains and 2 hydrophobic potassium-conducting pore helices, which comprise 43% of the protein's amino acid sequence. Initial expression and characterization of epitope-tagged HA-KCNK3 in PC12 used the classical radioimmunoprecipitation assay (RIPA) buffer for lysis, which contains the detergents 1% Triton X-100, 1% sodium deoxycholate, and 0.1% sodium dodecyl sulfate. Following immunoblotting, the anti-HA immunoreactivity exhibited minimal electrophorectic mobility and was concentrated primarily in the stacking gel, consistent with protein aggregation (Fig 3.3). To circumvent this obstacle, we optimized the solubilization conditions for KCNK3, testing previous approaches in which potassium channels were expressed and solubilized. The bacterial potassium channel KcsA was cloned and purified, ultimately leading to its crystallization and structural determination, using the amphiphile detergent decyl maltoside. We tested whether a related detergent, dodecyl maltoside, could more efficiently solubilize KCNK3 transiently expressed in HEK 293T cells. This detergent contains a two methyl addition to the aliphatic chain as well as a lower critical micelle concentration. Using this detergent, we observed show the

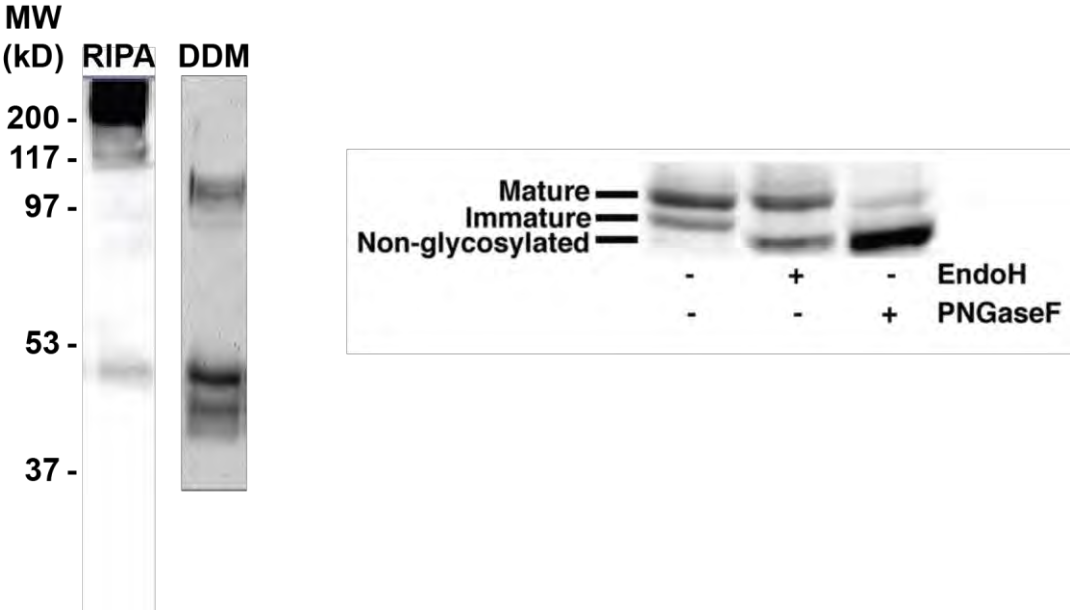

FIGURE 3.3: KCNK3 Requires a Specific Solubilization Protocol: Mature KCNK3 is insoluble in RIPA lysis buffer and present following solubilization in dodecyl maltoside. Left: Immunoblot of HA-KCNK3 lysed in either RIPA (Lane 1) or DDM (Lane 2). Right: HEK293T cells were transfected with HA-KCNK3, and cell lysates were analyzed 48 h post-transfection. Lysates were treated with 1 unit of endoglycosidase H (EndoH) or peptide:N-glycosidase F (PNGaseF) for 3 h at 30°C and resolved by SDS-PAGE, and immunoblots were probed using anti-HA antibody. Note detection of both KCNK3 mature (endoglycosidase H-insensitive) and immature (endoglycosidase H-sensitive) species.

presence of two anti-HA reactive bands, at ~50 and ~100 kD, whereas no immunoreactivity was detected in non-transfected cells (Fig 3.3).

The presence of two immunoreactive KCNK3 bands could be due to proteolysis, a mixture of KCNK3 biosynthetic intermediates, or the presence of monomeric and dimeric (i.e. non-dissociated) KCNK3 subunits. To distinguish between these possibilities, we differentially deglycosylated HEK lysates with endoglycosidase H (EndoH) or peptide-N-glycosidase F (PNGaseF) to inspect the core protein and the channel's glycosylation state. EndoH selectively cleaves high mannose N-linked glycans before they receive post-ER processing in the Golgi. Sensitivity to this enzyme indicates an immature channel and resistance shows post-ER trafficking. PNGase F cleaves all N-linked glycans and reveals the mobility of the non-glycosylated (core) protein. As can be seen in Figure 3.3, PNGase treatment reduced the 50 and 100 kDa bands to 45 and 90 kDa, respectively, demonstrating the presence of N-linked glycosylation. In contrast, neither the 50 nor 100 kDa bands were sensitive to Endo H treatment. These data suggest that both 50 and 100kDa KCNK3 species are biosynthetically mature (post-ER/Golgi) protein, and that they represent KCNK3 monomer and non-dissociated dimmers. KCNK3 is present in both mature and immature states at its monomeric size. Future experiments will only use the mature, higher monomeric and dimeric bands for surface protein quantification.

KCNK3 internalizes in response to PKC activation

PKC-mediated losses in KCNK3 activity could be due to changes in channel conductance, open probability or surface number due to acute endocytic trafficking**.** However, the timecourse of KCNK3 downregulation in response to PKC activation suggested a membrane trafficking event. To test whether PKC-mediated KCNK3 functional losses were due to surface losses, we first employed cell-surface biotinylation to measure KCNK3 surface levels in response to PKC activation in transfected HEK cells. The results are shown in Figure 3.4. Under vehicle-treated conditions, 65.0±6.9% total KCNK3 was at the cell surface. Treatment with 1 μM PMA, 30 min, 37°C significantly decreased KCNK3 surface levels to 47.4 ± 5.7% total KCNK3 ($p<0.04$, Student's *t* test, $n = 9$). Of note, both mature and immature KCNK3 species are detectable in total cell lysates, whereas only mature protein is detected in surface fractions.

We next asked whether PKC-induced losses in KCNK3 activity in CGNs were also due to rapid endocytosis. To detect native KCNK3, we first attempted to use a commercially available anti-KCNK3 antibody. While this reagent specifically detected KCNK3 via immunocytochemistry, it failed to detect a KCNK3-specific band by immunoblot in transfected HEK293 cells and was deemed unsuitable for use in biochemical studies. Thus, in order to perform biochemical studies in primary CGNs, we raised rabbit antisera directed against the KCNK3 carboxy terminus and, using affinity chromatography, purified the antisera using the

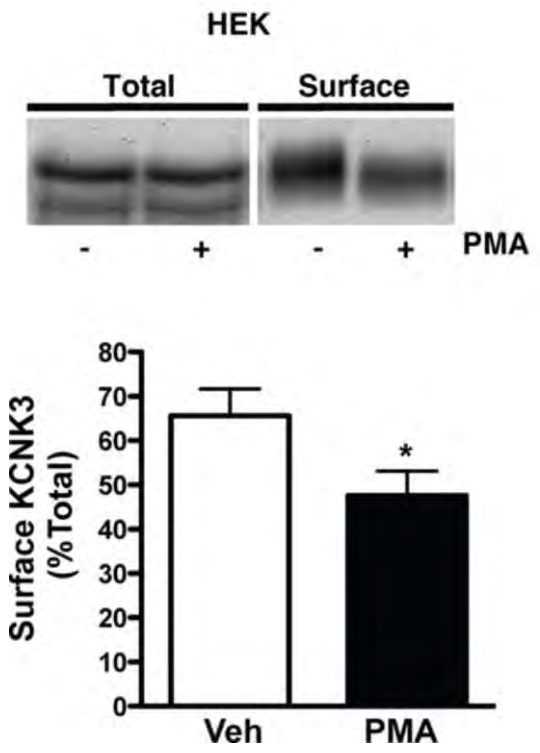

FIGURE 3.4: **PKC Activation Reduces KCNK3 Surface Levels in HEK 293T Cells**: HEK cells transfected with HA-KCNK3 were treated or not treated with 1 μM PMA for 30 min at 37 °C, and KCNK3 surface levels were measured by surface biotinylation as described in *Methods*. Top: representative immunoblot showing total and surface KCNK3 protein detected with anti-HA antibody. Bottom: average data expressed as KCNK3 surface levels ± S.E.M. (error bars). *$p < 0.04$, significantly different from vehicle control; Student's t test; $n = 9$.

antigenic peptide (Fig. 3.5). This reagent specifically detects KCNK3 monomers in transfected HEK cells and CGNs (Fig 3.5). We used this reagent to ask whether PKC-induced losses in KCNK3 activity in CGNs were due to KCNK3 internalization. CGNs were treated ±1 μM PMA for 20 minutes at 37°C, followed by cell-surface biotinylation. Following vehicle treatment, we observed 5.0 ± 0.4 % of total KCNK3 on the cell surface (Fig. 3.6). Treatment with 1μM PMA, 30 min, 37°C significantly decreased KCNK3 surface levels to 3.74 ± 0.2% of total KCNK3 ($p<0.04$, Student's *t* test, n = 7) (Fig. 3.6). This translates to a 25.2% loss in surface KCNK3 protein, which is consistent with PMA-induced reduction of KCNK3 currents in HEK cells and acid-sensitive leak currents in CGNs.

We next used cellular imaging to examine KCNK3 cellular distribution in HEK cells. Under basal conditions, KCNK3 expressed prominently at the cell perimeter and co-localized with the IL2α receptor (Tac), co-expressed as a plasma membrane marker, (Fig. 3.7). Following treatment with 1μM PMA for 30 minutes at 37°C, we observed a marked loss of KCNK3 from the cell surface, and redistribution into intracellular puncta (Fig. 3.7), whereas Tac remained on the cell surface. PMA-induced losses from the cell surface were completely blocked by pre-treating cells with 1 μM BIM (Fig. 3.7), demonstrating that PMA-induced losses were PKC-mediated. In order to test whether KCNK3 traffics via the endocytic pathway we next labeled endosomes with Alexa^{594}-transferrin (Tf) during PMA-induced KCNK3

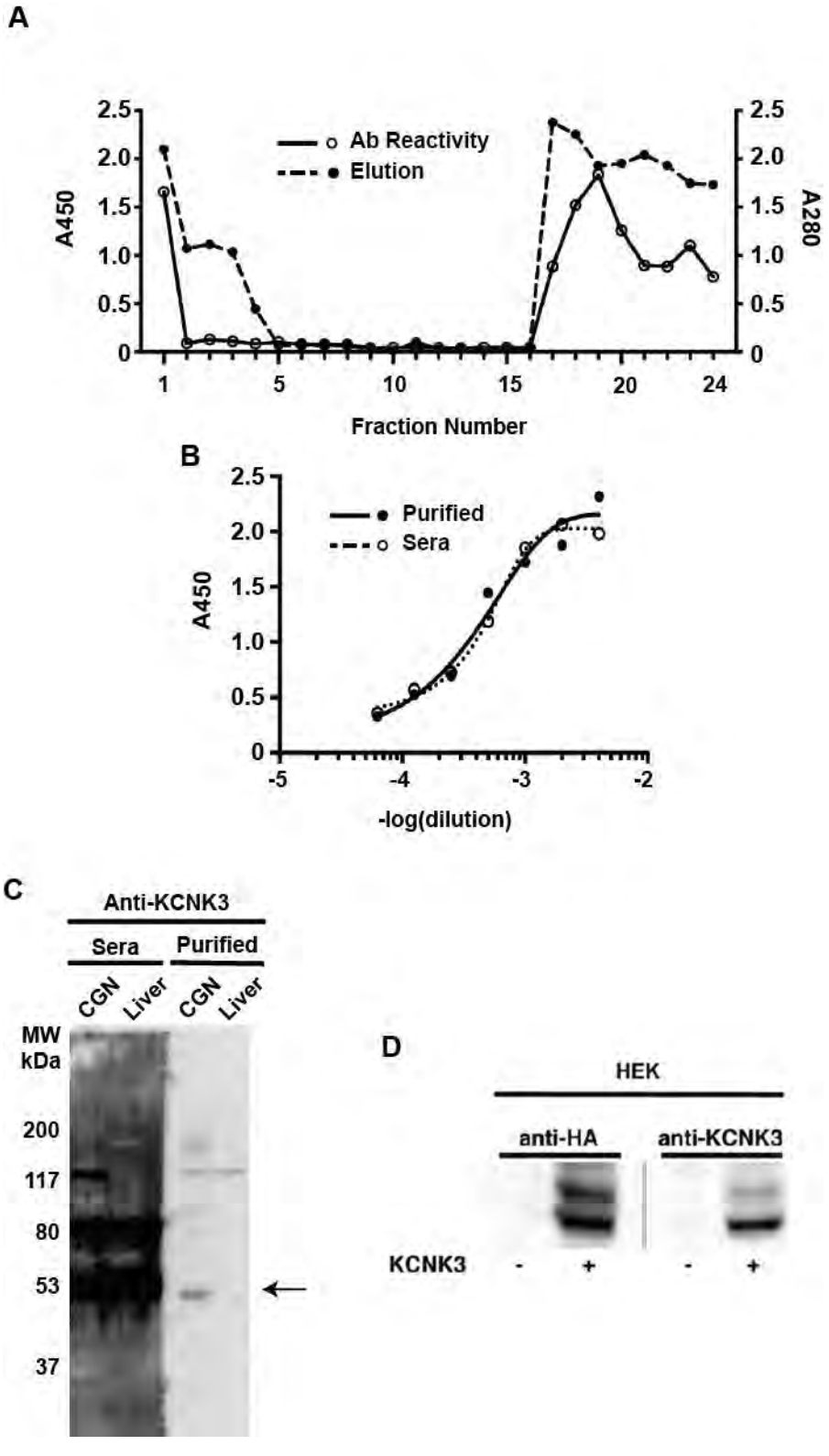
A
Ab Reactivity
Elution
A450
A280
Fraction Number
B
Purified
Sera
A450
-log(dilution)
C
Anti-KCNK3
Sera
Purified
CGN
Liver
CGN
Liver
MW
kDa
200
117
80
53
37
D
HEK
anti-HA
anti-KCNK3
KCNK3
-
+
-
+

FIGURE 3.5: Production and Purification of an Antibody that Specifically Recognizes KCNK3: A C-terminal-directed rabbit anti-KCNK3 antibody specifically recognizes KCNK3 in cultured cerebellar granule neurons and transfected HEK cells. (A) Antigen purification and immunoreactivity graph. (●; dotted line) A280 absorbance from antibody affinity purification. (○) A450 absorbance from ELISA measuring immunoreactivity. Fractions: Flowthrough (1-4), column washes (5-15), and competitive antigen elution (16-24). (B) Antibody immunoreactivity following antigen affinity chromatography. Sera EC_{50} = 1.01; Purified antibody EC_{50} = 0.99. (C) The indicated tissues were harvested from P6 rat pups, lysed, and resolved by SDS-PAGE. Immunoblots were probed with anti-KCNK3 sera or affinity purified anti-KCNK3 antibody. The arrow indicates KCNK3 monomer. (D) HEK cells were transfected with either vector (−) or HA-KCNK3 (+), cell lysates were resolved by SDS-PAGE, and immunoblots were probed with anti-HA and rabbit anti-KCNK3 antibodies, in parallel.

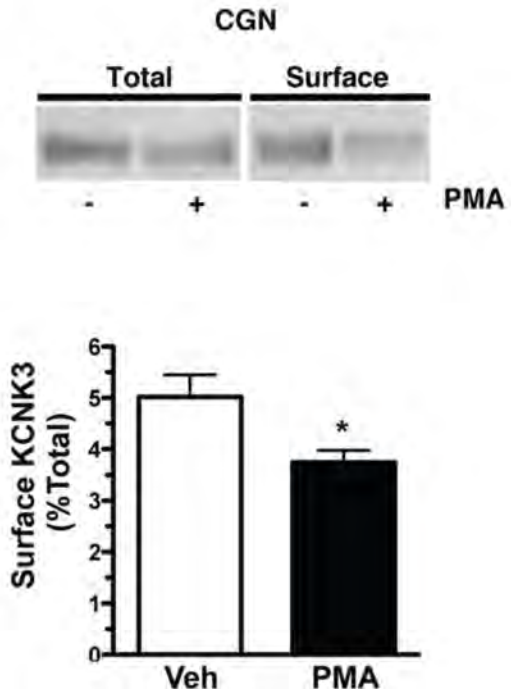

FIGURE 3.6: PKC Activation Reduces KCNK3 Surface Levels in Cerebellar Granule Neurons: Immunoblots with rabbit anti-KCNK3 antibody reveal specific KCNK3. Cell surface biotinylation. CGNs were treated or not treated with 1 μM PMA for 30 min at 37 °C, and KCNK3 surface levels were measured by biotinylation as described in *Methods*. Top: representative immunoblot showing total and surface KCNK3 protein. Bottom: average KCNK3 surface levels expressed as a percentage of total KCNK3 ± S.E.M. *$p < 0.04$, significantly different from vehicle control; Student's t test; n = 7.

internalization. As seen in Figure 3.7, KCNK3 internalized into a subset of Tf-positive endosomes, suggesting that KCNK3 traffics via the endosomal pathway and, specifically, through Tf-positive endosomes. Following internalization, proteins can divert to either degradative or recycling endocytic pathways. To test whether KCNK3 is subject to degradation following internalization, we monitored KCNK3 stability over time ± 1 μM PMA, following pretreatment with the translational inhibitor cyclohexamide. KCNK3 was highly stable over a 60 minute period, and PMA treatment had no effect on total KCNK3 protein levels (Fig. 3.8), suggesting that following internalization KCNK3 traffics through a non-degradative pathway. Taken together, these data indicate that KCNK3 undergoes PKC-stimulated, non-degradative endocytosis.

Group I mGluR activation induces KCNK3 downregulation and internalization

To investigate physiologically relevant stimuli that may regulate KCNK3 trafficking, we tested whether activating Group I mGluRs would alter KCNK3 function in CGNs. Group I mGluRs couple to G_q activation, which ultimately activates PKC, and are abundantly expressed in CGNs (Prezeau et al., 1994). Moreover, Group I mGluR activation has been shown to decrease acid-sensitive currents in motor neurons (Talley, Lei, Sirois, & Bayliss, 2000). CGNs were treated with the Group I mGluR agonist dihydroxy-phenyl-glycine (DHPG, 1 μM) during whole cell recording. We observed a rapid and significant reduction in KCNK3-associated

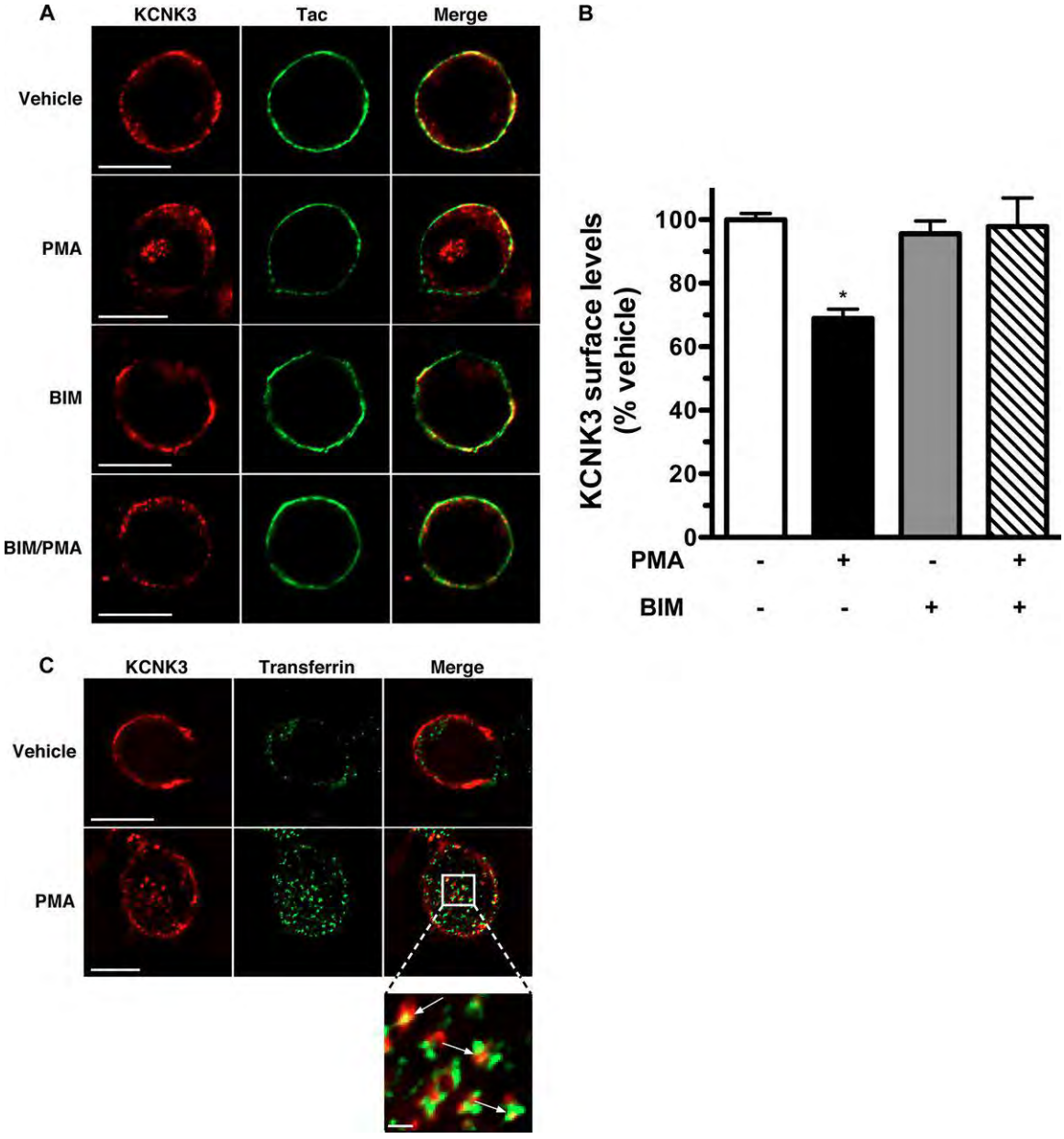
A
KCNK3
Tac
Merge
Vehicle
PMA
BIM
BIM/PMA
B
KCNK3 surface levels (% vehicle)
100
80
60
40
20
0
*
PMA - + - +
BIM - - + +
C
KCNK3
Transferrin
Merge
Vehicle
PMA

FIGURE 3.7: KCNK3 Internalization Specifically Requires PKC Activation and Traffics to Transferrin-positive Endosomes: HEK cells were co-transfected with KCNK3 and the cell surface marker IL2αR (Tac) and were pretreated with or without 1 μM BIM, followed by treatment with or without 1 μM PMA for 30 min at 37°C. Surface Tac was labeled on non-permeabilized cells with αTac antibody (green). Cells were then permeabilized and stained for KCNK3 (red). Images were captured and analyzed as described under *Methods.* Scale bars, 10 μm. (A) representative images; (B) image quantification. Data are expressed as percentage of vehicle surface levels ± S.E.M. (error bars). *$p<0.05$, significantly different from vehicle, BIM, and BIM/PMA; one-way analysis of variance with Tukey's multiple comparison test; n = 12. (C) Cells were treated or not treated with 1 μM PMA for 30 min at 37°C in the presence of Alexa594-Tf (green), fixed, permeabilized, and stained for KCNK3 (red). Scale bars, 10 μm. Enlarged view, scale bar, 1 μm.

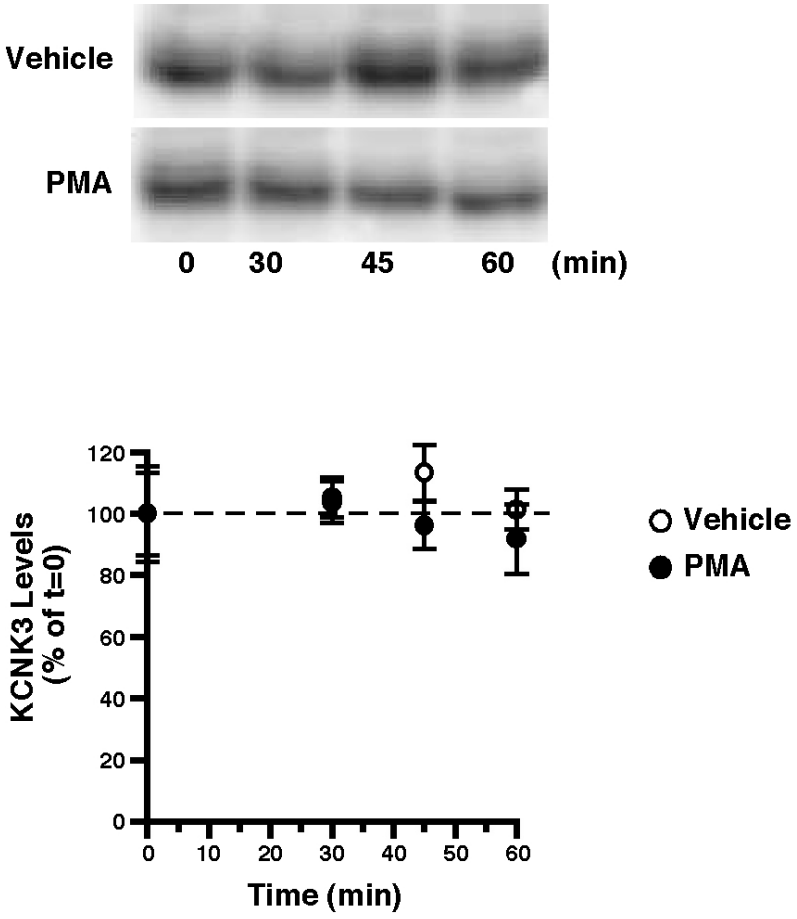

FIGURE 3.8: KCNK3 is Not Degraded Following PKC-Mediated Internalization: HEK cells transfected with HA-KCNK3 were treated or not treated 10 μM cycloheximide for the indicated times at 37°C, and KCNK3 surface levels were measured by surface biotinylation as described in *Methods*. Top: representative immunoblot showing total and surface KCNK3 protein detected with anti-HA antibody. Bottom: average data expressed as KCNK3 surface levels normalized to t=0 ± S.E.M. (error bars).

current in response to DHPG treatment, which was comparable in magnitude to that observed following PMA treatment (56 ± 10% current remaining; n = 8; $p<0.01$) (Fig 3.9). To determine whether DHPG-mediated losses in current were PKC-dependent, CGNs were pretreated with 1μM BIM prior to DHPG application. BIM alone had no effect on acid-sensitive currents (Fig. 3.9), but completely blocked DHPG-mediated loss in KCNK3 currents. These results indicate that KCNK3 undergoes PKC-mediated functional downregulation in response to Group I mGluR activation.

We next asked whether Group I mGluR activation stimulates KCNK3 internalization and, if so, whether PKC activation was required. HEK cells were co-transfected with KCNK3 and either GFP alone or with mGluR5 in a bicistronic expression vector. Treatment with 1 μM DHPG for 20 min at 37°C, had no effect on KCNK3 surface levels in cells expressing KCNK3 and GFP ($p= 0.89$; Student's *t* test; n=6) (Fig. 3.10). In contrast, when KCNK3 was co-expressed with mGluR5, 1μM DHPG treatment decreased KCNK3 surface levels to 70.7 ± 5.0% of KCNK3 levels in vehicle-treated cells. (Fig. 3.10). mGluR5-mediated KCNK3 internalization required PKC activation, as pretreatment with 1μM BIM completely blocked mGluR5-mediated KCNK3 surface losses (Fig. 3.10). Taken together, our results indicate that KCNK3 is subject to acute internalization in response to PKC activation, and that Group I mGluR activation can trigger KCNK3 endocytosis.

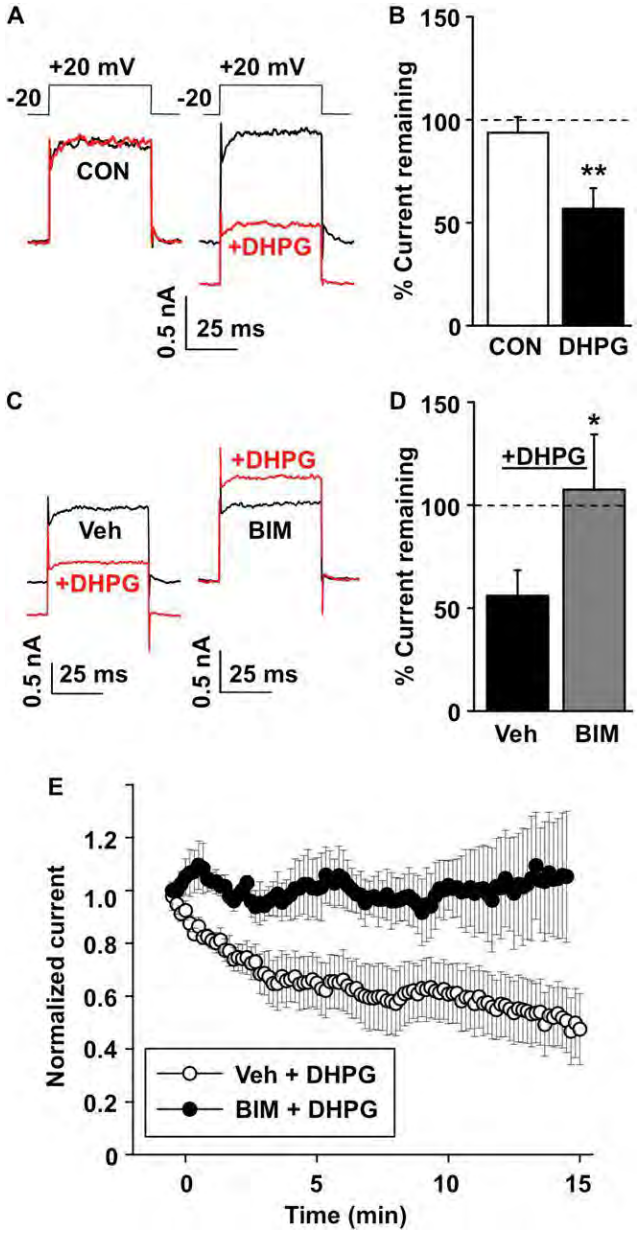
A
+20 mV
-20
+20 mV
-20
CON
+DHPG
0.5 nA
25 ms
B
150
100
50
0
% Current remaining
**
CON
DHPG
C
+DHPG
Veh
+DHPG
BIM
0.5 nA
25 ms
0.5 nA
25 ms
D
150
100
50
0
% Current remaining
+DHPG
*
Veh
BIM
E
1.2
1.0
0.8
0.6
0.4
0.2
0
Normalized current
Veh + DHPG
BIM + DHPG
0
5
10
15
Time (min)

FIGURE 3.9: KCNK3 Currents Are Specifically Downregulated by mGluR1/5 Agonists in Cerebellar Granule Neurons: Whole-cell recordings of K^+ leak current in the presence of 0.5 μM TTX and 10 mM TEA (7–14 days *in vitro*) were tested for sensitivity to the group I mGluR agonist DHPG. (A) selected sweeps at time 0 min (black line) and 15 min (red line). Left: representative traces (CON) show leak current amplitude with no additions. Right: representative traces with and without 1 μM DHPG. (B) average percentage of current remaining after 15 min of no additions (CON) or DHPG (n = 6–8/group). Cells exposed to DHPG exhibited significant inhibition of leak current compared with no addition (**, $p < 0.02$; two-way Student's t test for two means). (C) Left: cells were preincubated for at least 8 min in 0.005% DMSO (Veh) while recording whole-cell leak currents. Representative current traces versus time exhibit substantial decreases in amplitude after 15 min of 1 μM DHPG compared with time 0 min (Veh). Right: representative traces document that preincubating cells with 1 μM BIM for at least 8 min while in the whole-cell configuration minimized leak current inhibition by DHPG. (D) average percentage of current remaining after 15 min of DHPG following preincubation with either 1 μM BIM (n = 3) or DMSO (Veh; n = 4). *$p < 0.05$, compared with the presence of BIM using a two-way Student's t test for two means). (E) time course of the average decrease in normalized leak currents over 15 min. DHPG was applied at time 0 min (n = 3–4/data point) in the presence of DMSO (○) or BIM (●). Error bars, S.E.M.

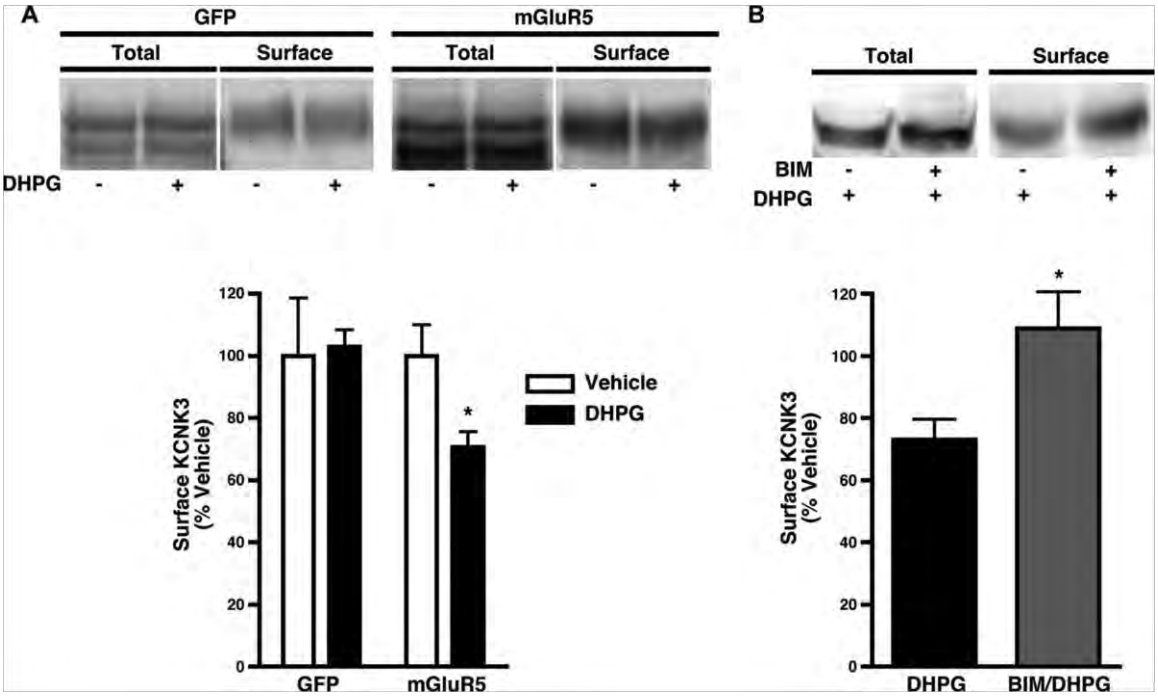

FIGURE 3.10: KCNK3 Internalizes in Response to mGluR1/5 Agonists via a PKC-specific Mechanism: (A) Cell surface biotinylation. Cells were treated or not treated with 1 μM DHPG for 20 min at 37°C, and KCNK3 surface levels were measured as described under *Methods*. Top: representative immunoblot showing total and surface KCNK3 protein. Bottom: average KCNK3 surface levels expressed as percentage of vehicle ± S.E.M. (error bars). *$p < 0.03$, significantly different from vehicle control; Student's t test; n = 6. (B) cells were treated or not treated with 1 μM BIM for 20 min at 37 °C followed by treatment with or without 1 μM DHPG for 20 min at 37°C, and KCNK3 surface levels were measured as described under *Methods.* Top: representative immunoblot showing KCNK3 total and surface protein. Bottom: average KCNK3 surface levels expressed as percentage of vehicle ± S.E.M. *$p < 0.03$, significantly different from vehicle control; Student's t test; n = 6.

KCNK3 carboxy terminal residues are both necessary and sufficient for PKC-regulated KCNK3 internalization

We next sought to identify the molecular determinants of PKC-mediated KCNK3 internalization. We previously reported that the dopamine transporter (DAT) encodes a novel carboxy terminal endocytic signal, FREKLAYAIA, that regulates both constitutive internalization, as well as trafficking in response to PKC activation (Boudanova et al., 2008b; Holton et al., 2005). In particular, the REK residues have been shown by our laboratory to be sensitive to PKC activation. The tandem pore potassium channel KCNK3 (TASK-1) encodes a homologous sequence, SREKLQYSIP, in carboxy terminal residues 334-343, which is absent in the KCNK3 homolog, KCNK9 (Fig. 3.11). We used a gain-of-function assay to ask whether the KCNK3 carboxy terminus was sufficient to drive internalization of an endocytic-defective reporter protein, Tac. As seen in Figure 3.10, Tac is highly expressed at the cell surface under trafficking restrictive conditions (4°C), and remains at the surface in trafficking permissive conditions (37°C). In contrast, a Tac fusion protein expressing the KCNK3 carboxy terminus robustly internalized at 37°C. Internalization was specific to the KCNK3 carboxy terminus, as a Tac-KCNK9 fusion protein failed to internalize (Fig. 3.11). These results indicate that the KCNK3 carboxy terminus encodes residues sufficient to drive endocytosis.

Given the homology between the DAT endocytic signal with the SREKLQYSIP motif in KCNK3, we next tested whether residues involved in PKC-regulated DAT

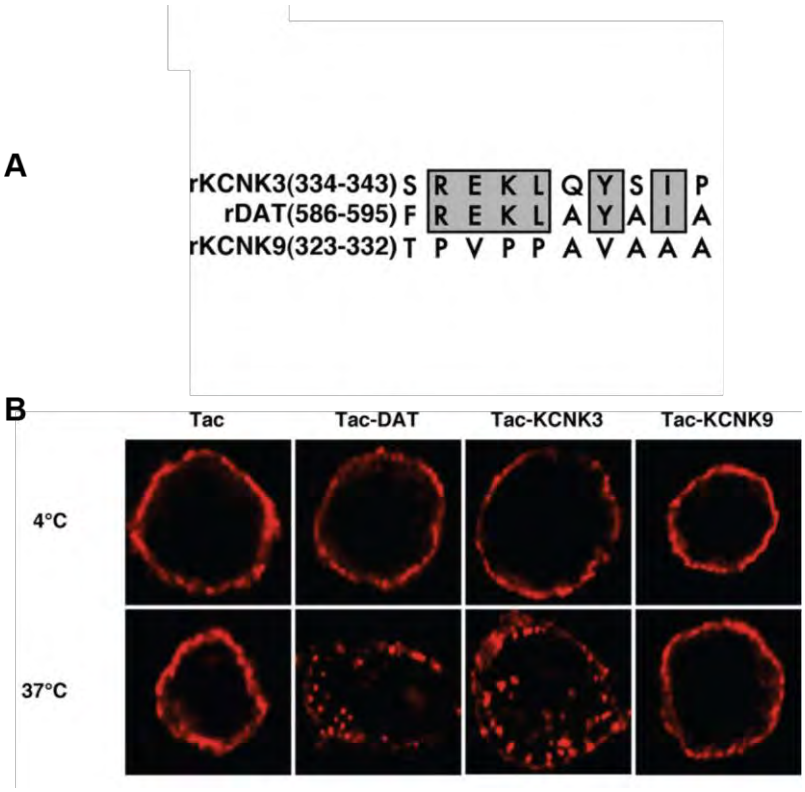

FIGURE 3.11: The KCNK3 Carboxy Terminus Contains an Endocytic Signal: PC12 were transfected with the indicated constructs and assayed 24–48 h post-transfection. (A) Sequence alignment between DAT and the potassium channel KCNK3 and KCNK9 C-terminal subregions. (B) Immunocytochemistry. Intact cells were incubated in anti-Tac antibody at 4°C, shifted to 37°C for 30 min, and then fixed and imaged as described under *Methods*.

internalization were also necessary for KCNK3 downregulation and internalization. To test this possibility, we mutated KCNK3 residues 335-337 (REK) to alanines and tested the capacity of this mutant to undergo PKC-mediated downregulation and internalization. The KCNK3 335-337(3A) mutant expressed and exhibited whole cell currents comparable to those measured for wildtype channel (Fig. 3.12). As observed previously, treatment with 1μM PMA resulted in a significant, time-dependent decrease in wildtype KCNK3 currents (Fig. 3.12). In contrast, KCNK3 335-337(3A) was completely insensitive to PMA treatment, and no current loss was observed (Fig. 3.12). We next investigated whether abolished PKC-mediated KCNK3 335-337(3A) current losses were due to perturbation of KCNK3 internalization. Cellular imaging revealed that KCNK3 335-337(3A) expressed at the cell surface, but failed to internalize following PKC activation (Fig. 3.12). We next used surface biotinylation to compare wildtype and KCNK3 335-337(3A) surface levels ±PKC activation. As shown in Figure 3.12, we confirmed that mutating KCNK3 residues 335–337 significantly blocked PKC-mediated KCNK3 surface losses (wild type: 63.7 ± 7.5% of vehicle levels; REK/AAA: 114.4 ± 12.4% of vehicle levels, $p<0.02$, Student's t test, $n = 4$), demonstrating that these three residues are key determinants of PKC-mediated KCNK3 functional down-regulation and internalization.

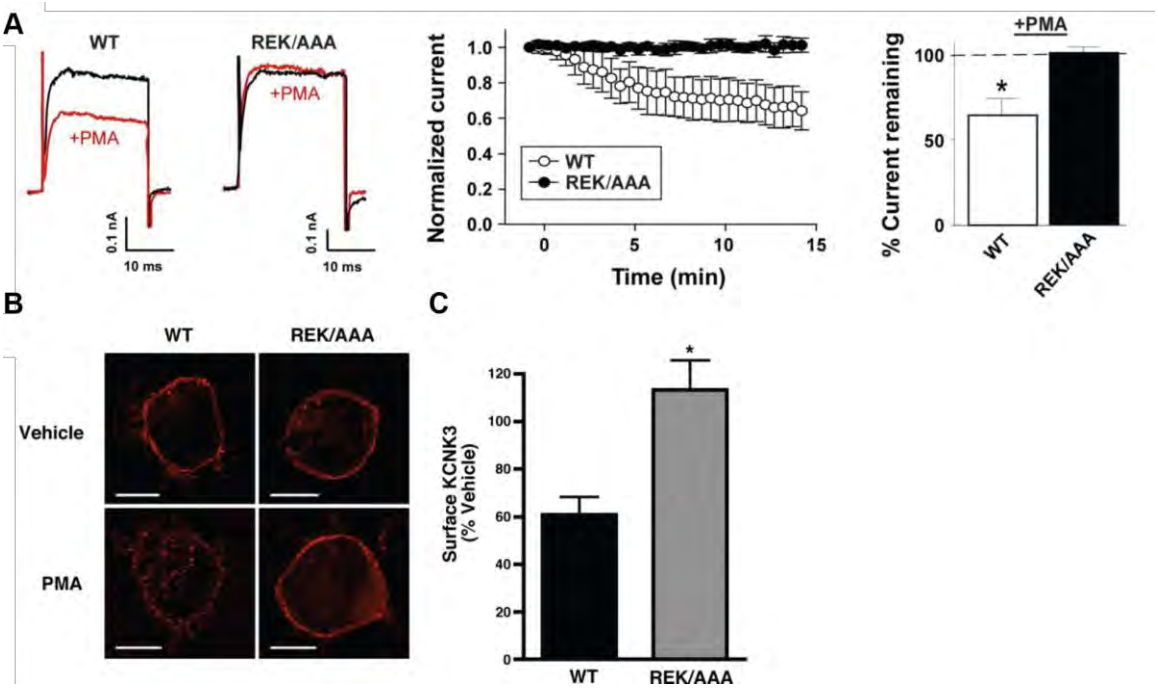

FIGURE 3.12: Residues 335-337 in the KCNK3 Carboxy Terminus are Required for PKC-mediated Functional and Surface Losses: HEK cells were transfected with the indicated constructs and assayed 24–48 h post-transfection. The REK/AAA mutation prevents PMA-induced inhibition of KCNK3 current. (A) Left: representative traces of KCNK3 current recorded from HEK293T cells expressing either WT or REK/AAA mutant channels recorded before (*black*) and after (*red*) 1 μM PMA treatment (40-mV test pulse). Middle: average normalized time course of WT (*open circles*; *n*= 3) or REK/AAA (*filled circles*; *n*= 5) currents recorded during a 15-min exposure to 1 μM PMA. Right: mean ± S.E.M. of current remaining after a 15-min exposure to PMA (*p*= 0.007). (B) Immunocytochemistry. Cells were treated or not treated with 1 μM PMA for 30 min at 37°C, fixed, stained for KCNK3, and imaged as described under *Methods*. *Scale bars*, 10 μm. (D) cell surface biotinylation. Cells were treated or not treated with 1 μM PMA for 15 min at 37°C, and KCNK3 surface levels were measured as described under *Methods*. Average KCNK3 surface levels following PMA treatment are expressed as percentage of vehicle ± S.E.M. (*error bars*). **p*< 0.02, significantly different from WT; Student's *t*-test; *n*= 4.

PKC-mediated KCNK3 endocytosis requires 14-3-3β

Previous work from our laboratory demonstrated that PKC-induced DAT trafficking relies on a saturable factor (Loder & Melikian, 2003). In that study, increased DAT expression levels correlated with losses in PKC-induced transporter internalization. To test whether PKC-stimulated KCNK3 internalization also relied upon a saturable factor, we performed overexpression experiments in transiently transfected HEK cells in which 5-fold more KCNK3 cDNA was used for transfections, which translated into a 10-fold increase in KCNK3 protein expression (Fig 3.13). Under vehicle conditions, KCNK3 was readily apparent at the cell surface (Fig. 3.13). However, overexpression completely abolished PKC-mediated KCNK3 internalization (Fig 3.13). We next tested whether co-expression of a co-factor could rescue KCNK3 in an overexpression system. The phosphoserine binding protein 14-3-3β is reported to facilitate KCNK3 exit from the ER and to interact with the KCNK3 distal carboxy terminus. Importantly, KCNK3 encodes a canonical (R/K)XX(Y/F)pSXP 14-3-3 binding site in the SREKLQYSIP region (SREKLQYSIP), prompting us to ask whether 14-3-3β may also play a role in PKC-mediated KCNK3 endocytosis. We tested this possibility by co-overexpressing KCNK3 and 14-3-3β and assessing whether PKC-mediated KCNK3 internalization could be rescued by 14-3-3β. Co-expression of 14-3-3β completely rescued the ability of KCNK3 to internalize in response to PKC activation in the overexpression system (Fig. 3.13). This suggests that 14-3-3β

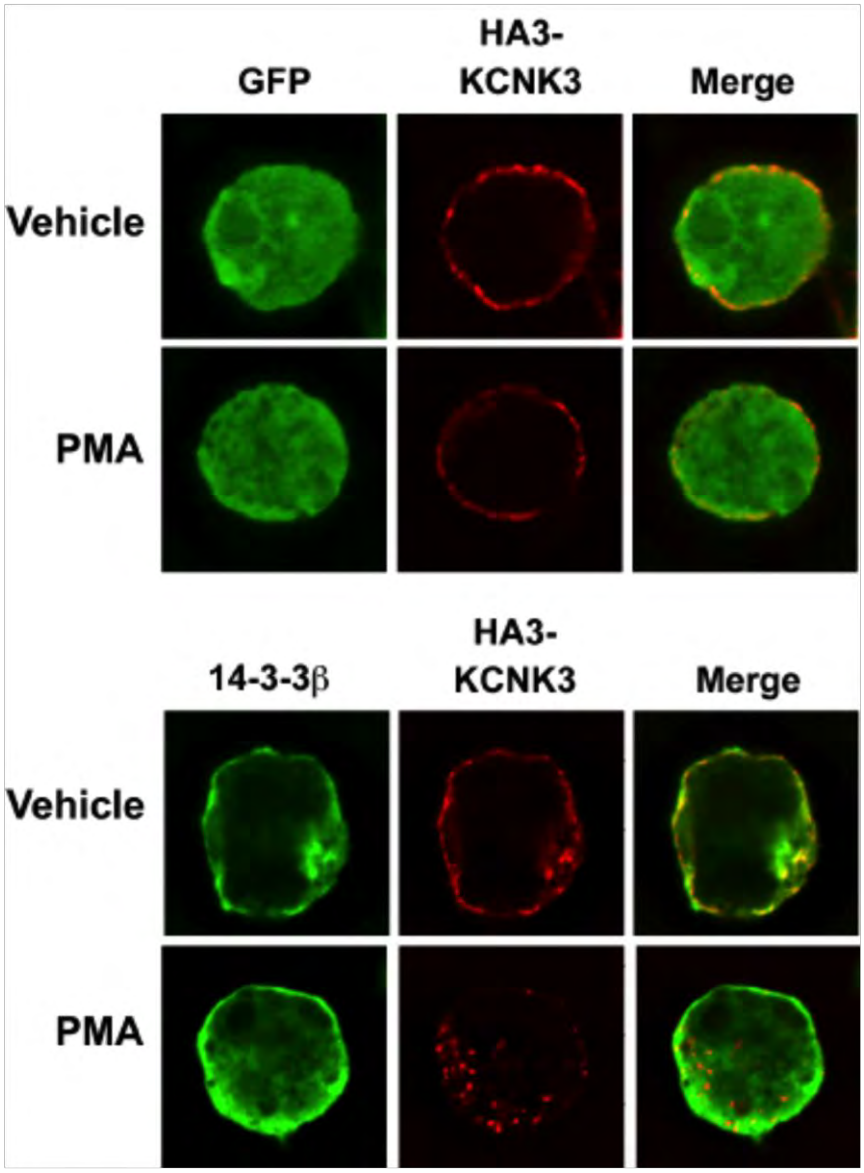

FIGURE 3.13: The Phosphoserine Binding Protein 14-3-3β is a Saturable Factor Required for PKC-mediated KCNK3 Internalization: HEK cells were transfected with 5X the normal HA-KCNK3 with or without 14-3-3β-GFP and assayed for trafficking 48 h post-transfection. Channel overexpression blocked PKC-mediated KCNK3 trafficking and 14-3-3 β co-expression rescued the trafficking blockade. Immunocytochemistry: Cells were treated or not treated with 1 μM PMA for 30 min at 37°C, fixed, stained for KCNK3 (red), and imaged as described under *Methods*. GFP expression indicates co-transfection (green).

may play a role in regulated endocytic trafficking in addition to its known role as an ER chaperone.

Using a knockdown approach to limit 14-3-3β availability, we further tested the whether 14-3-3β was required for PKC-mediated KCNK3 surface losses. Three shRNAs targeting human 14-3-3β were tested for their ability to decrease 14-3-3β expression levels. As seen in Figure 3.14, 14-3-3β shRNAs 6, 7, and 8 significantly decreased 14-3-3β levels 72 hours post-transfection, as compared to vector-transfected controls, whereas a scrambled shRNA had no significant effect on 14-3-3β levels. Significant 14-3-3β knockdowns were also achieved 48 hours post transfection (Fig. 3.14). HEK cells were co-transfected with KCNK3 with each of these shRNAs, and their ability to undergo PKC-stimulated internalization was assessed by cellular imaging following treatment with 1 μM PMA for 30 minutes at 37°C. Under basal conditions, KCNK3 prominently localized to the cell surface, both in the presence of control or 14-3-3β-directed shRNAs. PKC activation resulted in robust KCNK3 redistribution to intracellular puncta in cells co-expressing either GFP alone or GFP and scrambled shRNA (Fig. 3.14). In contrast, KCNK3 failed to redistribute to intracellular puncta in cells co-expressing any of the three 14-3-3β-directed shRNAs (Fig. 3.14). We additionally tested whether 14-3-3β was required for PKC-mediated functional downregulation of KCNK3. Cells were co-transfected with either GFP, scrambled shRNA or 14-3-3β shRNA#7 and whole cell currents were recorded. Application of 1 μM PMA

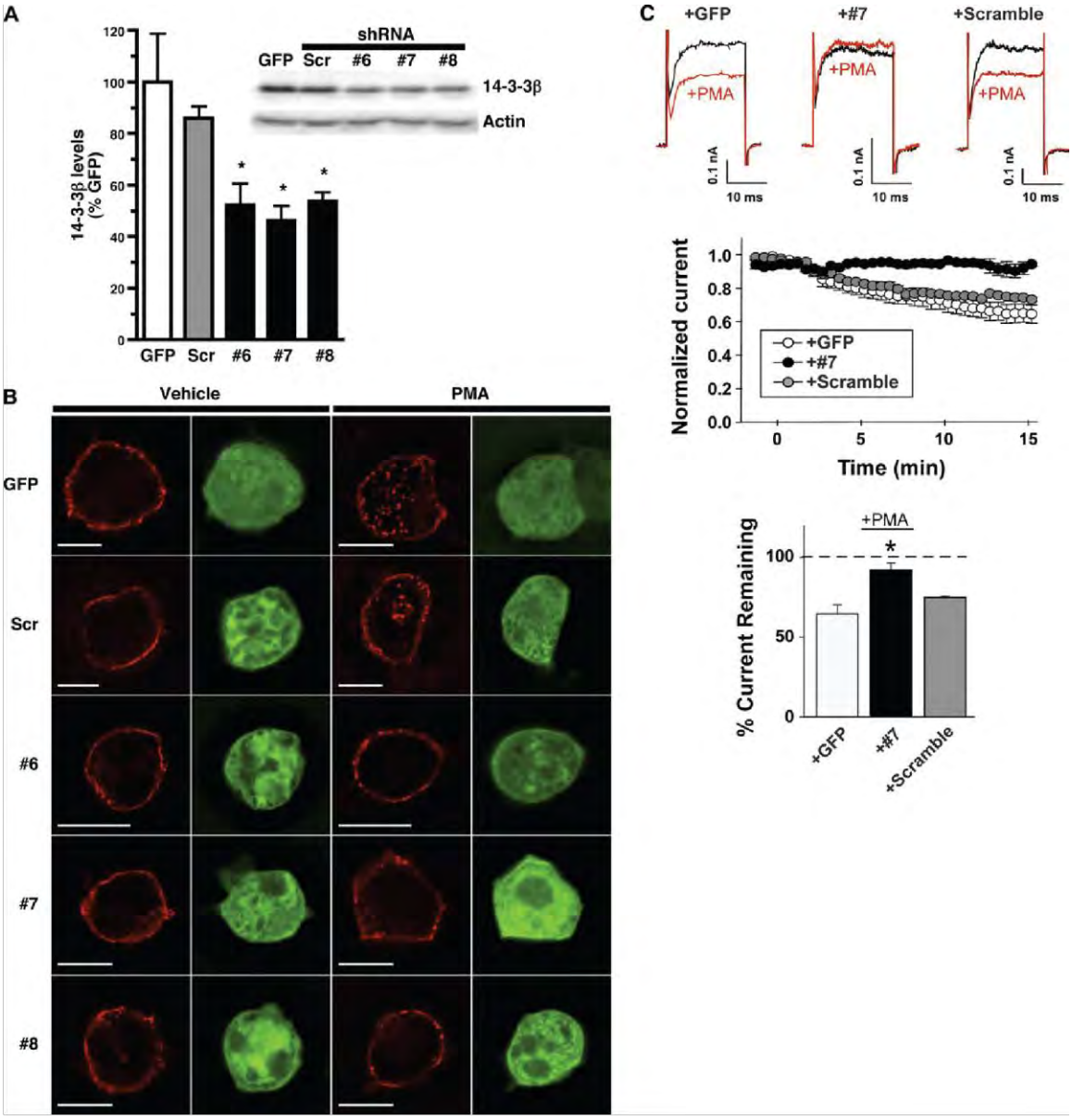
A
shRNA
GFP Scr #6 #7 #8
14-3-3β
Actin
14-3-3β levels (% GFP)
120
100
80
60
40
20
0
GFP Scr #6 #7 #8
B
Vehicle
PMA
GFP
Scr
#6
#7
#8
C
+GFP
+#7
+Scramble
+PMA
0.1 nA
10 ms
Normalized current
1.0
0.8
0.6
0.4
0.2
0.0
+GFP
+#7
+Scramble
0
5
10
15
Time (min)
+PMA
% Current Remaining
100
50
0
+GFP
+#7
+Scramble

FIGURE 3.14: The Phosphoserine Binding Protein 14-3-3β is Required for PKC-mediated KCNK3 Functional and Surface Losses: HEK cells were transfected with the indicated constructs and assayed 48 h (A) or 72 h (B and C) post-transfection. (A) shRNA-mediated 14-3-3β knockdown. Average 14-3-3β protein levels are expressed as percentage of control levels ± S.E.M. *p < 0.004, significantly different from GFP-transfected controls; one-way analysis of variance with Dunnett's post hoc analysis; n=4. *Inset*, representative immunoblot probed for 14-3-3β and actin (loading control). (B) Immunocytochemistry. Cells were treated or not treated with 1 μM PMA for 30 min at 37 °C, fixed, and stained for KCNK3 (red). GFP expression indicates shRNA co-transfection (green). Images were captured and analyzed as described under *Methods*. Scale bars, 10 μm. (C) PKC-mediated inhibition of KCNK3 current requires 14-3-3β. Top: representative whole-cell current traces from HEK293T cells co-expressing KCNK3 with either GFP, shRNA 7, or scrambled shRNA recorded before (black) and after (red) 1 μM PMA treatment (40-mV test pulse). Average normalized time course (middle) and mean ± S.E.M. (error bars) of current remaining (bottom) after 15 min of PMA treatment are shown; n=9 for GFP control; n=4 for scrambled and #7 shRNAs. *p < .02, significantly different from wildtype, , one-way ANOVA with Bonferroni's multiple comparison test.

resulted in a time-dependent decrease in KCNK3 currents in cells co-expressing either GFP or scrambled shRNA (Fig. 3.14). However, 14-3-3β-directed shRNA#7 completely blocked the PMA-induced downregulation of KCNK3 (Fig. 3.14). Taken together, these results indicate that 14-3-3β plays a requisite role in PKC-mediated KCNK3 internalization, and implicates 14-3-3β in regulated endocytosis, in addition to its previously defined role in ER export.

DISCUSSION

Membrane protein trafficking is a central mechanism controlling neuronal excitability and plasticity in the brain. Regulated internalization of ligand-gated ion channels, such as AMPA (Bredt & Nicoll, 2003), NMDA (Perez-Otano & Ehlers, 2005) and $GABA_A$ receptors (Kittler, McAinsh, & Moss, 2002), is a key factor in synaptic plasticity. Recent studies indicate that endocytic trafficking acutely regulates several different types of K^+ channels, including K_{ATP} (Manna et al., 2010) and $K_{Ca.2.1}$ (Correa, Muller, Collingridge, & Marrion, 2009), suggesting that regulated membrane trafficking is a means to rapidly control K^+ channel density. Indeed, a recent study demonstrated that TWIK1 undergoes regulated internalization via a classic dileucine endocytic signal (Feliciangeli et al., 2010). In the current study, our data reveal that dynamic endocytic trafficking regulates acid-sensitive K^+ leak channel surface expression. This finding suggests a role for KCNK3 to uniquely contribute to synaptic plasticity. KCNK3 internalization would be predicted to depolarize the membrane potential, which would inactivate Na_v

channels, causing the membrane to reach threshold more slowly, fail in firing, and/or spike at a slower frequency of bursting. Alternatively, membrane depolarization mediated by regulated KCNK3 trafficking could relieve Mg^{2+} block of NMDA receptors, increasing the probability of NMDA receptor firing and downstream plasticity events in response to an excitatory postsynaptic potential. Thus, in combination with established ligand-gated ion channel trafficking, acutely regulating KCNK3 surface levels would give rise to a multimodal, context-dependent plasticity of membrane excitability that could last for many minutes.

Prior studies using phorbol esters (Lopes et al., 2000), Group I mGluR agonists (Talley et al., 2000), and M1/M3 muscarinic agonists (Meuth et al., 2003) demonstrated a PKC-mediated functional down-regulation of KCNK3 and/or acid-sensitive currents, respectively. However, the mechanisms underlying this down-regulation have not been well defined. We observed significant loss of KCNK3 activity in response to PMA treatment over a 15-min time course in both CGNs and HEK cells, which is consistent with the time course for endocytosis. We used surface biotinylation and cellular imaging to directly test whether PKC-stimulated KCNK3 current losses were due to internalization. We observed significant PKC-dependent losses in surface KCNK3 following PMA treatment both in HEK cells and CGNs, which were completely blocked by the PKC inhibitor BIM. The magnitude of KCNK3 surface losses paralleled PKC-mediated KCNK3 currents losses, consistent with endocytosis as the primary mechanism responsible for

PKC-mediated KCNK3 inhibition. Moreover, we observed losses in acid-sensitive leak currents and KCNK3 internalization via activation of endogenously expressed Group I mGluRs, consistent with previous reports demonstrating Group I mGluR-mediated KCNK3 down-regulation Previous studies reported rapid KCNK3 activity losses in response to direct G_q activation (X. Chen et al., 2006) or via glutamatergic signaling (Chemin et al., 2003) in heterologous expression systems and CGNs, whereas we observed a slower time course of KCNK3 inhibition. These differences may be due to direct G_q activation in a heterologous expression system *versus* indirect via G_q coupling in our experiments. This difference may also reflect the much higher DHPG concentrations used in previous studies, compared with those used in our studies (10 and 100 μM *versus* 1 μM in our study). Indeed, decreased cAMP production in response to high DHPG concentrations has been reported, which is likely mediated by Group III mGluR activation. It is not known whether PKC activation results in KCNK3 phosphorylation, either directly or indirectly. A recent report demonstrated that endothelin-1 down-regulates KCNK3 and leads to PKC-dependent KCNK3 phosphorylation in pulmonary artery smooth muscle cells (Tang et al., 2009). However, it should be noted that these phosphorylation studies relied upon the commercially available anti-KCNK3 antibody that, in our hands, does not recognize a KNCK3-specific band. It is interesting to note that under basal conditions, KNCK3 surface expression in primary CGN cultures was <6% total KCNK3 protein, which differed markedly from observed surface levels in transfected HEK cells. Nevertheless, these values are consistent with those

reported for other channels in both primary cultured neurons (Gross, Yao, Pong, Jeromin, & Bassell, 2011) and acute brain slices (D. Y. Kim, Gersbacher, Inquimbert, & Kovacs, 2011). Low channel surface density (as a fraction of the total available channel) may reflect large intracellular endocytic pools tightly regulated by neuron-specific mechanisms. Alternatively, they may reflect a high degree of turnover in neuronal systems, with large, forward trafficking protein pools to maintain steady state channel levels in the membrane.

Following internalization from the cell surface, proteins can diverge to either recycling or degradative endocytic pathways (Bonifacino & Traub, 2003). For example, EGFR (Huang, Kirkpatrick, Jiang, Gygi, & Sorkin, 2006) and δ-opioid receptors (von Zastrow, 2010) enter late endosomes and are degraded upon internalization, whereas the TfR is primarily recycled. We observed KCNK3 co-localization in an early endosome/TfR-positive vesicle population following internalization and detected no losses in total KCNK3 protein following PKC stimulation. These results suggest that internalized KCNK3 is likely to enter a recycling, rather than a degradative, pathway.

Previous studies from our laboratory investigating mechanisms responsible for PKC-stimulated DAT trafficking revealed a novel endocytic regulatory domain (FREKLAYAIA) encoded in the DAT C-terminus that is highly conserved across the SLC6 transporter gene family and is the locus for an endocytic braking

mechanism (Boudanova et al., 2008b). Sequence comparison across the mammalian genome revealed that KCNK3 is the only membrane protein outside of the SLC6 transporter gene family to encode a homologous endocytic signal. Gain-of-function assays revealed that the KCNK3 C terminus is sufficient for endocytosis, and that the REK residues are absolutely required for PKC-mediated KCNK3 down-regulation and internalization. These results offer further insight into the previous results of Talley and Bayliss (Talley & Bayliss, 2002), in which KCNK3 C-terminal deletions that encompassed the 335–344 region abolished TRH receptor-mediated KCNK3 inhibition, which also occurs via G_q activation. It is currently not clear how these charged residues function to target either DAT or KCNK3 to the endocytic machinery. Answers to this question await future studies.

PKC-stimulated KCNK3 endocytosis absolutely required the phosphoserine-binding protein 14-3-3β. 14-3-3β belongs to the family of 14-3-3 phosphoserine-binding proteins, which are widely expressed in the brain and periphery and exist as homo- or heterodimers (Obsilova, Silhan, Boura, Teisinger, & Obsil, 2008). 14-3-3 binds target proteins primarily at either RS*X*pS*X*P or (R/K)*X*φ*X*(pS/pT)*X*P motifs (Yaffe et al., 1997), and several proteins encode multiple 14-3-3 binding sites (Tzivion, Luo, & Avruch, 2000). 14-3-3 binding can 1) induce conformation changes that facilitate catalytic activity or protein-protein interactions, 2) mask domains to prevent protein-protein interactions, or 3) facilitate protein co-localization. Previous work demonstrated that 14-3-3β binds to a non-canonical

14-3-3 binding motif in the distal KCNK3 C terminus and is required for KCNK3 egress from the ER (Zuzarte et al., 2009). In addition, other 14-3-3 isoforms can interact with the KCNK3 C-terminus and promote increased KCNK3 surface density (Rajan et al., 2002); however, it is not clear whether the increased KCNK3 surface expression is due to ER egress or endocytic trafficking. Our results indicate that 14-3-3β is also necessary for PKC-mediated KNCK3 internalization. We noted that a ~50% 14-3-3β knockdown did not markedly disrupt KCNK3 surface targeting, whereas PKC-mediated endocytosis was abolished. This may suggest that forward trafficking from the ER is less sensitive to 14-3-3β levels than KCNK3 surface populations. Alternatively, other accessory proteins working in consort with 14-3-3β at the cell surface may be expressed in limited quantities and are thereby more sensitive to losses in 14-3-3β. Interestingly, the epithelial sodium channel, ENaC, constitutively internalizes in a 14-3-3- and Nedd4-2-dependent manner, and aldosterone increases ENaC surface expression via blocking 14-3-3-dependent ENaC internalization and degradation (Ichimura et al., 2005). The mechanism by which 14-3-3β promotes KCNK3 internalization is not known; nor is it clear whether a mechanism distinct from 14-3-3β-dependent ER exit is at play. It is interesting to note that the SREKLQYSIP region is similar to the mode II 14-3-3β binding motif (R/K)*X*φ*X*(pS/pT)*X*P. Although we do not currently know whether 14-3-3β controls KCNK3 internalization directly or indirectly, this site is a candidate locus for potential 14-3-3β/KCNK3 endocytic interactions, distinct from the identified sequence controlling KCNK3 egress from the ER. Future studies

exploring the possibility of this sequence as a *bona fide* 14-3-3β binding site should be illuminating.

CHAPTER IV

Dopamine Transporter Endocytic Trafficking: Differential Dependence on Dynamin and the Actin Cytoskeleton

INTRODUCTION

The plasma membrane dopamine transporter (DAT) is expressed exclusively in dopaminergic neurons in the central nervous system and functions to transport extracellular dopamine (DA) back into these neurons, thus providing temporal and spatial regulation of DA neurotransmission. Mutations in DAT have been reported in neurological diseases, such as attention deficit hyperactivity disorder (ADHD), Parkinson's disease and schizophrenia. The psychostimulants amphetamine (AMPH) (Horn et al., 1971), cocaine (Calligaro & Eldefrawi, 1987), and methylphenidate (Schweri et al., 1985) all competitively inhibit DAT, and DAT binding to cocaine is requisite for the rewarding properties of this drug (R. Chen et al., 2006; Thomsen et al., 2009). DAT surface expression determines the DA clearance efficiency and is acutely regulated by endocytic trafficking (Buckley, Melikian, Provoda, & Waring, 2000). DAT undergoes constitutive endocytosis and recycling (Melikian & Buckley, 1999; Sorkina et al., 2005). Importantly, DAT endocytic trafficking is acutely modulated by PKC activation and exposure to AMPH (Saunders et al., 2000), as well as trafficking regulated by cell signaling

pathways, as well as by DAT substrates (AMPH) and inhibitors (cocaine) (Daws et al., 2002).

The molecular mechanism regulating DAT endocytosis and recycling is still under investigation, and previous studies have reported conflicting results. Previous work has shown that constitutive and PKC-mediated DAT endocytosis require the classical clathrin-mediated endocytic molecules clathrin and dynamin (Daniels & Amara, 1999; Eriksen et al., 2009; Saunders et al., 2000). Conversely, it has been shown that the lipid-raft associated protein flotillin-1 is required for PKC-mediated DAT internalization, in a clathrin-independent process (Cremona et al., 2011). These studies relied upon chronic shRNA-mediated depletion of endocytic molecules or co-expression of dominant negative mutant molecules and were primarily carried out in heterologous expression systems. Chronic trafficking protein depletion over several days may act to perturb all membrane trafficking, which could mask or overstate the necessity for DAT trafficking. Moreover, DAT is expressed in a small subset of neurons and heterologous expression systems may not contain the full complement of proteins required for physiological DAT regulation. Here, we test DAT's trafficking dependence on dynamin in acute mouse striatal slices using pharmacological dynamin inhibitors in order to assess trafficking requirements in a physiologically relevant and minimally perturbed milieu. Our results demonstrate a differential dependence on dynamin for constitutive and PKC-regulated DAT endocytic trafficking.

RESULTS

DAT is functionally downregulated by dynamin inhibition

Previous studies reported dynamin-dependent DAT trafficking in heterologous expression systems and cultured dopaminergic neurons (Daniels & Amara, 1999; Eriksen et al., 2009). These studies depended on shRNA-mediated depletion or co-expression of dominant negative mutant trafficking proteins, which block cellular membrane trafficking for several days. We took advantage of a newly developed dynamin inhibitor, dynasore, to acutely perturb dynamin activity and test whether DAT trafficking is dynamin-dependent.

We first tested whether dynamin inhibition altered dopamine transporter activity and ability to undergo PKC-mediated downregulation. DAT-PC12 cells were pretreated with either ±80 μM dynasore, 30 min, 37°C, followed by treatment ±1 μM PMA, 30 min, 37°C to activate PKC, and [^{3}H]DA uptake was assessed. Dynamin inhibition significantly decreased DAT activity to 62.9 ± 7.7% of control levels (Fig. 4.1). Losses in DAT activity were not due to disruption of the transmembrane sodium gradient, as Na^+-dependent alanine transport was unaffected by dynasore treatment (Fig. 4.1). PMA treatment alone significantly decreased DAT activity (33.2% compared to Veh) and dynasore pre-treatment did not block PKC-stimulated DAT downregulation (33.2% PMA vs 23.1% Dyn/PMA) (Fig. 4.1).

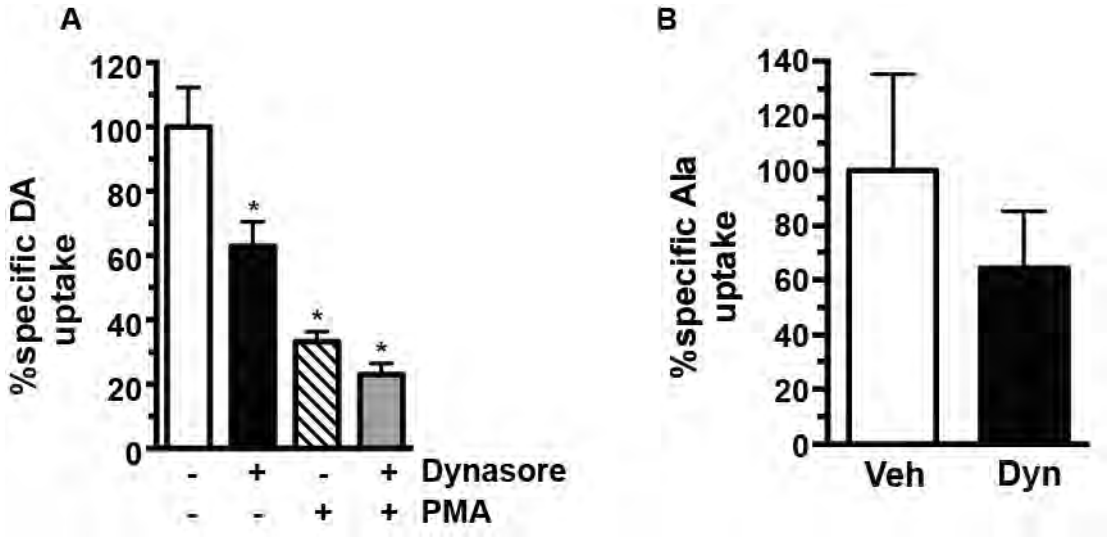

FIGURE 4.1: Dynamin Inhibition Reduces DAT Activity but Does Not Block PKC-Mediated DAT Downregulation in PC12 Cells: Uptake assays following dynasore treatment in DAT-PC12 cells. DAT-PC12 cells were treated ± 80 μM dynasore (Dyn), 30 min, 37°C followed by ± 1 μM PMA, 30 min, 37°C and DAT function and surface levels were measured by [^{3}H]dopamine uptake assay as described in *Methods*. (A) Data are expressed as % of vehicle specific DA uptake ±S.E.M. *p<0.002, (one way ANOVA with Bonferroni's post-hoc test, n=9 (Veh and Dynasore) or n=6 (PMA and Dynasore/PMA). (B) Data are expressed as % of vehicle specific alanine uptake ±S.E.M, p=0.45 (Student's t test, n=3).

Dynamin inhibition decreases DAT surface levels

To test whether dynasore-mediated losses in DAT function were due to losses in DAT surface protein, we treated DAT-PC12 cells ±80 μM dynasore, 30 min, 37°C and measured DAT surface levels using surface biotinylation. As can be seen in Figure 4.2, at steady state, there was 25.5 ± 1.0% of DAT on the surface. Dynasore treatment significantly reduced DAT surface levels to 14.5 ± 2.9% (Fig 4.2). To test for dynasore-mediated off-target effects we used dynole 34-2, which has a higher affinity (10 μM vs 80 μM) and acts allosterically to inhibit dynamin, whereas dynasore is a competitive inhibitor at dynamin's GTP binding site. As dynole 34-2 has not been extensively characterized, we tested if this inhibitor effectively blocked transferrin receptor (TfR) internalization, a dynamin-dependent endocytic event. We treated PC12 cells with 10 μM dynole for 30 min at 37°C and measured fluorescent transferrin internalization (a marker for TfR endocytosis). In vehicle-treated cells, transferrin was internalized and found in internal puncta, which is indicative of normal endocytosis. However, in dynole treated cells there was no visible puncta, consistent with a TfR endocytic blockade (Fig. 4.3). To measure DAT surface levels, we performed surface biotinylation on DAT-PC12 cells. Following 10 μM dynole treatment, DAT surface levels significantly decreased to 15.8 ± 0.9%. Additionally, we determined if PKC-mediated surface losses were dynamin dependent. Following 1 μM PMA treatment for 30 minutes at 37°C, DAT surface levels were significantly decreased from Veh (10.3 ± 1.3% compared to 25.5 ± 1.0%), as has been shown previously (Fig. 4.2). Moreover,

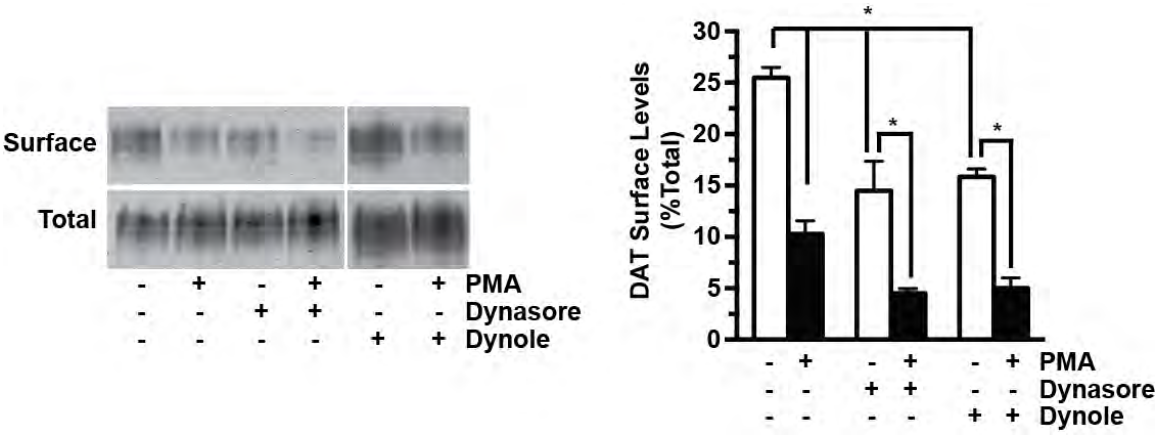

FIGURE 4.2: PKC-mediated DAT Internalization is Dynamin Independent in DAT-PC12 Cells: Surface biotinylations following dynasore treatment in DAT PC12 cells. DAT-PC12 cells were treated ± 80 µM dynasore or 10 µM dynole for 30 min at 37°C followed by ± 1 µM PMA for 30 minutes at 37°C and DAT and surface levels were measured by and surface biotinylation, as described in *Methods*. Left: Surface biotinylation - representative immunoblot. Right: Averaged data. Data are expressed as %vehicle surface DAT levels ± S.E.M. *p<0.001, (one way ANOVA with Bonferonni's post-hoc test, n=3-4).

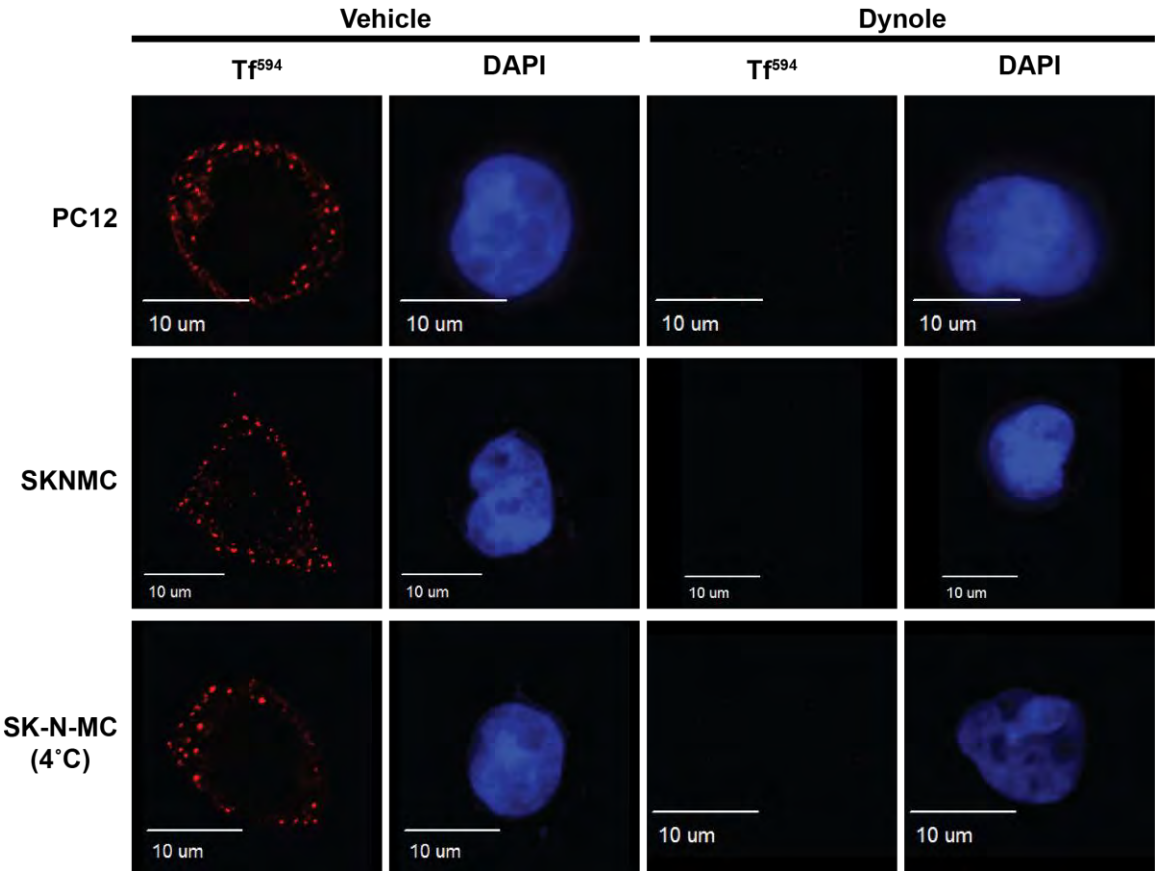

FIGURE 4.3: Dynole treatment blocks transferrin receptor internalization: DAT-PC12 and DAT-SK-N-MC were treated with 10 μM dynole for 30 minutes at 37°C (top and middle rows) or treated with 10 μM dynole for 20 minutes at 37°C (bottom row) followed by incubation at 4°C for 60 minutes and transferrin receptor internalization was measured and visualized as described in *Methods*.

both dynasore and dynole treatment did not block the PKC-mediated DAT internalization (Dynole: 15.8 ± 0.8% compared to 5.0 ± 1.0%; Dynasore: 14.5 ± 2.9% compared 4.5 ± 0.5%) (Fig 4.2). These data suggest that, in PC12 cells, PKC-mediated DAT internalization is dynamin–independent.

To test whether DAT surface losses in response to dynamin inhibition were dependent on cellular context, we also tested the effect of dynasore in the dopaminergic neuroblastoma cell line SK-N-MC, stably transfected with DAT (DAT-SK-N-MC). Similar to results observed in DAT-PC12 cells, 80 μM dynasore treatment, 30 min, 37°C significantly decreased surface DAT to 77.0 ± 5.6% control levels (Fig. 4.4). To assure that effects on DAT surface levels were not due to possible off-target dynasore effects, we also tested dynole 34-2, and its inactive analog dynole 31-2. Similar to our results with dynasore, 10 μM dynole treatment, 30 min, 37°C significantly decreased DAT surface levels to 68.0 ± 6.8**%** of vehicle-treated cells, whereas dynole 31-2 had no significant effect on DAT surface levels (97.6 ± 8.4% of control; (Fig 4.4). To test if PKC-mediated surface losses were dynamin dependent, DAT-SK-N-MC cells were pretreated ± 10 μM dynole, 30 min, 37°C followed by PKC activation with 1μM PMA, 30 min, 37°C. PKC activation induced a significant decrease in DAT surface levels following vehicle pretreatment to 78.6 ± 6.0% of control levels. In contrast, dynole pretreatment completely blocked any additional PKC-mediate DAT surface losses (68.0 ± 6.8% versus 69.8 ± 3.8%; Fig. 4.4). In order to assess cell permeability to the biotinylation reagent,

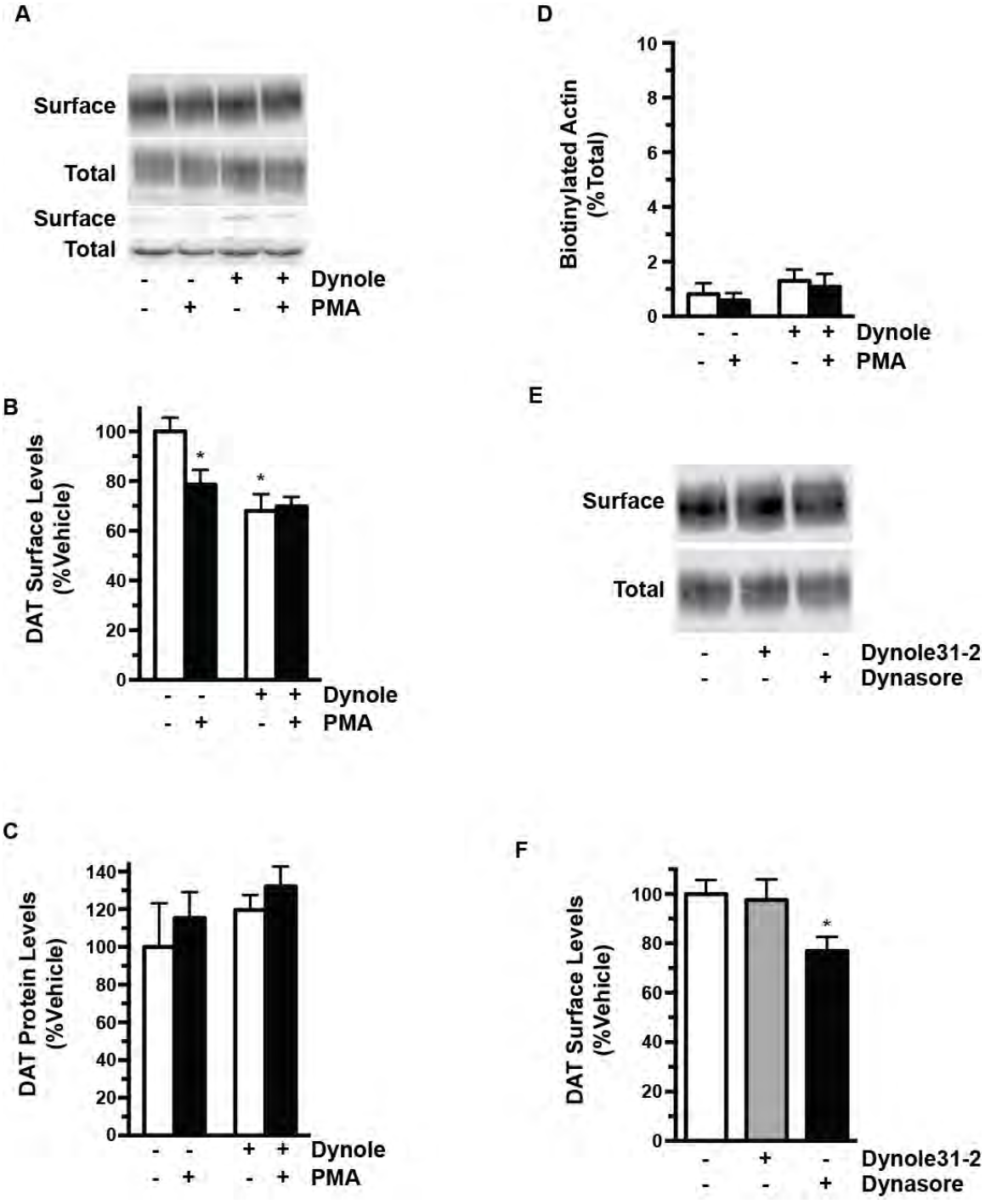
A
Surface
Total
Surface
Total
- - + + Dynole
- + - + PMA
B
DAT Surface Levels (%Vehicle)
100
80
60
40
20
0
*
*
- - + + Dynole
- + - + PMA
C
DAT Protein Levels (%Vehicle)
140
120
100
80
60
40
20
0
- - + + Dynole
- + - + PMA
D
Biotinylated Actin (%Total)
10
8
6
4
2
0
- - + + Dynole
- + - + PMA
E
Surface
Total
- + - Dynole31-2
- - + Dynasore
F
DAT Surface Levels (%Vehicle)
100
80
60
40
20
0
*
- + - Dynole31-2
- - + Dynasore

FIGURE 4.4: Dynamin Inhibition Reduces DAT Surface Levels in DAT SK-N-MC Cells: *Surface biotinylation studies*: (A-D) DAT-SK-N-MC cells were treated ± 10 μM dynole for 30 minutes at 37°C followed by treatment ± 1 μM PMA for 30 minutes at 37°C or were treated 10 μM dynole 31-2 or 80 μM dynasore for 30 minutes at 37°C and DAT surface levels were measured by surface biotinylation, as described in *Methods*. (A) 10 μM dynole, representative blot. (B) 10 μM dynole, averaged data: DAT surface levels: Data are expressed as %vehicle surface DAT levels ±S.E.M. *Significantly different than vehicle, one-way ANOVA with Bonferonni's post hoc test, $p<0.002$, $n=8$. (C) Total DAT protein: Data are expressed as %vehicle total DAT levels ±S.E.M. $p=0.51$, (one way ANOVA with Bonferonni's post-hoc test, $n=5$). (D) Biotinylated actin levels: Data are expressed as %biotinylated actin of total actin ±S.E.M $p=0.62$, (one way ANOVA with Bonferonni's post-hoc test, $n=5$). (E) 80 μM dynasore and 10 μM dynole 31-2, representative immunoblot. (F) 80 μM dynasore and 10 μM dynole 31-2, averaged data: DAT surface levels: Data are expressed as %vehicle surface DAT levels ±S.E.M. *Significantly different than vehicle, one-way ANOVA with Bonferonni's post hoc test, $p<0.05$, $n=8$.

we measured the biotinylated actin population. We saw low levels of biotinylated actin (~1.0%) across all experimental conditions indicating that the SK-N-MC cells were intact and that trafficking could occur normally (Fig. 4.4). Previous reports have indicated that internalized DAT is targeted for degradation (Miranda et al., 2005). To test if this was occurring in SK-N-MC cells, we compared the total DAT levels across experimental conditions. Total DAT protein was not significantly different following either dynole (119.6 ± 7.9% vehicle levels) or PMA (115.4 ± 13.6% vehicle levels) treatments over the experimental time-course (Fig. 4.4). The conflicting results between PC12 and SK-N-MC cells prompted us to ask whether dynamin was required for basal and PKC-stimulated DAT trafficking in a native preparation.

The incongruity in the results regarding dynamin's role in DAT trafficking between these two cell lines prompted us to develop a new tool to ask these questions about dynamin's role in DAT trafficking. Consequently, we performed surface biotinylation on acute mouse striatal slices, a highly enriched dopaminergic terminal region. As can be seen in Figure 4.5, we detected robust DAT surface expression in the striatum (43.7 ± 3.8% total DAT on the surface) under vehicle-treated conditions. PKC activation with 1 μM PMA, 30 min, 37°C significantly decreased DAT surface levels to 77.3 ± 3.6% compared to Veh). In slices treated with 10μM dynole, 30 min, 37°C, we observed a significant reduction in DAT surface levels (80.7 ± 4.6% compared to Veh). Dynole pretreatment completely

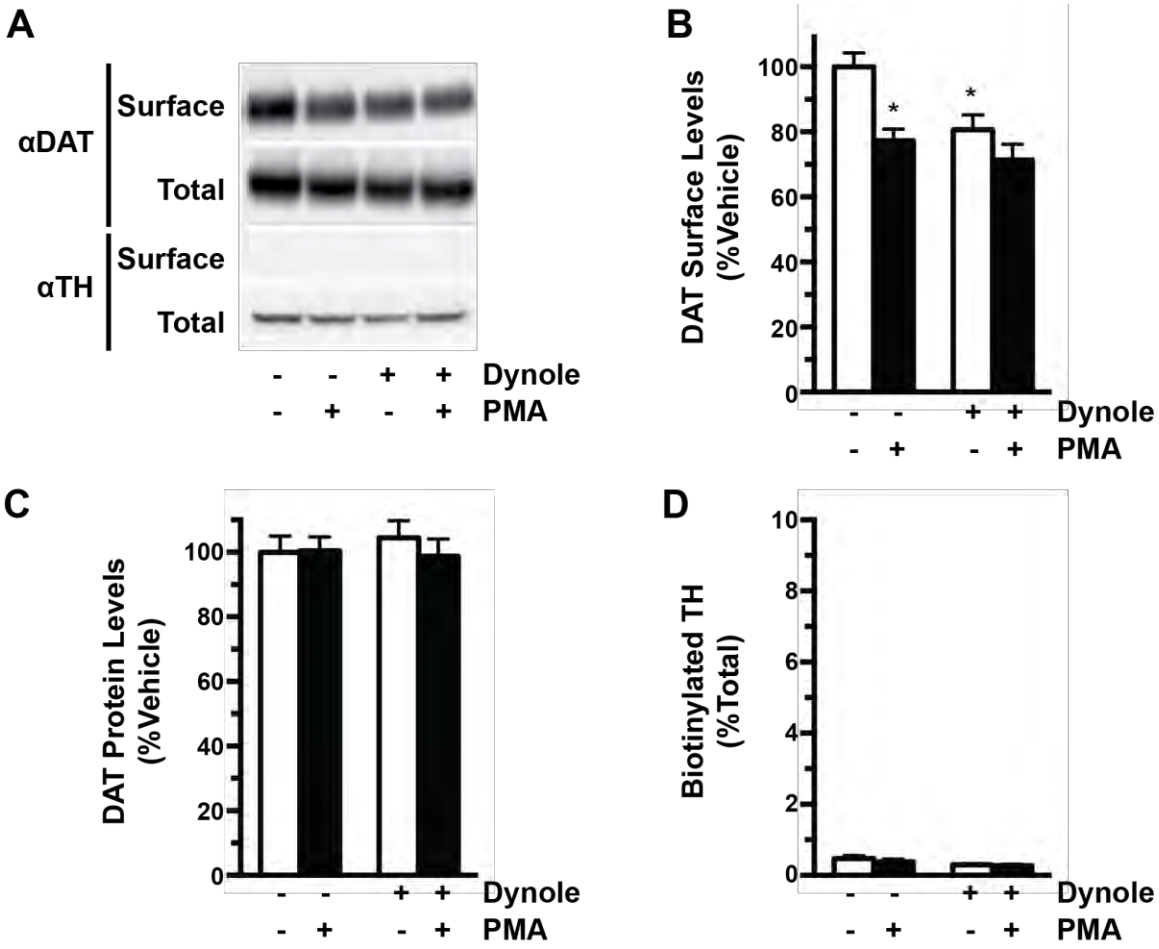

FIGURE 4.5: Dynamin Inhibition Reduces DAT Surface Levels and Blocks PKC-Stimulated DAT Internalization in Acute Mouse Striatal Slice: Surface biotinylation following dynole treatment in mouse striatal slices. Slices were treated ± 10 μM dynole for 30 minutes at 37°C followed by treatment ± 1 μM PMA for 30 mintues at 37°C and DAT surface levels were measured by surface biotinylation, as described in *Methods*. (A) Surface biotinylation – Representative immunoblot. (B) Averaged data: DAT surface levels: Data are expressed as %vehicle surface DAT levels ±S.E.M. *Significantly different than vehicle, one-way ANOVA with Tukey's post hoc analysis, $p<0.001$, n=12. (C) Total DAT protein: Data are expressed as %vehicle total DAT levels ±S.E.M. $p=0.87$, (one way ANOVA with Bonferonni's post-hoc test, n=12). (D) Biotinylated TH levels: Data are expressed as %biotinylated TH of total TH ±S.E.M $p=0.13$, (one way ANOVA with Bonferonni's post-hoc test, n=12).

abolished further PMA stimulated losses (80.7 ± 4.6% vs 71.4 ± 4.3%). To test the slice integrity and assure that the biotinylation reagent did not gain access to intraceullar proteins in dopaminergic neurons, we immunoblotted for tyrosine hydroxylase (TH) in parallel. Biotinylated TH levels averaged ~0.4% (Fig. 4.5), consistent with the striatal slices being intact and the assay reflecting accurate DAT surface measurements. To test whether dynyamin inhibition or PKC activation target DAT for degradation in the striatal slices, we compared the total DAT levels across experimental conditions. Total DAT protein was not significantly different following either dynole (104 ± 5.3% vehicle levels) or PMA (100.4 ± 4.3% vehicle levels) treatments over the experimental time-course (Fig. 4.5). Thus, we conclude that 1) DAT traffics in SK-N-MC cells similarly to that observed in mouse striatum and 2) the surface loss seen during PKC activation and dynamin inhibition was the same magnitude.

Recycling blockade reveals DAT is in two surface pools

The observed DAT surface losses in SK-N-MC cells and striatal slices in response to dynamin inhibition suggest that dynamin is not required for basal DAT internalization, but may be required for PKC-stimulated DAT surface losses. Another possible interpretation is that there is a finite pool of endocytic-competent DAT in SK-N-MC cells and adult dopaminergic neurons that was depleted during the dynole treatment, and that the remaining DAT surface pool is endocytic-incompetent and therefore unable to internalize following PKC activation. To

distinguish between these possibilities, we used two independent approaches to deplete surface DAT by blocking endocytic recycling in DAT-SK-N-MC cells: Monensin treatment, which blocks the vacuolar H^+ ATPase, and 18°C temperature blockade, which we previously demonstrated blocks DAT endocytic recycling (Loder & Melikian, 2003). To test whether the DAT pool that was resistant to basal internalization had the capacity to internalize in response to PKC activation, we initially depleted surface DAT in striatal slices by blocking endosomal recycling by treatment with the ionophore, monensin. Monensin is a Na^+/H^+ antiporter inhibitor whose action has been shown to block DAT recycling back to the plasma membrane (Sorkina et al., 2005). We reasoned that if all surface DAT is endocytic competent, we would expect continual surface DAT losses over time, whereas if there is an endocytic-incompetent pool we would expect initial surface losses that plateau over time. Treatment with 25 μM monensin, 37°C resulted in an initial surface DAT loss that plateaued by 60 min (Fig 4.6). To test whether monensin was effectively blocking endocytic recycling in our hands, we used a pulse-chase approach to measure TfR recycling in SK-N-MC cells. Cells were treated with 25 μM monensin for 60 minutes at 37°C to block endocytic recycling. A 5 min Tf-Alexa^{594} pulse, followed by a 20 min unlabeled Tf chase, was applied to the cells to monitor endocytic recycling, which would be detectable as an intracellular fluorescence loss following the Tf chase. In vehicle-treated cells, we observed robust Tf loading after 5 min that was completely chased from the cells. In contrast, monensin treatment markedly blocked recycling, indicated by the retention of

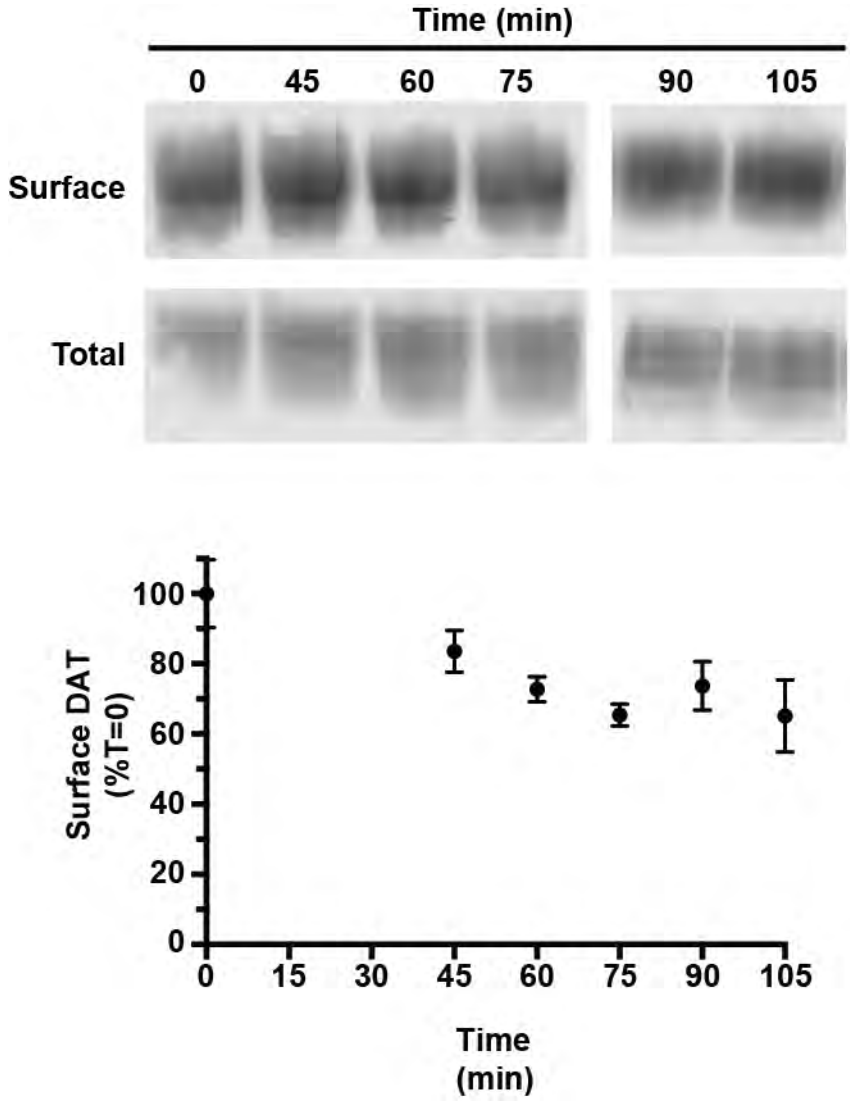

FIGURE 4.6: Monensin Treatment Blocks DAT Recycling: DAT-SK-N-MC were treated with 25 μM monensin for the indicated duration at 37°C. Surface DAT was measured by biotinylation as described in *Methods*. Top: Representative immunoblot. Bottom: Averaged data: DAT surface levels: data are expressed as %T=0 surface DAT ± S.E.M.

fluorescent transferrin (Fig. 4.7). Using these recycling block conditions, we depleted the trafficking-competent DAT surface pool and tested whether the remaining DAT surface population was capable of PKC-stimulated internalization. Mouse striatal slices were pretreated with either vehicle or 25 μM Monensin, 60 min, 37°C, followed by treatment with either vehicle or 1 μM PMA, 30 min, 37°C and surface biotinylation to measure DAT surface expression. Monensin treatment significantly reduced DAT surface levels to 73.1 ± 5.0% as compared to vehicle-treated slices, consistent with DAT surface depletion due to recycling blockade (Fig. 4.8). PKC activation significantly decreased DAT surface levels, and monensin pretreatment completely blocked further PKC-stimulated DAT surface losses (73.1 ± 5.0% compared to 63.2 ± 4.6%). These data support the hypothesis that surface DAT is segregated between trafficking-competent and –incompetent pools. Recycling blockade also did not target DAT to a degradative fate, as total DAT protein levels were unchanged over the course of the experiment for either monensin (92.3 ± 7.7% vehicle levels) or PMA (98.5 ± 5.5% vehicle levels) (Fig. 4.8). It should be noted that monensin treatment also increased neuronal permeability to the biotinylation reagent, as biotinylated TH levels were higher than those seen in the vehicle-treated slices (vehicle: 1.7 ± 0.3% vs. monensin: 8.5 ± 0.9%; Fig. 4.8).

To further test whether DAT was segregated between trafficking -competent and -incompetent surface pools, we performed 18°C recycling blockade in DAT-SK-N-

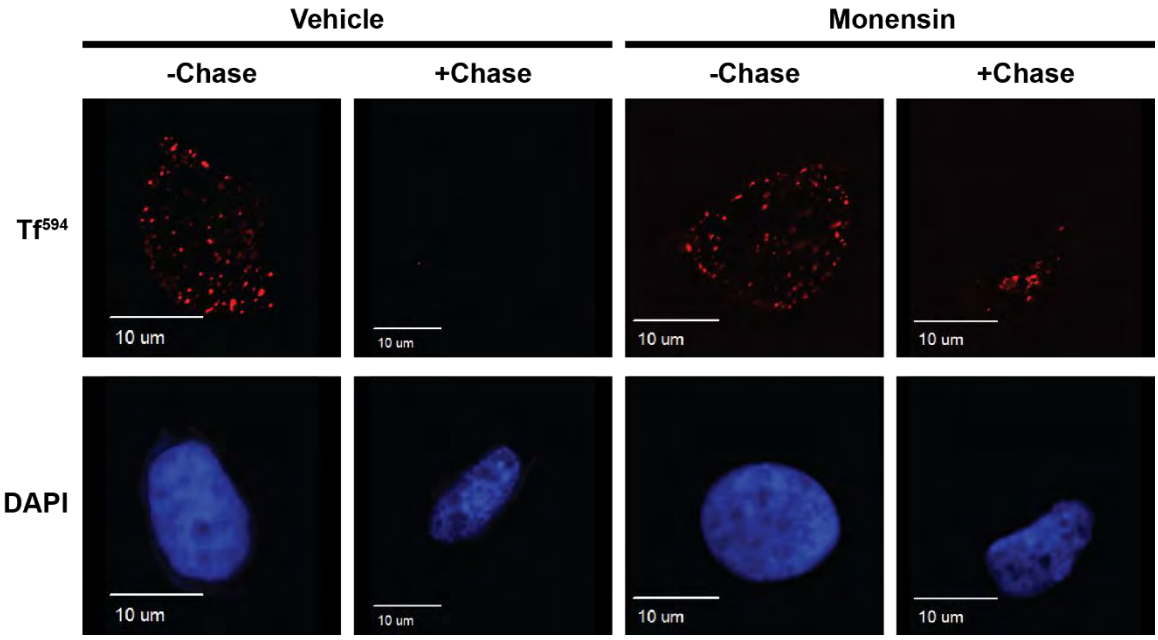

FIGURE 4.7: Monensin Treatment Blocks Transferrin Receptor Recycling: DAT-SK-N-MC were treated with 25 μM monensin for 60 minutes at 37°C and transferrin receptor (red) recycling was measured and visualized as described in *Methods*.

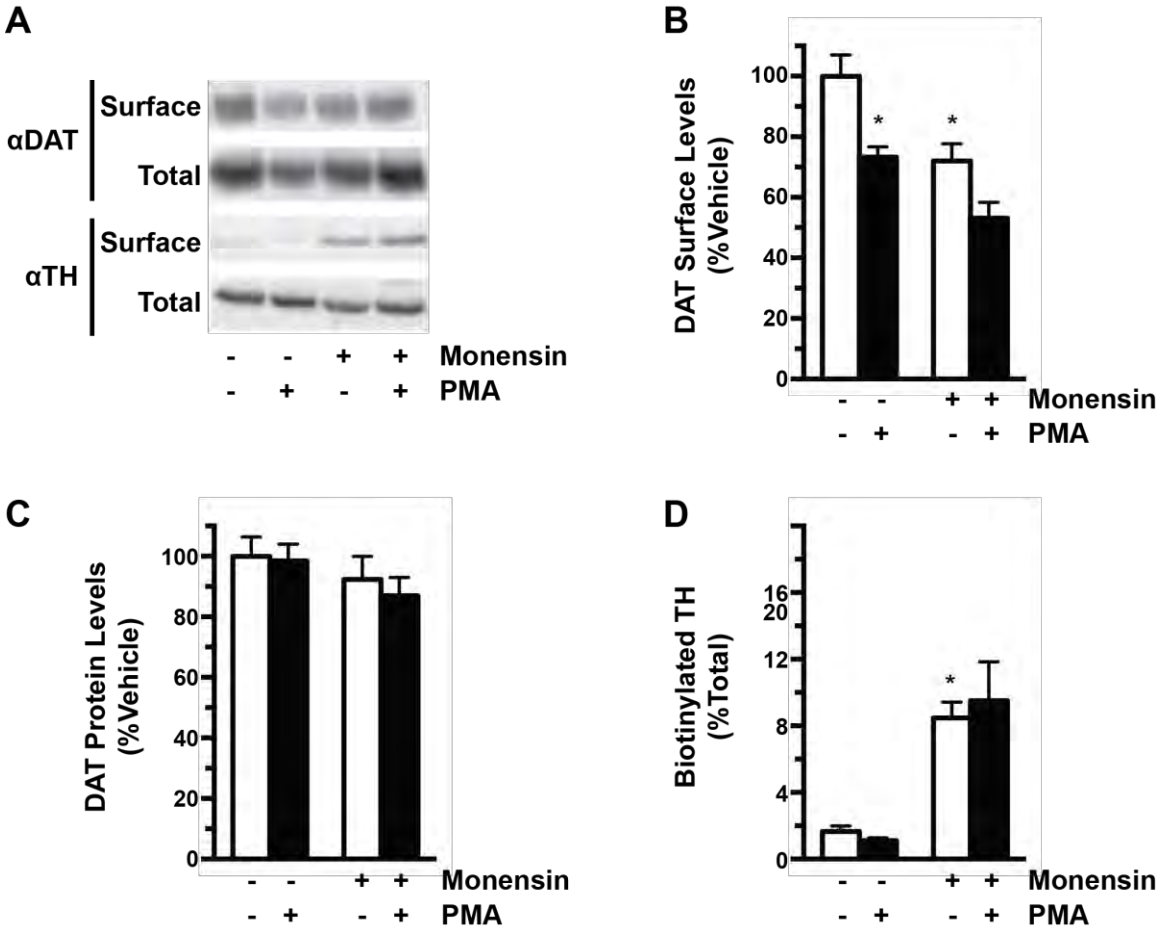

FIGURE 4.8: Recycling Blockade with Monensin Prevents PKC-Mediated DAT Internalization in acute mouse striatal slices. Surface biotinylations following recycling blockade with monensin treatment in mouse striatal slices. Slices were treated ± 25 μM monensin for 60 mintues at 37°C followed by treatment ± 1 μM PMA for 30 minutes at 37°C. DAT surface levels were measured by surface biotinylation, as described in *Methods*. (A) Surface biotinylation – mouse striatal slice - representative immunoblot. (B) Averaged data. Data are expressed as %vehicle surface DAT levels ±S.E.M, *p<0.0001. (one-way ANOVA with Bonferroni post hoc analysis, n=21). (C) Total DAT protein: Data are expressed as %vehicle DAT total levels ±S.E.M., p=0.46 (one-way ANOVA with Bonferroni post hoc analysis, n=21). (D) Biotinylated tyrosine hydroxylase levels: Data are expressed as %biotinylated TH of total TH ±S.E.M *p<0.001 (one-way ANOVA with Bonferroni post hoc analysis, n=21).

MC cells. DAT-SK-N-MC cells were incubated at 18°C for 45 minutes followed by treatment with 1 μM PMA for 45 minutes to activate PKC. As can be seen in Figure 4.9, DAT surface depletion using an 18°C recycling blockade also blocked PKC-regulated DAT surface loss (98.3 ± 9.4% vehicle levels), consistent with the existence of a trafficking-incompetent DAT surface pool. It is possible that a lack of PMA effect at 18°C was due to inability of PMA to activate PKC at 18°C. To control for this possibility we tested whether PMA could drive DAT internalization at 18°C in DAT-PC12 cells, which did not exhibit a trafficking incompetent DAT pool (see Fig. 4.2). As can be seen in Figure 4.10, PKC activation at 18°C decreased DAT surface levels (47.1 ± 9.4% vehicle levels) in DAT-PC12 cells, demonstrating PMA activity at 18°C and that lack of PMA-induced DAT internalization following 18°C recycling blockade was not due to lack of PKC activation.

DAT internalization does not require dynamin

Since trafficking-competent DAT was fully depleted during the course of our dynole treatment, we were not able to address whether PKC-mediated DAT internalization is dynamin-dependent. In order to test whether PKC-mediated DAT internalization is dynamin dependent, we used reversible biotinylation to directly measure basal and PKC-stimulated DAT internalization rates during dynole treatment in DAT-SK-N-MC cells. In order to assure that dynole incubations were sufficiently long to impact dynamin-dependent endocytosis, but not so long as to deplete the

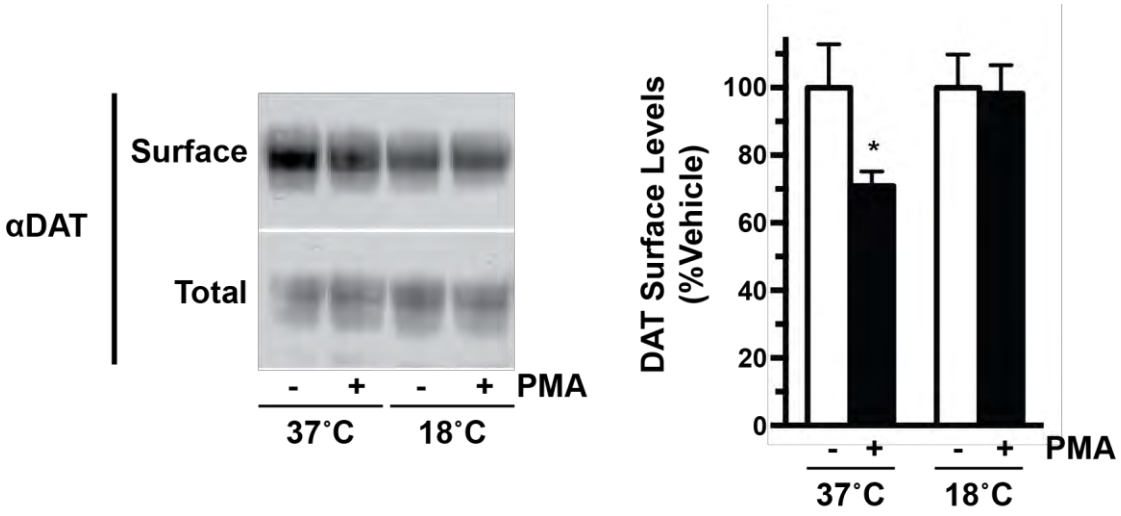

FIGURE 4.9: Recycling Blockade by 18°C Incubation Prevents PKC-mediated DAT Internalization in DAT-SK-N-MC Cells: Surface biotinylations following recycling blockade with 18°C incubation of neuroblastoma SK-N-MC cells. DAT-SK-N-MC cells were incubated at 18°C or 37°C for 45 minutes followed by treatment ± 1 μM PMA for 45 minutes at 18°C. DAT surface levels were measured by surface biotinylation, as described in *Methods*. Left: representative immunoblot. Right: Averaged data. Data are expressed as %vehicle surface DAT levels ±S.E.M. *Significantly different than vehicle, *p<.03, (Student's t test, n=12 (37°C) and n=15 (18°C)).

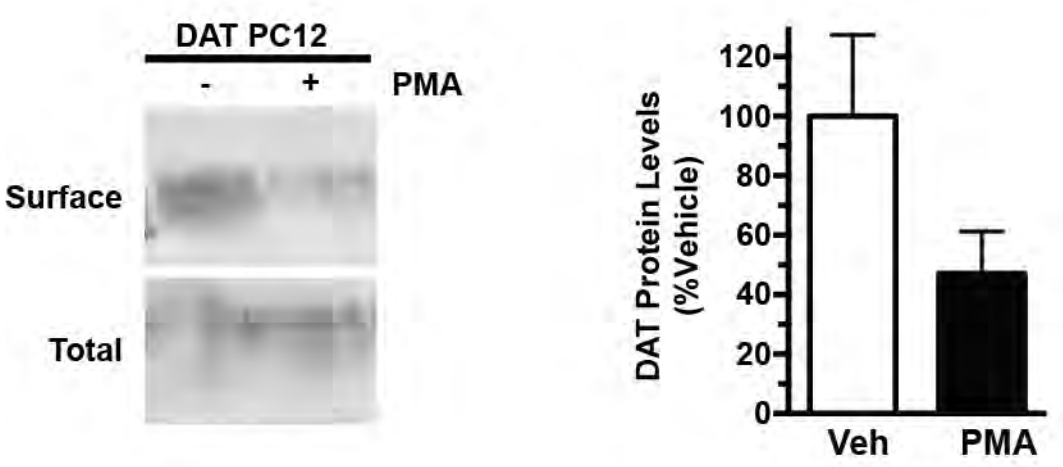

FIGURE 4.10: PMA Decreases DAT Surface Expression at 18°C in DAT-PC12 cells: DAT-PC12 cells were treated with 1 **µ**M PMA for 45 minutes at 18°C. DAT surface levels were measured by surface biotinylation as described in *Methods*. Left: Representative immunoblot. Right: Averaged Data: Data are expressed as %vehicle surface DAT levels ±S.E.M. p=0.14, (Student's t test, n=4).

trafficking competent DAT pool, we developed an altered internalization protocol in which cells were treated with dynole for 20 min, 37°C prior to biotinylating. This short dynole pre-incubation was sufficient to block dynamin-dependent TfR internalization (Fig. 4.3). Using the reversible biotinylation protocol, we directly measured DAT internalization rates in DAT-SK-N-MC cells following this short dynole pre-incubation. Under control conditions, dynole had no significant effect on DAT internalization (68.8 ± 9.3% of Veh; Fig 4.11), consistent with the hypothesis that constitutive DAT trafficking is dynamin independent. PKC activation with 1 μM PMA increased DAT internalization rates to 179.1 ± 20.5% of Veh), but did not increase DAT internalization in dynole-treated cells (68.8 ± 9.3% compared 71.4 ± 11.6% if Veh). These results demonstrate that constitutive DAT internalization is dynamin-independent, but that dynamin is required for PKC-stimulation of DAT internalization rates. These results further suggest that dynamin is required for DAT endocytic recycling back to the plasma membrane, and that dynole treatment depleted DAT surface levels by imposing a recycling blockade.

Dynamin regulates DAT trafficking via an actin-dependent mechanism

Given that DAT recycling appeared dynamin-dependent, we next aimed to test what mechanisms were facilitating dynamin-dependent DAT recycling. The cytoskeletal protein actin is known to regulate protein trafficking (Swiatecka-Urban et al., 2002) and dynamin has been shown to be required for small actin stress

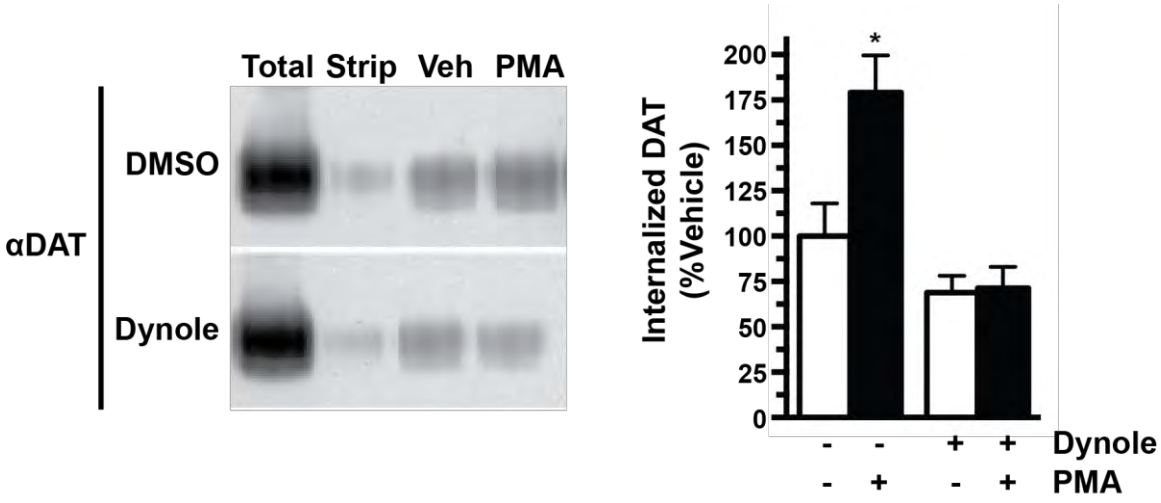

FIGURE 4.11: Dynamin is Required for PKC-mediated DAT Internalization but Not Constitutive Endocytosis: Internalization assay following dynole-treated DAT-SK-N-MC cells. Cells were treated ± 10 μM dynole, 20 min, 37°C, then biotinylated at 4°C, followed by ± 1 μM PMA, ± 10 μM dynole for 10 min at 37°C. Left: Internalization assay – representative immunoblot of internalized DAT. Right: Averaged data. Data are expressed as %vehicle surface DAT levels ±S.E.M. * $p<0.001$ (one-way ANOVA with Bonferroni post hoc analysis, n=4)

fibre polymerization (Cao, Deacon, Reczek, Bretscher, & von Zastrow, 1999; Mooren, Kotova, Moore, & Schafer, 2009), making this protein a likely candidate in the DAT trafficking mechanism. To test a putative role for actin in dynamin-dependent DAT endocytic recycling, we disrupted the actin cytoskeleton with cytochalasin D in mouse striatal slices and tested whether DAT surface levels were sensitive to dynole. Slices were pretreated with either vehicle or 0.2 µg/mL cytochalasin D (CytoD), 30 min, 37°C, followed by treatment with either vehicle or 10 µM dynole, 30 min, 37°C. CytoD treatment alone significantly reduced DAT surface levels (69.9 ± 5.1% compared to Veh; Fig. 4.12), consistent with a role for actin in DAT endocytic trafficking. As previously described (Fig. 4.5), dynole treatment significantly reduce DAT surface levels to 67.2 ± 5.0% vehicle levels, and pretreatment with CytoD completely blocked further dynole-mediated DAT surface losses (67.2 ± 5.0% compared to 66.6 ± 7.0% of Veh; Fig. 4.12). CytoD treatment had no effect on slice permeability to the biotinylation reagent, as seen in immunoblots probed for TH in parallel (Fig. 4.12). CytoD treatment also did not target DAT to a degradative fate, as total DAT protein levels were unchanged over the course of the experiment for CytoD (91.7 ± 10.1% vehicle levels) (Fig. 4.12). To test whether CytoD treatment globally effected endocytic trafficking, we measured TfR surface levels in the mouse striatal slices. Using surface biotinylation, we observed no detectable differences in surface TfR levels (118 ± 12.6% compare to Veh; Fig. 4.12) demonstrating that CytoD treatment did not globally reduce surface protein levels.

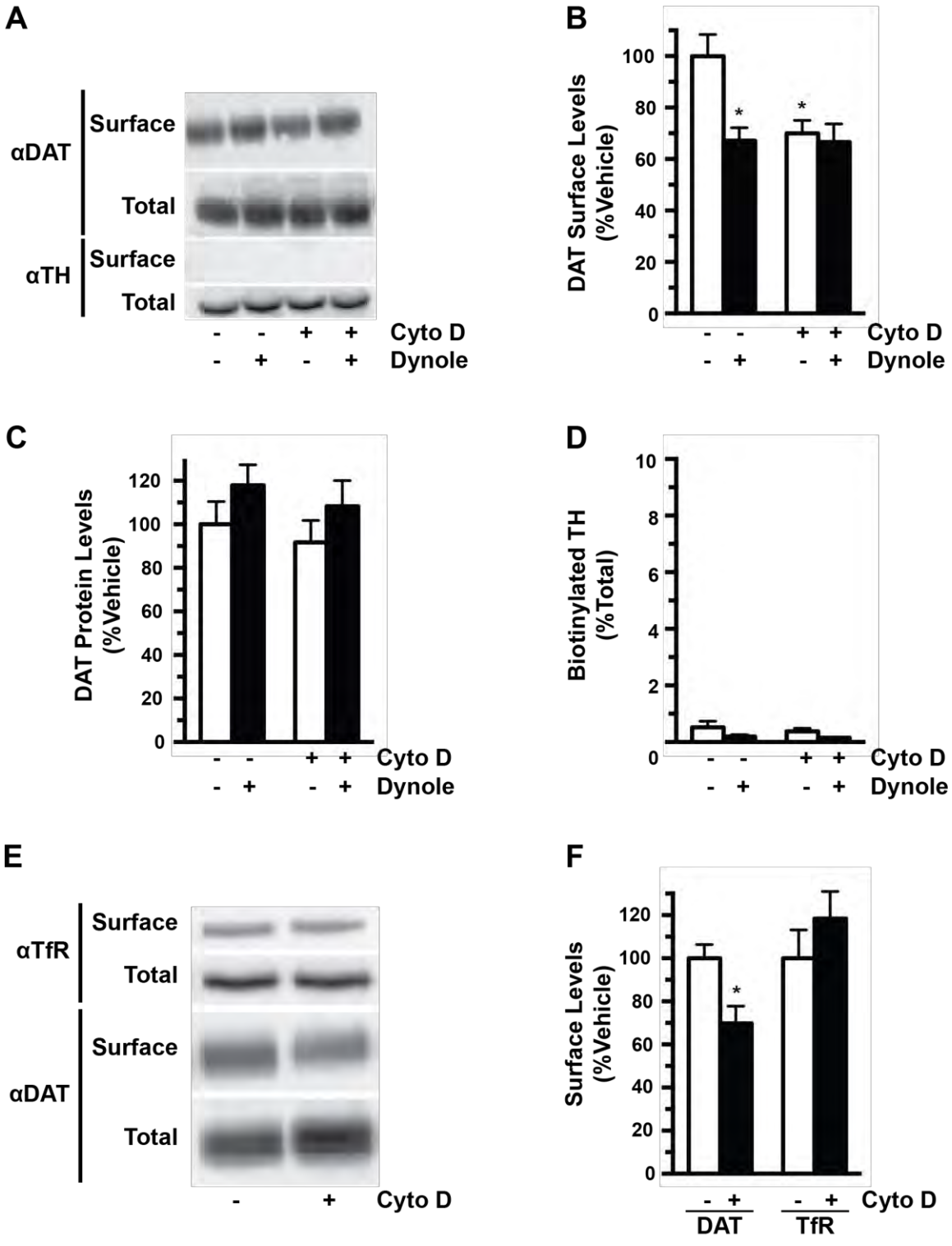
A
αDAT
Surface
Total
αTH
Surface
Total
- - + + Cyto D
- + - + Dynole
B
DAT Surface Levels (%Vehicle)
100
80
60
40
20
0
*
*
- - + + Cyto D
- + - + Dynole
C
DAT Protein Levels (%Vehicle)
120
100
80
60
40
20
0
- - + + Cyto D
- + - + Dynole
D
Biotinylated TH (%Total)
10
8
6
4
2
0
- - + + Cyto D
- + - + Dynole
E
αTfR
Surface
Total
αDAT
Surface
Total
- + Cyto D
F
Surface Levels (%Vehicle)
120
100
80
60
40
20
0
*
- + - + Cyto D
DAT
TfR

FIGURE 4.12: DAT Plasma Membrane Recycling Requires Dynamin via an Actin-Dependent Mechanism: Surface biotinylations following cytochalasin D (Cyto D) treatment mouse striatal slices. (A-D) Slices were treated ± 0.2 ug/mL cytochalasin D for 30 minutes at 37°C followed by treatment ± 10 μM dynole for 30 minutes at 37°C and DAT surface levels were measured by surface biotinylation, as described in *Methods*. (E-F) Slices were treated ± 0.2 ug/mL cytochalasin D for 30 minutes at 37°C and TfR and DAT surface levels were measured by surface biotinylation. (A) Surface biotinylation – Representative immunoblot. (B) Averaged data. Data are expressed as %vehicle surface DAT levels ±S.E.M. *$p<0.004$ (one-way ANOVA with Bonferroni's post hoc analysis, $p<0.004$, n=7). (C) Total DAT protein: Data are expressed as %vehicle total DAT levels ±S.E.M. $p=0.35$, (one way ANOVA with Bonferonni's post-hoc test, n=7). (D) Biotinylated TH levels: Data are expressed as %biotinylated TH of total TH ±S.E.M $p=0.18$, (one way ANOVA with Bonferonni's post-hoc test, n=7). (E) Surface biotinylation – Representative immunoblot. (F) Averaged data. Data are expressed as %vehicle surface DAT or %vehicle surface TfR levels ±S.E.M. DAT: *$p<0.02$ (Student's *t* test, n=6) and TfR: $p=0.34$ (Student's *t* test, n=6).

DISCUSSION

Dopamine transporter activity is the major mechanism mediating synaptic dopamine clearance and signal latency (Giros et al., 1996). Membrane trafficking constitutes an important role in regulating transporter function. Recent studies indicate that DAT trafficking requires the classical endocytic molecules clathrin and dynamin (Eriksen et al., 2009; Sorkina et al., 2005). These studies depended on chronic trafficking perturbation through shRNA-mediated knockdown or co-expression of dominant negative mutant proteins, as well as heterologous cell expression or cultured dopaminergic neurons. We took advantage of newly developed pharmacological dynamin inhibitors acutely to block dynamin function and test whether DAT trafficking is dynamin-dependent in mouse striatal slices. Our results clearly demonstrate a differential dependence on dynamin for endocytic recycling and PKC-mediated DAT internalization, but not for constitutive DAT endocytosis (Fig. 4.5).

Using the pharmacological dynamin inhibitor, we teased out dynamin's role in DAT trafficking at presynaptic termini, which is the site for DAT regulation in neurotransmitter clearance. We show that dynamin is not required for constitutive DAT internalization (Fig. 4.11), as dynole treatment did not alter basal DAT internalization rates. In contrast, PKC-mediated DAT internalization is strictly dynamin-dependent. There have been other reports demonstrating that DAT endocytosis may not require dynamin. The membrane raft associated protein

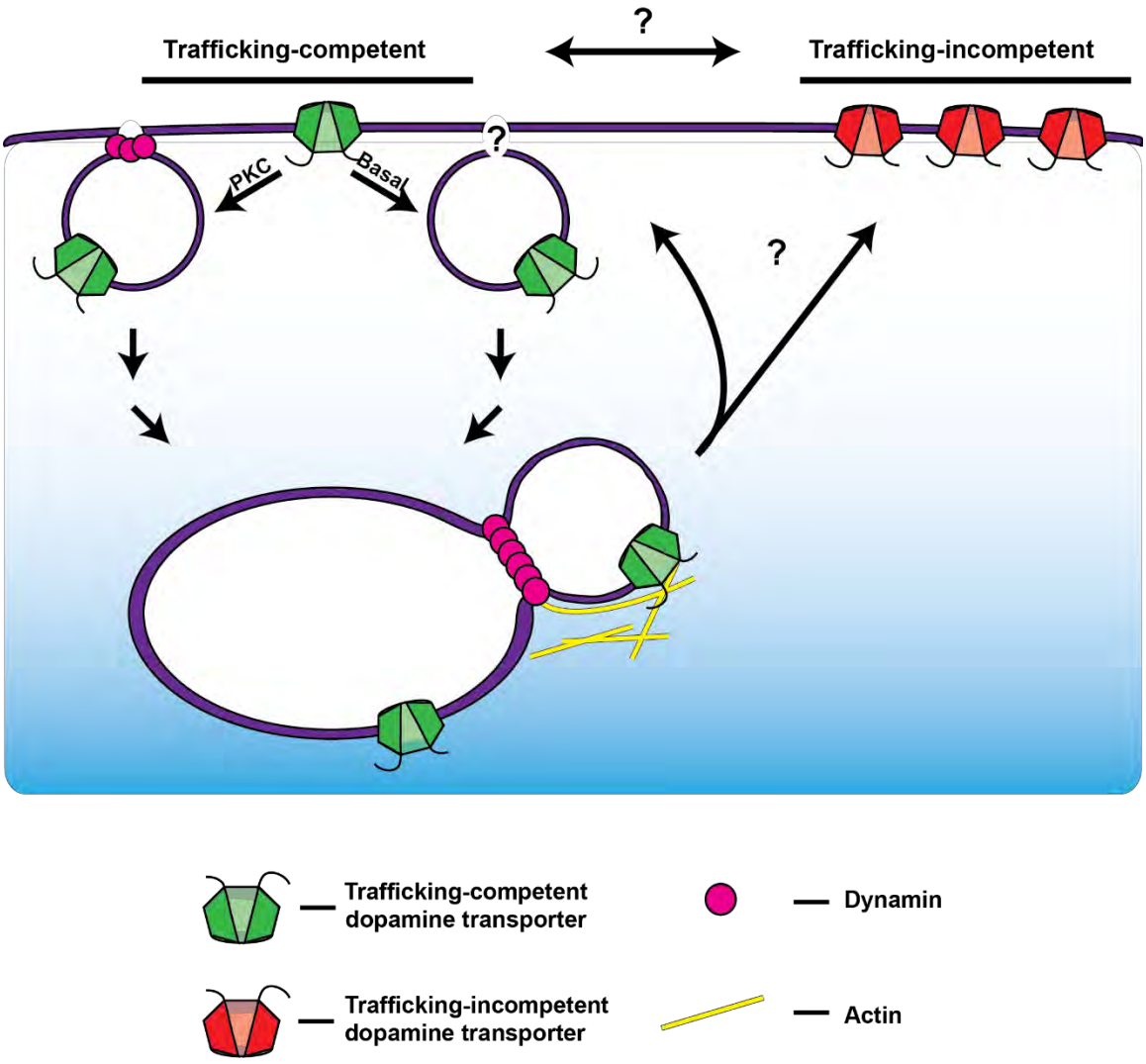

FIGURE 4.13: DAT is Segregated Between Trafficking-Competent and –Incompetent Pools at the Surface: DAT Trafficking model. Surface DAT is segregated between two surface pools: trafficking-competent and -incompetent. Basal DAT internalization occurs via a dynamin-independent mechanism whereas PKC mediated DAT trafficking occurs via a dynamin-dependent mechanism. DAT recycling back to the plasma membrane is dynamin and actin dependent.

flotillin-1 has been shown to be required for PKC-mediated DAT trafficking (Cremona et al., 2011). The role for dynamin in that process was not specifically explored, but trafficking from lipid rafts has been shown to be both dynamin dependent and independent. Furthermore, DAT internalization is regulated by presynaptic D_2 receptors, where receptor activation ultimately elicits decreased DAT surface levels, as well as D_2 trafficking (Lee et al., 2007). D_2 receptor trafficking has been shown to be insensitive to dynamin inhibition (Kotowski, Hopf, Seif, Bonci, & von Zastrow, 2011; Vickery & von Zastrow, 1999). Since DAT and D_2 interact, this raises the possibility that they are co-trafficking via a dynamin-independent mechanism into endosomal compartments.

Interestingly, we see that surface resident DAT is not present in a uniform pool, but rather two pools: one of which undergoes constitutive and PKC-mediated trafficking and one which does not respond to either of these two regulatory events (Fig. 4.8). A previous study from Foster and associates reported that DAT is segregated between lipid raft and non-raft domains at the cell surface (Foster et al., 2008), raising the possibility that either raft or non-raft microdomains may facilitate trafficking competent and incompetent DAT populations. Additionally, a DAT trafficking mutant, R615C, found in an ADHD patient, has been shown to constitutively internalize at a higher rate and is found in a different distribution compared to wild-type between raft and non-raft membrane domains at the surface (Sakrikar et al., 2012). Future work measuring DAT trafficking specifically from

these two membrane domains will be informative regarding if this is the segregation is used to delineate trafficking requirements.

Conflicting results have been reported regarding DAT's endocytic fate during basal and PKC-stimulated internalization, both in neurons and heterologous expression systems. Previous reports show that DAT ubiquitylation is required for PKC-mediated DAT trafficking (Miranda et al., 2005). This post-translational modification is then required for DAT degradation, as mutations in N-terminal lysines prevent ubiquitylation and slow DAT turnover (Vina-Vilaseca & Sorkin, 2010). These studies were done in heterologous cells treated with PMA for 1-2 hours, potentially masking DAT fate as this does not likely reflect physiologically relevant stimuli. Additionally, work done in the Gether lab in cultured dopaminergic neurons reports that internalized DAT preferentially sorts to Rab7-positive endosomes, indicating a predominantly degradative fate (Eriksen et al., 2009). This study tracked a fluorescent cocaine analog bound to DAT to test internalization and endosomal sorting. Persistent ligand binding has been reported to alter DAT endocytic fate, tempering the interpretation for this result (Daws et al., 2002). Moreover, DAT trafficking was PMA-insensitive and no DAT recycling was observed, inconsistent with our results in the striatal slice as well as DAT trafficking studies in heterologous cells. We observe DAT surface losses in dynole-treated slices, consistent with a role for dynamin in constitutive DAT recycling, and DAT was not significantly degraded over the experimental time-course (Fig. 4.5).

DAT has been described to constitutively recycle to the plasma membrane and co-localize in Rab11 endosomal compartments in heterologous cells (Furman, Lo, et al., 2009). We show for the first time that DAT recycles in striatal presynaptic termini (Fig. 4.8). Recent work has shown that D_2 activation will cause a rapidly observed increase in DAT surface levels in striatal synaptosomes followed by the aforementioned DAT surface reduction (Chen et al., 2013). This rapid release to increase surface expression is reminiscent of the regulated recycling seen in the glucose transporter GLUT4. There, insulin signaling will elicit an Akt-mediated cascade releasing GLUT4-positive endosomes to fuse at the cell surface, rapidly increasing glucose uptake in response food intake (Foley, Boguslavsky, & Klip, 2011). Insulin treatment also acutely increases DAT activity and increases transporter suface expression through PI3K signaling (Carvelli et al., 2002). AMPH will also cause a rapidly observed increase in DAT surface levels followed by a slower occurring reduction in surface DAT (Chen et al., 2009). Moreover, AMPH-induced DAT trafficking is correlated with decreased Akt activity via a CaMKII-dependent pathway and can be inhibited by insulin treatment (Garcia et al., 2005). Rapid DAT recycling was also observed following dopamine uptake, with maximal DAT surface levels observed after 80 seconds (Furman, Chen, et al., 2009). This could provide a mechanism for neurons to mute consequent neurotransmittory events by providing greater uptake following dopamine release. Whether the

molecules required for the DAT surface reduction are also mediating the increase in DAT surface levels remain to be seen.

The precise mechanism for this recycling is not fully known, but we show that that the cytoskeletal protein actin is required for this trafficking destination. Actin filaments have been shown to mediate recycling endosome transport to the cell. The cystic fibrosis conductance regulator requires actin association for recycling back to the plasma membrane via the channel's C-terminal PDZ domain (Swiatecka-Urban et al., 2002). Furthermore, actin is involved in tubular endosome formation that recycle β_2-adrenergic receptor back to the cell surface in a dynamin-dependent process (Cao et al., 1999). This is consistent with our results in which dynamin and actin work in concert to regulate DAT surface levels in the striatum (Fig. 4.12). Nevertheless, the full complement of molecular components necessary for the DAT recycling pathway are still under study.

We found that the dopamine transporter constitutively internalizes via a dynamin-independent mechanism, whereas PKC-mediated DAT internalization is dynamin-dependent, as has been previously described (Fig. 4.13). We show that constitutively internalized DAT does not result in DAT degradation, and that DAT recycling back to the plasma membrane occurs via a dynamin-dependent, actin-mediated mechanism. Futhermore, we show that not all DAT surface molecules

are able to constitutively internalize and that constitutive and PKC-mediated DAT trafficking draw from the same trafficking-competent surface pool.

CHAPTER V

Discussion

KCNK3 Undergoes PKC-mediated Trafficking via a 14-3-3β-Dependent Mechanism

Endocytic trafficking is a mechanism to regulate the plasma membrane function of membrane proteins. Recent studies indicate that endocytic trafficking acutely regulates several different types of K^+ channels, including K_{ATP} (Manna et al., 2010) and $K_{Ca.2.1}$ (Correa et al., 2009), suggesting that regulated membrane trafficking is a means to rapidly control K^+ channel surface density. In the current studies, our data revealed that dynamic endocytic trafficking regulates acid-sensitive K^+ leak channel surface expression. This finding suggests a role for KCNK3 trafficking could potentially contribute to neuronal excitability. KCNK3 internalization would be predicted to depolarize the membrane potential, and prohibit Na_v channel activation, resulting in a slower frequency of action potential initiation. Alternatively, membrane depolarization mediated by regulated KCNK3 trafficking could potentially be sufficient to relieve Mg^{2+} block of NMDA receptors, increasing the probability of NMDA receptor firing and downstream plasticity events in response to an excitatory postsynaptic potential. Thus, in combination with established ligand-gated ion channel trafficking, acutely regulating KCNK3 surface levels could give rise to a context-dependent plasticity of membrane.

Prior studies using phorbol esters (Lopes et al., 2000), Group I mGluR agonists (Talley et al., 2000), and M1/M3 muscarinic agonists (Meuth et al., 2003) demonstrated a PKC-mediated functional down-regulation of KCNK3 and/or acid-sensitive currents, respectively. However, the mechanisms underlying this down-regulation have not been well defined. We observed significant loss of KCNK3 activity in response to PMA treatment over a 15-min time course in both CGNs and HEK cells, which is consistent with the time course for endocytosis. We used surface biotinylation and cellular imaging to directly test whether PKC-stimulated KCNK3 current losses were due to internalization. We observed significant PKC-dependent losses in surface KCNK3 following PMA treatment both in HEK cells and CGNs, which were completely blocked by the PKC inhibitor BIM. The magnitude of KCNK3 surface losses paralleled PKC-mediated KCNK3 currents losses, consistent with endocytosis as the primary mechanism responsible for PKC-mediated KCNK3 inhibition. Moreover, we observed losses in acid-sensitive leak currents and KCNK3 internalization via activation of endogenously expressed Group I mGluRs, consistent with previous reports demonstrating Group I mGluR-mediated KCNK3 down-regulation (Talley et al., 2000). Previous studies reported rapid KCNK3 activity losses in response to direct G_q activation (X. Chen et al., 2006) or via glutamatergic signaling (Chemin et al., 2003; Talley et al., 2000) in heterologous expression systems and CGNs, whereas we observed a slower time course of KCNK3 inhibition. This difference may also reflect the much higher DHPG concentrations used in previous studies, compared with those used in our

studies (10 and 100 μM *versus* 1 μM in our study). Decreased cAMP production in response to high DHPG concentrations has been reported, which is likely mediated by Group III mGluR activation (Sekiyama et al., 1996). It is not known whether PKC activation results in KCNK3 phosphorylation, either directly or indirectly. A recent report demonstrated that endothelin-1 down-regulates KCNK3 and leads to PKC-dependent KCNK3 phosphorylation in pulmonary artery smooth muscle cells (Tang et al., 2009). However, it should be noted that these phosphorylation studies relied upon the commercially available anti-KCNK3 antibody that, in our hands, does not recognize a KNCK3-specific band. It is interesting to note that under basal conditions, KNCK3 surface expression in primary CGN cultures was <6% total KCNK3 protein, which differed markedly from observed surface levels in transfected HEK cells. Nevertheless, these values are consistent with those reported for other channels in both primary cultured neurons and acute brain slices (Gross et al., 2011; D. Y. Kim et al., 2011). Low channel surface density (as a fraction of the total available channel) may reflect large intracellular endocytic pools tightly regulated by neuron-specific mechanisms. Alternatively, they may reflect a high degree of turnover in neuronal systems, with large, forward trafficking protein pools to maintain steady state channel levels in the membrane.

The large intracellular pool may also reflect a mechanism by which neurons can initiate KCNK3 trafficking to the membrane leading to neuronal quiescence or in response to extracellular cues. Indeed, KCNK3 activity is required for mediating

neurodegeneration induced by stroke-induced ischemia (Hawkins & Butt, 2013). The mechanistic understanding for this apoptosis-supporting function could open new avenues to acutely treat stroke and diminish damage during the cerebrovascular incident. Additionally, acute regulation of KCNK3 surface expression has implications in nociception and pharmacological pain management. KCNK3 is expressed in nociceptive dorsal root ganglia (Cooper, Johnson, & Rau, 2004). As we observed a large intracellular KCNK3 pool (Fig 3.6), channel recycling to the surface would act to inhibit these neurons. Although recycling determinants for the channel have not been described, KCNK3 shares a trafficking motif with DAT (Fig. 3.11) and may share trafficking mechanisms between the two proteins. Acute release from intracellular pools for KCNK3, and DAT, is an interesting area of study and should be illuminating regarding its effect on neuronal function.

KCNK3 activity has been shown to be required for multiple sclerosis progression. $CD4^+$ T-lymphocytes that target myelin and cause its degradation are activated in a KCNK3-dependent process (Bittner et al., 2012). A newly developed pharmacological KCNK3 inhibitor, A293, is able to inhibit T-cell activation, prevent myelin loss, and extend longevity in a multiple sclerosis mouse model. Although this is mediated through direct channel inactivation, pharmacological KCNK3 trafficking induction could also be a mechanism to slow disease progression and have broader application in auto-immune disease treatment.

KCNK3 and a closely related leak channel KCNK9 have been show to form heterodimers in neurons (Berg et al., 2004). Whether PKC-mediated KCNK3 trafficking will occur in the heterodimer is not known, but it offers a possibility that KCNK9's insensitivity to PKC will act dominantly and prevent potential KCNK3/KCNK9 trafficking. Conversely, KCNK3 may act dominantly and induce KCNK9 surface losses following PKC activation. Differential targeting in response to hetero-oligomerization and competing endocytic signals has been reported in the asialoglycoprotein receptor and alters the receptor's polarized distribution from apical to basolateral (Fuhrer, Geffen, Huggel, & Spiess, 1994). Whether KCNK3/KCNK9 dimers display differential regulation is an area of ongoing study.

Following internalization from the cell surface, proteins can diverge to either recycling or degradative endocytic pathways. For example, EGFR (Huang et al., 2006) and δ-opioid receptors (von Zastrow, 2010) enter late endosomes and are degraded upon internalization, whereas the TfR and μ opioid receptors (Jennifer Whistler lab) are primarily recycled. We observed KCNK3 co-localization in an early endosome/TfR-positive vesicle population following internalization and detected no losses in total KCNK3 protein following PKC stimulation. These results suggest that internalized KCNK3 is likely to enter a recycling, rather than a degradative, pathway.

Previous studies from our laboratory investigating mechanisms responsible for PKC-stimulated DAT trafficking revealed a novel endocytic regulatory domain (FREKLAYAIA) encoded in the DAT C-terminus (Holton et al., 2005) that is highly conserved across the SLC6 transporter gene family and is the locus for an endocytic braking mechanism (Boudanova, Navaroli, Stevens, & Melikian, 2008a). These results offer further insight into the previous results of Talley and Bayliss (Talley & Bayliss, 2002), in which KCNK3 C-terminal deletions that encompassed the 335–344 region abolished TRH receptor-mediated KCNK3 inhibition, which also occurs via G_q activation. It is currently not clear how these charged residues function to target either DAT or KCNK3 to the endocytic machinery. Also, FREKLAYAIA mediates constitutive DAT internalization and the question remains if KCNK3 constitituvely internalizes and was not directly addressed in this study. An interesting area to further characterize the similarity between these homologous sequences would be to exchange the endocytic signals and test for sufficiency for the more completely described DAT FREKLAYAIA to drive KCNK3 trafficking in response to physiological cues known to mediate DAT trafficking, such as insulin stimulation. Previous reports observed that KCNK3 activity is modulated by metabolic cues, since glucose treatment in orexinergic neurons will decrease channel activity (Burdakov et al., 2006). Whether DAT and KCNK3 share a cell signaling response to metabolic cues could be addressed, such as Akt signaling for DAT and insulin, is an interesting area of study.

PKC-stimulated KCNK3 endocytosis absolutely required the phosphoserine-binding protein 14-3-3β. 14-3-3 binds target proteins primarily at either RS*X*pS*X*P or (R/K)*X*φ*X*(pS/pT)*X*P motifs, and several proteins encode multiple 14-3-3 binding sites (Tzivion et al., 2000; Yaffe et al., 1997). 14-3-3 binding can induce conformation changes that facilitate catalytic activity or protein-protein interactions, mask domains to prevent protein-protein interactions, or facilitate protein co-localization. Previous work demonstrated that 14-3-3β binds to a non-canonical 14-3-3 binding motif in the distal KCNK3 C terminus and is required for KCNK3 egress from the ER (O'Kelly et al., 2002). Our results indicate that 14-3-3β is also necessary for PKC-mediated KNCK3 internalization. We noted that a ~50% 14-3-3β knockdown did not markedly disrupt KCNK3 surface targeting, whereas PKC-mediated endocytosis was abolished. This may suggest that forward trafficking from the ER is less sensitive to 14-3-3β levels than KCNK3 surface populations. Alternatively, other accessory proteins working in consort with 14-3-3β at the cell surface may be expressed in limited quantities and are thereby more sensitive to losses in 14-3-3β. Interestingly, the epithelial sodium channel, ENaC, constitutively internalizes in a 14-3-3- and Nedd4-2-dependent manner, and aldosterone increases ENaC surface expression via blocking 14-3-3-dependent ENaC internalization and degradation (Ichimura et al., 2005). Furthermore, 14-3-3 interaction with the α2 adrenergic receptor supports receptor surface expression and dephosphorylation followed by subsequent 14-3-3 dissociation initiates endocytosis, consistent with a role for 14-3-3 as an endocytic brake (Wang &

Limbird, 2007). . Although we do not currently know whether 14-3-3β controls KCNK3 internalization directly or indirectly, this site is a candidate locus for potential 14-3-3β/KCNK3 endocytic interactions, distinct from the identified sequence controlling KCNK3 egress from the ER. Future studies exploring the possibility of this sequence as a *bona fide* 14-3-3β binding site and/or endocytic braking mechanism should be informative.

DOPAMINE TRANSPORTER ENDOCYTIC TRAFFICKING: DIFFERENTIAL DEPENDENCE ON DYNAMIN AND THE ACTIN CYTOSKELETON

Dopamine transporter activity is the major mechanism mediating synaptic dopamine clearance and signal latency. Membrane trafficking constitutes an important role in regulating transporter function. Recent studies indicate that DAT trafficking requires the classical endocytic molecules clathrin and dynamin (Eriksen et al., 2009; Sorkina et al., 2005). These studies depended on chronic trafficking perturbation through shRNA-mediated knockdown or co-expression of dominant negative mutant proteins, as well as heterologous cell expression or cultured dopaminergic neurons. We took advantage of newly developed pharmacological dynamin inhibitors acutely to block dynamin function and test whether DAT trafficking is dynamin-dependent in mouse striatal slices. Our results clearly demonstrate a differential dependence on dynamin for endocytic recycling and PKC-mediated DAT internalization, but not for constitutive DAT endocytosis.

Using the pharmacological dynamin inhibitor, we teased out dynamin's role in DAT trafficking at presynaptic termini, which is the site for DAT regulation in neurotransmitter clearance. We show that dynamin is not required for constitutive DAT internalization, as dynole treatment did not alter basal DAT internalization rates. In contrast, PKC-mediated DAT internalization is strictly dynamin-dependent. There have been other reports demonstrating that DAT endocytosis may not require dynamin. The membrane raft associated protein flotillin-1 has been shown to be required for PKC-mediated DAT trafficking (Cremona et al., 2011). The role for dynamin in that process was not specifically explored, but trafficking from lipid rafts has been shown to be both dynamin-dependent and -independent. Furthermore, DAT internalization is regulated by presynaptic D_2 receptors, where receptor activation ultimately elicits decreased DAT surface levels, as well as D_2 trafficking (Lee et al., 2007). D_2 receptor trafficking has been shown to be insensitive to dynamin inhibition (Kotowski et al., 2011; Vickery & von Zastrow, 1999). Since DAT and D_2 interact, this raises the possibility that they are co-trafficking via a dynamin-independent mechanism into endosomal compartments.

Interestingly, we see that surface resident DAT is not present in a uniform pool, but rather two pools: one of which undergoes constitutive and PKC-mediated trafficking and one which does not respond to either of these two regulatory events. A previous study from Foster and associates reported that DAT is segregated

between lipid raft and non-raft domains at the cell surface (Foster et al., 2008), raising the possibility that either raft or non-raft microdomains may facilitate trafficking competent and incompetent DAT populations. Additionally, a DAT trafficking mutant, R615C, found in an ADHD patient, has been shown to constitutively internalize at a higher rate and is found in a different distribution compared to wild-type between raft and non-raft membrane domains at the surface (Sakrikar et al., 2012). Future work measuring DAT trafficking specifically from these two membrane domains will be informative regarding if this is the segregation is used to delineate trafficking requirements.

The functional implications for segregated DAT populations at the cell surface are not known. This could provide a mechanism by which dopaminergic neurons can mute responses to cell signaling pathways, preventing profound DAT surface loss. As $DAT^{(-/-)}$ mice display behavioural deficits (Giros et al., 1996) and dopaminergic signal latency has been implicated in mood (Chaudhury et al., 2013) and cognitive disorders (Brunelin et al., 2013), potential 'over-trafficking' would have deleterious effects. Finite surface pools have been described for the potassium channel K(V)10.1, where constitutively internalizing channel will plateau after 45 minutes, consistent with the DAT model ((Kohl, Lorinczi, Pardo, & Stuhmer, 2011). Moreover, this channel was observed to internalize via two different mechanisms (clathrin-deoendent and clathrin-independent fluid phase uptake), also consistent with our observed dynamin-dependent and –independent DAT trafficking

pathways. Furthermore, whether related neurotransmitter transporter, like NET or SERT, are also segregated between trafficking-competent and –incompetent pools is an interesting question. NET and SERT have been shown to localize to raft and non-raft membrane domains (Matthies et al., 2009; Muller, Wiborg, & Haase, 2006). Studies testing whether they contain a finite trafficking-competent surface pool could have broader implications for the SLC6 protein family.

Conflicting results have been reported regarding DAT's endocytic fate during basal and PKC-stimulated internalization, both in neurons and heterologous expression systems. Previous reports show that DAT ubiquitylation is required for PKC-mediated DAT trafficking (Miranda et al., 2005). This post-translational modification is then required for DAT degradation, as mutations in N-terminal lysines prevent ubiquitylation and slow DAT turnover (Vina-Vilaseca & Sorkin, 2010). These studies were performed in a non-neuronal heterologous expression system and imposed 1-2 hour PMA treatments, resulting in an extensive PKC activation that may not reflect a physiologically relevant stimulus. This approach could have artifactually targeted DAT to a degradative fate. Additionally, work from Eriksen and associates in cultured dopaminergic neurons demonstrated that internalized DAT preferentially sorts to Rab7-positive endosomes, indicating a predominantly degradative fate (Eriksen et al., 2009). This study tracked a fluorescent cocaine analog bound to DAT to test internalization and endosomal sorting. Persistent ligand binding has been reported to alter DAT endocytic fate,

tempering the interpretation for this result (Daws et al., 2002). Moreover, DAT trafficking was PMA-insensitive and no DAT recycling was observed, inconsistent with our results in the striatal slice as well as DAT trafficking studies in heterologous cells. We observe DAT surface losses in dynole-treated slices, consistent with a role for dynamin in constitutive DAT recycling, and DAT was not significantly degraded over the experimental time-course. However, one caveat to our findings is that we, as yet, do not know the dynamin-dependent endocytic compartment in which DAT accumulates. If this is an early endosomal compartment, we may be blocking PKC-stimulated DAT degradation by arresting progression to degradative endocytic vesicles. Future studies tracking DAT endocytic trafficking should be illuminating in this regard.

DAT has been described to constitutively recycle to the plasma membrane and co-localize in Rab11 endosomal compartments in heterologous cells (Furman, Lo, et al., 2009). Our results suggest that DAT recycles in striatal presynaptic termini. Recent work has shown that D_2 activation will cause a rapidly observed increase in DAT surface levels in striatal synaptosomes followed by the aforementioned DAT surface reduction (Chen et al., 2013). This rapid release to increase surface expression is reminiscent of the regulated recycling seen in the glucose transporter GLUT4. There, insulin signaling will elicit an Akt-mediated cascade releasing GLUT4-positive endosomes to fuse at the cell surface, rapidly increasing glucose uptake in response food intake (Foley et al., 2011). Insulin treatment also acutely

increases DAT activity and increases transporter surface expression through PI3K signaling (Carvelli et al., 2002). AMPH will also cause a rapidly (seconds) observed increase in DAT surface levels followed by a slower (minutes) occurring reduction in surface DAT (Chen et al., 2009). Moreover, AMPH-induced DAT trafficking is correlated with decreased Akt activity via a CaMKII-dependent pathway and can be inhibited by insulin treatment (Garcia et al., 2005). Rapid DAT recycling was also observed following dopamine uptake, with maximal DAT surface levels observed after 80 seconds (Furman, Chen, et al., 2009). This could provide a mechanism for neurons to mute dopaminergic neurotransmission by providing greater uptake following dopamine release. Whether the molecules required for the DAT surface reduction are also mediating the increase in DAT surface levels remain to be seen.

The precise mechanism for DAT recycling is not fully known, but we show that that the cytoskeletal protein actin is required at the dynamin-dependent step in the recycling process. Actin filaments have been shown to mediate recycling endosome transport to the cell. The cystic fibrosis conductance regulator requires actin association for recycling back to the plasma membrane via the channel's C-terminal PDZ domain (Swiatecka-Urban et al., 2002). Furthermore, actin is involved in tubular endosome formation that recycle β_2-adrenergic receptor back to the cell surface in a dynamin-dependent process (Cao et al., 1999). This is consistent with our results in which dynamin and actin work in concert to regulate

DAT surface levels in the striatum. Nevertheless, the full complement of molecular components necessary for the DAT recycling pathway are still under study.

Ahern, C. A., & Kobertz, W. R. (2009). Chemical tools for K(+) channel biology. *Biochemistry, 48*(3), 517-526. doi: 10.1021/bi8018515

Ait-Slimane, T., Galmes, R., Trugnan, G., & Maurice, M. (2009). Basolateral internalization of GPI-anchored proteins occurs via a clathrin-independent flotillin-dependent pathway in polarized hepatic cells. *Mol Biol Cell, 20*(17), 3792-3800. doi: 10.1091/mbc.E09-04-0275

Albright, T. D., Jessell, T. M., Kandel, E. R., & Posner, M. I. (2000). Neural science: a century of progress and the mysteries that remain. *Neuron, 25 Suppl*, S1-55.

Argyelan, M., Szabo, Z., Kanyo, B., Tanacs, A., Kovacs, Z., Janka, Z., & Pavics, L. (2005). Dopamine transporter availability in medication free and in bupropion treated depression: a 99mTc-TRODAT-1 SPECT study. *J Affect Disord, 89*(1-3), 115-123. doi: 10.1016/j.jad.2005.08.016

Balasubramanian, N., Scott, D. W., Castle, J. D., Casanova, J. E., & Schwartz, M. A. (2007). Arf6 and microtubules in adhesion-dependent trafficking of lipid rafts. *Nat Cell Biol, 9*(12), 1381-1391. doi: 10.1038/ncb1657

Balklava, Z., Pant, S., Fares, H., & Grant, B. D. (2007). Genome-wide analysis identifies a general requirement for polarity proteins in endocytic traffic. *Nat Cell Biol, 9*(9), 1066-1073. doi: 10.1038/ncb1627

Bautista, D. M., Sigal, Y. M., Milstein, A. D., Garrison, J. L., Zorn, J. A., Tsuruda, P. R., . . . Julius, D. (2008). Pungent agents from Szechuan peppers excite sensory neurons by inhibiting two-pore potassium channels. *Nat Neurosci, 11*(7), 772-779.

Bayliss, D. A., Sirois, J. E., & Talley, E. M. (2003). The TASK family: two-pore domain background K+ channels. *Mol Interv, 3*(4), 205-219. doi: 10.1124/mi.3.4.205

Bayliss, D. A., Talley, E. M., Sirois, J. E., & Lei, Q. (2001). TASK-1 is a highly modulated pH-sensitive 'leak' K(+) channel expressed in brainstem respiratory neurons. *Respir Physiol, 129*(1-2), 159-174.

Berg, A. P., Talley, E. M., Manger, J. P., & Bayliss, D. A. (2004). Motoneurons express heteromeric TWIK-related acid-sensitive K+ (TASK) channels containing TASK-1 (KCNK3) and TASK-3 (KCNK9) subunits. *J Neurosci, 24*(30), 6693-6702.

Besana, A., Barbuti, A., Tateyama, M. A., Symes, A. J., Robinson, R. B., & Feinmark, S. J. (2004). Activation of protein kinase C epsilon inhibits the two-pore domain K+ channel, TASK-1, inducing repolarization abnormalities in cardiac ventricular myocytes. *J Biol Chem, 279*(32), 33154-33160. doi: 10.1074/jbc.M403525200

Birmingham, A. T., & Iversen, L. L. (1969). Uptake and metabolism of 3H-noradrenaline by normal and by denervated vasa deferentia of guinea-pigs and rats. *Br J Pharmacol, 35*(2), P356-358.

Bittner, S., Bauer, M. A., Ehling, P., Bobak, N., Breuer, J., Herrmann, A. M., . . . Meuth, S. G. (2012). The TASK1 channel inhibitor A293 shows efficacy in a mouse model of multiple sclerosis. *Exp Neurol, 238*(2), 149-155. doi: 10.1016/j.expneurol.2012.08.021

Blakely, R. D., Berson, H. E., Fremeau, R. T., Jr., Caron, M. G., Peek, M. M., Prince, H. K., & Bradley, C. C. (1991). Cloning and expression of a functional serotonin transporter from rat brain. *Nature, 354*(6348), 66-70. doi: 10.1038/354066a0

Blakely, R. D., Robinson, M. B., & Amara, S. G. (1988). Expression of neurotransmitter transport from rat brain mRNA in Xenopus laevis oocytes. *Proc Natl Acad Sci U S A, 85*(24), 9846-9850.

Bogdanski, D. F., Blaszkowski, T. P., & Tissari, A. H. (1970). Mechanisms of biogenic amine transport and storage. IV. Relationship between K+ and the Na+ requirement for transport and storage of 5-hydroxytryptamine and norepinephrine in synaptosomes. *Biochim Biophys Acta, 211*(3), 521-532.

Bonifacino, J. S., & Traub, L. M. (2003). Signals for sorting of transmembrane proteins to endosomes and lysosomes. *Annu Rev Biochem, 72*, 395-447.

Boudanova, E., Navaroli, D. M., Stevens, Z., & Melikian, H. E. (2008a). Dopamine transporter endocytic determinants: Carboxy terminal residues critical for basal and PKC-stimulated internalization. *Mol Cell Neurosci*.

Boudanova, E., Navaroli, D. M., Stevens, Z., & Melikian, H. E. (2008b). Dopamine transporter endocytic determinants: carboxy terminal residues critical for basal and PKC-stimulated internalization. *Mol Cell Neurosci, 39*(2), 211-217. doi: 10.1016/j.mcn.2008.06.011

Bredt, D. S., & Nicoll, R. A. (2003). AMPA receptor trafficking at excitatory synapses. *Neuron, 40*(2), 361-379.

Browne, D. L., Gancher, S. T., Nutt, J. G., Brunt, E. R., Smith, E. A., Kramer, P., & Litt, M. (1994). Episodic ataxia/myokymia syndrome is associated with point mutations in the human potassium channel gene, KCNA1. *Nat Genet, 8*(2), 136-140. doi: 10.1038/ng1094-136

Brunelin, J., Fecteau, S., & Suaud-Chagny, M. F. (2013). Abnormal striatal dopamine transmission in schizophrenia. *Curr Med Chem, 20*(3), 397-404.

Buckingham, S. D., Kidd, J. F., Law, R. J., Franks, C. J., & Sattelle, D. B. (2005). Structure and function of two-pore-domain K+ channels: contributions from genetic model organisms. *Trends Pharmacol Sci, 26*(7), 361-367. doi: 10.1016/j.tips.2005.05.003

Buckler, K. J., Williams, B. A., & Honore, E. (2000). An oxygen-, acid- and anaesthetic-sensitive TASK-like background potassium channel in rat arterial chemoreceptor cells. *J Physiol, 525 Pt 1*, 135-142.

Buckley, K. M., Melikian, H. E., Provoda, C. J., & Waring, M. T. (2000). Regulation of neuronal function by protein trafficking: a role for the endosomal pathway. *J Physiol, 525 Pt 1*, 11-19.

Burdakov, D., Jensen, L. T., Alexopoulos, H., Williams, R. H., Fearon, I. M., O'Kelly, I., . . . Verkhratsky, A. (2006). Tandem-pore K+ channels mediate inhibition of orexin neurons by glucose. *Neuron, 50*(5), 711-722.

Burgueno, J., Enrich, C., Canela, E. I., Mallol, J., Lluis, C., Franco, R., & Ciruela, F. (2003). Metabotropic glutamate type 1alpha receptor localizes in low-density caveolin-rich plasma membrane fractions. *J Neurochem, 86*(4), 785-791.

Calligaro, D. O., & Eldefrawi, M. E. (1987). High affinity stereospecific binding of [3H] cocaine in striatum and its relationship to the dopamine transporter. *Membr Biochem, 7*(2), 87-106.

Cao, T. T., Deacon, H. W., Reczek, D., Bretscher, A., & von Zastrow, M. (1999). A kinase-regulated PDZ-domain interaction controls endocytic sorting of the beta2-adrenergic receptor. *Nature, 401*(6750), 286-290. doi: 10.1038/45816

Carvelli, L., Moron, J. A., Kahlig, K. M., Ferrer, J. V., Sen, N., Lechleiter, J. D., . . . Galli, A. (2002). PI 3-kinase regulation of dopamine uptake. *J Neurochem, 81*(4), 859-869.

Chaudhury, D., Walsh, J. J., Friedman, A. K., Juarez, B., Ku, S. M., Koo, J. W., . . . Han, M. H. (2013). Rapid regulation of depression-related behaviours by control of midbrain dopamine neurons. *Nature, 493*(7433), 532-536. doi: 10.1038/nature11713

Chemin, J., Girard, C., Duprat, F., Lesage, F., Romey, G., & Lazdunski, M. (2003). Mechanisms underlying excitatory effects of group I metabotropic glutamate receptors via inhibition of 2P domain K+ channels. *EMBO J, 22*(20), 5403-5411. doi: 10.1093/emboj/cdg528

Chen, R., Daining, C. P., Sun, H., Fraser, R., Stokes, S. L., Leitges, M., & Gnegy, M. E. (2013). Protein kinase Cbeta is a modulator of the dopamine D2 autoreceptor-activated trafficking of the dopamine transporter. *J Neurochem, 125*(5), 663-672. doi: 10.1111/jnc.12229

Chen, R., Furman, C. A., Zhang, M., Kim, M. N., Gereau, R. W. t., Leitges, M., & Gnegy, M. E. (2009). Protein kinase Cbeta is a critical regulator of dopamine transporter trafficking and regulates the behavioral response to amphetamine in mice. *J Pharmacol Exp Ther, 328*(3), 912-920. doi: 10.1124/jpet.108.147959

Chen, R., Tilley, M. R., Wei, H., Zhou, F., Zhou, F. M., Ching, S., . . . Gu, H. H. (2006). Abolished cocaine reward in mice with a cocaine-insensitive dopamine transporter. *Proc Natl Acad Sci U S A, 103*(24), 9333-9338. doi: 10.1073/pnas.0600905103

Chen, X., Talley, E. M., Patel, N., Gomis, A., McIntire, W. E., Dong, B., . . . Bayliss, D. A. (2006). Inhibition of a background potassium channel by Gq protein alpha-subunits. *Proc Natl Acad Sci U S A, 103*(9), 3422-3427.

Chi, L., & Reith, M. E. (2003). Substrate-induced trafficking of the dopamine transporter in heterologously expressing cells and in rat striatal synaptosomal preparations. *J Pharmacol Exp Ther, 307*(2), 729-736. doi: 10.1124/jpet.103.055095

Cooper, B. Y., Johnson, R. D., & Rau, K. K. (2004). Characterization and function of TWIK-related acid sensing K+ channels in a rat nociceptive cell. *Neuroscience, 129*(1), 209-224. doi: 10.1016/j.neuroscience.2004.06.066

Correa, S. A., Muller, J., Collingridge, G. L., & Marrion, N. V. (2009). Rapid endocytosis provides restricted somatic expression of a K+ channel in central neurons. *J Cell Sci, 122*(Pt 22), 4186-4194. doi: 10.1242/jcs.058420

Coyle, J. T., & Snyder, S. H. (1969). Antiparkinsonian drugs: inhibition of dopamine uptake in the corpus striatum as a possible mechanism of action. *Science, 166*(3907), 899-901.

Cremona, M. L., Matthies, H. J., Pau, K., Bowton, E., Speed, N., Lute, B. J., . . . Yamamoto, A. (2011). Flotillin-1 is essential for PKC-triggered endocytosis and membrane microdomain localization of DAT. *Nat Neurosci, 14*(4), 469-477. doi: 10.1038/nn.2781

Czirjak, G., & Enyedi, P. (2002). Formation of functional heterodimers between the TASK-1 and TASK-3 two-pore domain potassium channel subunits. *J Biol Chem, 277*(7), 5426-5432. doi: 10.1074/jbc.M107138200

D'Adamo, M. C., Liu, Z., Adelman, J. P., Maylie, J., & Pessia, M. (1998). Episodic ataxia type-1 mutations in the hKv1.1 cytoplasmic pore region alter the gating properties of the channel. *EMBO J, 17*(5), 1200-1207. doi: 10.1093/emboj/17.5.1200

Daniels, G. M., & Amara, S. G. (1999). Regulated trafficking of the human dopamine transporter. Clathrin-mediated internalization and lysosomal degradation in response to phorbol esters. *J Biol Chem, 274*(50), 35794-35801.

Davies, L. A., Hu, C., Guagliardo, N. A., Sen, N., Chen, X., Talley, E. M., . . . Barrett, P. Q. (2008). TASK channel deletion in mice causes primary hyperaldosteronism. *Proc Natl Acad Sci U S A, 105*(6), 2203-2208. doi: 10.1073/pnas.0712000105

Daws, L. C., Callaghan, P. D., Moron, J. A., Kahlig, K. M., Shippenberg, T. S., Javitch, J. A., & Galli, A. (2002). Cocaine increases dopamine uptake and cell surface expression of dopamine transporters. *Biochem Biophys Res Commun, 290*(5), 1545-1550. doi: 10.1006/bbrc.2002.6384

Dodson, P. D., & Forsythe, I. D. (2004). Presynaptic K+ channels: electrifying regulators of synaptic terminal excitability. *Trends Neurosci, 27*(4), 210-217. doi: 10.1016/j.tins.2004.02.012

Draper, R. K., Goda, Y., Brodsky, F. M., & Pfeffer, S. R. (1990). Antibodies to clathrin inhibit endocytosis but not recycling to the trans Golgi network in vitro. *Science, 248*(4962), 1539-1541.

Duprat, F., Lesage, F., Fink, M., Reyes, R., Heurteaux, C., & Lazdunski, M. (1997). TASK, a human background K+ channel to sense external pH variations near physiological pH. *EMBO J, 16*(17), 5464-5471.

Ehlers, M. D. (2000). Reinsertion or degradation of AMPA receptors determined by activity-dependent endocytic sorting. *Neuron, 28*(2), 511-525.

Enyedi, P., & Czirjak, G. (2010). Molecular background of leak K+ currents: two-pore domain potassium channels. *Physiol Rev, 90*(2), 559-605. doi: 10.1152/physrev.00029.2009

Eriksen, J., Rasmussen, S. G., Rasmussen, T. N., Vaegter, C. B., Cha, J. H., Zou, M. F., . . . Gether, U. (2009). Visualization of dopamine transporter trafficking in live neurons by use of fluorescent cocaine analogs. *J Neurosci, 29*(21), 6794-6808. doi: 10.1523/JNEUROSCI.4177-08.2009

Escayg, A., MacDonald, B. T., Meisler, M. H., Baulac, S., Huberfeld, G., An-Gourfinkel, I., . . . Malafosse, A. (2000). Mutations of SCN1A, encoding a neuronal sodium channel, in two families with GEFS+2. *Nat Genet, 24*(4), 343-345. doi: 10.1038/74159

Feliciangeli, S., Tardy, M. P., Sandoz, G., Chatelain, F. C., Warth, R., Barhanin, J., . . . Lesage, F. (2010). Potassium channel silencing by constitutive endocytosis and intracellular sequestration. *J Biol Chem, 285*(7), 4798-4805. doi: 10.1074/jbc.M109.078535

Floresco, S. B., West, A. R., Ash, B., Moore, H., & Grace, A. A. (2003). Afferent modulation of dopamine neuron firing differentially regulates tonic and phasic dopamine transmission. *Nat Neurosci, 6*(9), 968-973. doi: 10.1038/nn1103

Fog, J. U., Khoshbouei, H., Holy, M., Owens, W. A., Vaegter, C. B., Sen, N., . . . Gether, U. (2006). Calmodulin kinase II interacts with the dopamine transporter C terminus to regulate amphetamine-induced reverse transport. *Neuron, 51*(4), 417-429. doi: 10.1016/j.neuron.2006.06.028

Foley, K., Boguslavsky, S., & Klip, A. (2011). Endocytosis, recycling, and regulated exocytosis of glucose transporter 4. *Biochemistry, 50*(15), 3048-3061. doi: 10.1021/bi2000356

Foster, J. D., Adkins, S. D., Lever, J. R., & Vaughan, R. A. (2008). Phorbol ester induced trafficking-independent regulation and enhanced phosphorylation of the dopamine transporter associated with membrane rafts and cholesterol. *J Neurochem, 105*(5), 1683-1699. doi: 10.1111/j.1471-4159.2008.05262.x

Foster, J. D., & Vaughan, R. A. (2011). Palmitoylation controls dopamine transporter kinetics, degradation, and protein kinase C-dependent regulation. *J Biol Chem, 286*(7), 5175-5186. doi: 10.1074/jbc.M110.187872

Fuhrer, C., Geffen, I., Huggel, K., & Spiess, M. (1994). The two subunits of the asialoglycoprotein receptor contain different sorting information. *J Biol Chem, 269*(5), 3277-3282.

Furman, C. A., Chen, R., Guptaroy, B., Zhang, M., Holz, R. W., & Gnegy, M. (2009). Dopamine and amphetamine rapidly increase dopamine transporter trafficking to the surface: live-cell imaging using total internal reflection fluorescence microscopy. *J Neurosci, 29*(10), 3328-3336.

Furman, C. A., Lo, C. B., Stokes, S., Esteban, J. A., & Gnegy, M. E. (2009). Rab 11 regulates constitutive dopamine transporter trafficking and function in N2A neuroblastoma cells. *Neurosci Lett, 463*(1), 78-81. doi: 10.1016/j.neulet.2009.07.049

Garcia, B. G., Wei, Y., Moron, J. A., Lin, R. Z., Javitch, J. A., & Galli, A. (2005). Akt is essential for insulin modulation of amphetamine-induced human dopamine transporter cell-surface redistribution. *Mol Pharmacol, 68*(1), 102-109. doi: 10.1124/mol.104.009092

Georgiou, M., Marinari, E., Burden, J., & Baum, B. (2008). Cdc42, Par6, and aPKC regulate Arp2/3-mediated endocytosis to control local adherens junction stability. *Curr Biol, 18*(21), 1631-1638. doi: 10.1016/j.cub.2008.09.029

Girard, C., Tinel, N., Terrenoire, C., Romey, G., Lazdunski, M., & Borsotto, M. (2002). p11, an annexin II subunit, an auxiliary protein associated with the background K+ channel, TASK-1. *EMBO J, 21*(17), 4439-4448.

Giros, B., Jaber, M., Jones, S. R., Wightman, R. M., & Caron, M. G. (1996). Hyperlocomotion and indifference to cocaine and amphetamine in mice lacking the dopamine transporter. *Nature, 379*(6566), 606-612. doi: 10.1038/379606a0

Goldstein, S. A., Bockenhauer, D., O'Kelly, I., & Zilberberg, N. (2001). Potassium leak channels and the KCNK family of two-P-domain subunits. *Nat Rev Neurosci, 2*(3), 175-184.

Goldstein, S. A., Price, L. A., Rosenthal, D. N., & Pausch, M. H. (1996). ORK1, a potassium-selective leak channel with two pore domains cloned from Drosophila melanogaster by expression in Saccharomyces cerevisiae. *Proc Natl Acad Sci U S A, 93*(23), 13256-13261.

Goldstein, S. A., Wang, K. W., Ilan, N., & Pausch, M. H. (1998). Sequence and function of the two P domain potassium channels: implications of an emerging superfamily. *J Mol Med (Berl), 76*(1), 13-20.

Gouaux, E., & Mackinnon, R. (2005). Principles of selective ion transport in channels and pumps. *Science, 310*(5753), 1461-1465. doi: 10.1126/science.1113666

Grace, A. A., & Bunney, B. S. (1983). Intracellular and extracellular electrophysiology of nigral dopaminergic neurons--1. Identification and characterization. *Neuroscience, 10*(2), 301-315.

Gross, C., Yao, X., Pong, D. L., Jeromin, A., & Bassell, G. J. (2011). Fragile X mental retardation protein regulates protein expression and mRNA translation of the potassium channel Kv4.2. *J Neurosci, 31*(15), 5693-5698. doi: 10.1523/JNEUROSCI.6661-10.2011

Gruss, M., Bushell, T. J., Bright, D. P., Lieb, W. R., Mathie, A., & Franks, N. P. (2004). Two-pore-domain K+ channels are a novel target for the anesthetic gases xenon, nitrous oxide, and cyclopropane. *Mol Pharmacol, 65*(2), 443-452. doi: 10.1124/mol.65.2.443

Guastella, J., Nelson, N., Nelson, H., Czyzyk, L., Keynan, S., Miedel, M. C., . . . Kanner, B. I. (1990). Cloning and expression of a rat brain GABA transporter. *Science, 249*(4974), 1303-1306.

Harleton, E., Besana, A., Comas, G. M., Danilo, P., Jr., Rosen, T. S., Argenziano, M., . . . Feinmark, S. J. (2013). Ability to induce atrial fibrillation in the peri-operative

period is associated with phosphorylation-dependent inhibition of TWIK protein-related acid-sensitive potassium channel 1 (TASK-1). *J Biol Chem, 288*(4), 2829-2838. doi: 10.1074/jbc.M112.404095

Hattan, D., Nesti, E., Cachero, T. G., & Morielli, A. D. (2002). Tyrosine phosphorylation of Kv1.2 modulates its interaction with the actin-binding protein cortactin. *J Biol Chem, 277*(41), 38596-38606. doi: 10.1074/jbc.M205005200

Hauber, W. (1998). Involvement of basal ganglia transmitter systems in movement initiation. *Prog Neurobiol, 56*(5), 507-540.

Hawkins, V., & Butt, A. (2013). TASK-1 channels in oligodendrocytes: A role in ischemia mediated disruption. *Neurobiol Dis, 55*, 87-94. doi: 10.1016/j.nbd.2013.03.016

Hodgkin, A. L., & Huxley, A. F. (1952). A quantitative description of membrane current and its application to conduction and excitation in nerve. *J Physiol, 117*(4), 500-544.

Holton, K. L., Loder, M. K., & Melikian, H. E. (2005). Nonclassical, distinct endocytic signals dictate constitutive and PKC-regulated neurotransmitter transporter internalization. *Nat Neurosci, 8*(7), 881-888. doi: 10.1038/nn1478

Honing, S., Sandoval, I. V., & von Figura, K. (1998). A di-leucine-based motif in the cytoplasmic tail of LIMP-II and tyrosinase mediates selective binding of AP-3. *EMBO J, 17*(5), 1304-1314. doi: 10.1093/emboj/17.5.1304

Horn, A. S., Coyle, J. T., & Snyder, S. H. (1971). Catecholamine uptake by synaptosomes from rat brain. Structure-activity relationships of drugs with differential effects on dopamine and norepinephrine neurons. *Mol Pharmacol, 7*(1), 66-80.

Hsu, K., Seharaseyon, J., Dong, P., Bour, S., & Marban, E. (2004). Mutual functional destruction of HIV-1 Vpu and host TASK-1 channel. *Mol Cell, 14*(2), 259-267.

Huang, F., Kirkpatrick, D., Jiang, X., Gygi, S., & Sorkin, A. (2006). Differential regulation of EGF receptor internalization and degradation by multiubiquitination within the kinase domain. *Mol Cell, 21*(6), 737-748. doi: 10.1016/j.molcel.2006.02.018

Ichimura, T., Yamamura, H., Sasamoto, K., Tominaga, Y., Taoka, M., Kakiuchi, K., . . . Isobe, T. (2005). 14-3-3 proteins modulate the expression of epithelial Na+ channels by phosphorylation-dependent interaction with Nedd4-2 ubiquitin ligase. *J Biol Chem, 280*(13), 13187-13194. doi: 10.1074/jbc.M412884200

Ingram, S. L., Prasad, B. M., & Amara, S. G. (2002). Dopamine transporter-mediated conductances increase excitability of midbrain dopamine neurons. *Nat Neurosci, 5*(10), 971-978. doi: 10.1038/nn920

Iversen, L. L. (1974). Uptake mechanisms for neurotransmitter amines. *Biochem Pharmacol, 23*(14), 1927-1935.

Jing, S. Q., Spencer, T., Miller, K., Hopkins, C., & Trowbridge, I. S. (1990). Role of the human transferrin receptor cytoplasmic domain in endocytosis: localization of a specific signal sequence for internalization. *J Cell Biol, 110*(2), 283-294.

Johnson, L. A., Furman, C. A., Zhang, M., Guptaroy, B., & Gnegy, M. E. (2005). Rapid delivery of the dopamine transporter to the plasmalemmal membrane upon

amphetamine stimulation. *Neuropharmacology, 49*(6), 750-758. doi: 10.1016/j.neuropharm.2005.08.018

Johnston, J., Forsythe, I. D., & Kopp-Scheinpflug, C. (2010). Going native: voltage-gated potassium channels controlling neuronal excitability. *J Physiol, 588*(Pt 17), 3187-3200. doi: 10.1113/jphysiol.2010.191973

Kahlig, K. M., Lute, B. J., Wei, Y., Loland, C. J., Gether, U., Javitch, J. A., & Galli, A. (2006). Regulation of dopamine transporter trafficking by intracellular amphetamine. *Mol Pharmacol, 70*(2), 542-548. doi: 10.1124/mol.106.023952

Kang, D., Han, J., Talley, E. M., Bayliss, D. A., & Kim, D. (2004). Functional expression of TASK-1/TASK-3 heteromers in cerebellar granule cells. *J Physiol, 554*(Pt 1), 64-77.

Keyel, P. A., Mishra, S. K., Roth, R., Heuser, J. E., Watkins, S. C., & Traub, L. M. (2006). A single common portal for clathrin-mediated endocytosis of distinct cargo governed by cargo-selective adaptors. *Mol Biol Cell, 17*(10), 4300-4317. doi: 10.1091/mbc.E06-05-0421

Khoshbouei, H., Wang, H., Lechleiter, J. D., Javitch, J. A., & Galli, A. (2003). Amphetamine-induced dopamine efflux. A voltage-sensitive and intracellular Na+-dependent mechanism. *J Biol Chem, 278*(14), 12070-12077. doi: 10.1074/jbc.M212815200

Kilty, J. E., Lorang, D., & Amara, S. G. (1991). Cloning and expression of a cocaine-sensitive rat dopamine transporter. *Science, 254*(5031), 578-579.

Kim, D. Y., Gersbacher, M. T., Inquimbert, P., & Kovacs, D. M. (2011). Reduced sodium channel Na(v)1.1 levels in BACE1-null mice. *J Biol Chem, 286*(10), 8106-8116. doi: 10.1074/jbc.M110.134692

Kim, Y., Bang, H., & Kim, D. (1999). TBAK-1 and TASK-1, two-pore K(+) channel subunits: kinetic properties and expression in rat heart. *Am J Physiol, 277*(5 Pt 2), H1669-1678.

Kindler, C. H., Yost, C. S., & Gray, A. T. (1999). Local anesthetic inhibition of baseline potassium channels with two pore domains in tandem. *Anesthesiology, 90*(4), 1092-1102.

Kirkham, M., Fujita, A., Chadda, R., Nixon, S. J., Kurzchalia, T. V., Sharma, D. K., . . . Parton, R. G. (2005). Ultrastructural identification of uncoated caveolin-independent early endocytic vehicles. *J Cell Biol, 168*(3), 465-476. doi: 10.1083/jcb.200407078

Kittler, J. T., Chen, G., Kukhtina, V., Vahedi-Faridi, A., Gu, Z., Tretter, V., . . . Moss, S. J. (2008). Regulation of synaptic inhibition by phospho-dependent binding of the AP2 complex to a YECL motif in the GABAA receptor gamma2 subunit. *Proc Natl Acad Sci U S A, 105*(9), 3616-3621. doi: 10.1073/pnas.0707920105

Kittler, J. T., McAinsh, K., & Moss, S. J. (2002). Mechanisms of GABAA receptor assembly and trafficking: implications for the modulation of inhibitory neurotransmission. *Mol Neurobiol, 26*(2-3), 251-268. doi: 10.1385/MN:26:2-3:251

Kohl, T., Lorinczi, E., Pardo, L. A., & Stuhmer, W. (2011). Rapid internalization of the oncogenic K+ channel K(V)10.1. *PLoS One, 6*(10), e26329. doi: 10.1371/journal.pone.0026329

Kotowski, S. J., Hopf, F. W., Seif, T., Bonci, A., & von Zastrow, M. (2011). Endocytosis promotes rapid dopaminergic signaling. *Neuron, 71*(2), 278-290. doi: 10.1016/j.neuron.2011.05.036

Kuhar, M. J., & Zarbin, M. A. (1978). Synaptosomal transport: a chloride dependence for choline, GABA, glycine and several other compounds. *J Neurochem, 31*(1), 251-256.

Lamaze, C., Dujeancourt, A., Baba, T., Lo, C. G., Benmerah, A., & Dautry-Varsat, A. (2001). Interleukin 2 receptors and detergent-resistant membrane domains define a clathrin-independent endocytic pathway. *Mol Cell, 7*(3), 661-671.

Langhorst, M. F., Solis, G. P., Hannbeck, S., Plattner, H., & Stuermer, C. A. (2007). Linking membrane microdomains to the cytoskeleton: regulation of the lateral mobility of reggie-1/flotillin-2 by interaction with actin. *FEBS Lett, 581*(24), 4697-4703. doi: 10.1016/j.febslet.2007.08.074

Lee, F. J., Pei, L., Moszczynska, A., Vukusic, B., Fletcher, P. J., & Liu, F. (2007). Dopamine transporter cell surface localization facilitated by a direct interaction with the dopamine D2 receptor. *EMBO J, 26*(8), 2127-2136. doi: 10.1038/sj.emboj.7601656

Lesage, F., Guillemare, E., Fink, M., Duprat, F., Lazdunski, M., Romey, G., & Barhanin, J. (1996). TWIK-1, a ubiquitous human weakly inward rectifying K+ channel with a novel structure. *EMBO J, 15*(5), 1004-1011.

Lisman, J. (2012). Excitation, inhibition, local oscillations, or large-scale loops: what causes the symptoms of schizophrenia? *Curr Opin Neurobiol, 22*(3), 537-544. doi: 10.1016/j.conb.2011.10.018

Loder, M. K., & Melikian, H. E. (2003). The dopamine transporter constitutively internalizes and recycles in a protein kinase C-regulated manner in stably transfected PC12 cell lines. *J Biol Chem, 278*(24), 22168-22174. doi: 10.1074/jbc.M301845200

Lopes, C. M., Gallagher, P. G., Buck, M. E., Butler, M. H., & Goldstein, S. A. (2000). Proton block and voltage gating are potassium-dependent in the cardiac leak channel Kcnk3. *J Biol Chem, 275*(22), 16969-16978.

Lopes, C. M., Zilberberg, N., & Goldstein, S. A. (2001). Block of Kcnk3 by protons. Evidence that 2-P-domain potassium channel subunits function as homodimers. *J Biol Chem, 276*(27), 24449-24452.

Lossin, C., Wang, D. W., Rhodes, T. H., Vanoye, C. G., & George, A. L., Jr. (2002). Molecular basis of an inherited epilepsy. *Neuron, 34*(6), 877-884.

Manna, P. T., Smith, A. J., Taneja, T. K., Howell, G. J., Lippiat, J. D., & Sivaprasadarao, A. (2010). Constitutive endocytic recycling and protein kinase C-mediated lysosomal

degradation control K(ATP) channel surface density. *J Biol Chem, 285*(8), 5963-5973. doi: 10.1074/jbc.M109.066902

Mant, A., Elliott, D., Eyers, P. A., & O'Kelly, I. M. (2011). Protein kinase A is central for forward transport of two-pore domain potassium channels K2P3.1 and K2P9.1. *J Biol Chem, 286*(16), 14110-14119. doi: 10.1074/jbc.M110.190702

Mathie, A. (2007). Neuronal two-pore-domain potassium channels and their regulation by G protein-coupled receptors. *J Physiol, 578*(Pt 2), 377-385. doi: 10.1113/jphysiol.2006.121582

Mathie, A., Al-Moubarak, E., & Veale, E. L. (2010). Gating of two pore domain potassium channels. *J Physiol, 588*(Pt 17), 3149-3156. doi: 10.1113/jphysiol.2010.192344

Matthies, H. J., Han, Q., Shields, A., Wright, J., Moore, J. L., Winder, D. G., . . . Blakely, R. D. (2009). Subcellular localization of the antidepressant-sensitive norepinephrine transporter. *BMC Neurosci, 10*, 65. doi: 10.1186/1471-2202-10-65

Melikian, H. E., & Buckley, K. M. (1999). Membrane trafficking regulates the activity of the human dopamine transporter. *J Neurosci, 19*(18), 7699-7710.

Mello, R. J., Brown, M. S., Goldstein, J. L., & Anderson, R. G. (1980). LDL receptors in coated vesicles isolated from bovine adrenal cortex: binding sites unmasked by detergent treatment. *Cell, 20*(3), 829-837.

Meuth, S. G., Budde, T., Kanyshkova, T., Broicher, T., Munsch, T., & Pape, H. C. (2003). Contribution of TWIK-related acid-sensitive K+ channel 1 (TASK1) and TASK3 channels to the control of activity modes in thalamocortical neurons. *J Neurosci, 23*(16), 6460-6469.

Meuth, S. G., Kleinschnitz, C., Broicher, T., Austinat, M., Braeuninger, S., Bittner, S., . . . Wiendl, H. (2009). The neuroprotective impact of the leak potassium channel TASK1 on stroke development in mice. *Neurobiol Dis, 33*(1), 1-11. doi: 10.1016/j.nbd.2008.09.006

Michel, P. P., Toulorge, D., Guerreiro, S., & Hirsch, E. C. (2013). Specific needs of dopamine neurons for stimulation in order to survive: implication for Parkinson disease. *FASEB J*. doi: 10.1096/fj.12-220418

Millar, J. A., Barratt, L., Southan, A. P., Page, K. M., Fyffe, R. E., Robertson, B., & Mathie, A. (2000). A functional role for the two-pore domain potassium channel TASK-1 in cerebellar granule neurons. *Proc Natl Acad Sci U S A, 97*(7), 3614-3618. doi: 10.1073/pnas.050012597

Miranda, M., Wu, C. C., Sorkina, T., Korstjens, D. R., & Sorkin, A. (2005). Enhanced ubiquitylation and accelerated degradation of the dopamine transporter mediated by protein kinase C. *J Biol Chem, 280*(42), 35617-35624. doi: 10.1074/jbc.M506618200

Mooren, O. L., Kotova, T. I., Moore, A. J., & Schafer, D. A. (2009). Dynamin2 GTPase and cortactin remodel actin filaments. *J Biol Chem, 284*(36), 23995-24005. doi: 10.1074/jbc.M109.024398

Muller, H. K., Wiborg, O., & Haase, J. (2006). Subcellular redistribution of the serotonin transporter by secretory carrier membrane protein 2. *J Biol Chem, 281*(39), 28901-28909. doi: 10.1074/jbc.M602848200

Murotani, T., Ishizuka, T., Hattori, S., Hashimoto, R., Matsuzaki, S., & Yamatodani, A. (2007). High dopamine turnover in the brains of Sandy mice. *Neurosci Lett, 421*(1), 47-51. doi: 10.1016/j.neulet.2007.05.019

Naslavsky, N., Weigert, R., & Donaldson, J. G. (2003). Convergence of non-clathrin- and clathrin-derived endosomes involves Arf6 inactivation and changes in phosphoinositides. *Mol Biol Cell, 14*(2), 417-431. doi: 10.1091/mbc.02-04-0053

Navaroli, D. M., Stevens, Z. H., Uzelac, Z., Gabriel, L., King, M. J., Lifshitz, L. M., . . . Melikian, H. E. (2011). The plasma membrane-associated GTPase Rin interacts with the dopamine transporter and is required for protein kinase C-regulated dopamine transporter trafficking. *J Neurosci, 31*(39), 13758-13770. doi: 10.1523/JNEUROSCI.2649-11.2011

Nirenberg, M. J., Chan, J., Pohorille, A., Vaughan, R. A., Uhl, G. R., Kuhar, M. J., & Pickel, V. M. (1997). The dopamine transporter: comparative ultrastructure of dopaminergic axons in limbic and motor compartments of the nucleus accumbens. *J Neurosci, 17*(18), 6899-6907.

O'Kelly, I., Butler, M. H., Zilberberg, N., & Goldstein, S. A. (2002). Forward transport. 14-3-3 binding overcomes retention in endoplasmic reticulum by dibasic signals. *Cell, 111*(4), 577-588.

Obsilova, V., Silhan, J., Boura, E., Teisinger, J., & Obsil, T. (2008). 14-3-3 proteins: a family of versatile molecular regulators. *Physiol Res, 57 Suppl 3*, S11-21.

Pacholczyk, T., Blakely, R. D., & Amara, S. G. (1991). Expression cloning of a cocaine- and antidepressant-sensitive human noradrenaline transporter. *Nature, 350*(6316), 350-354. doi: 10.1038/350350a0

Payne, C. K., Jones, S. A., Chen, C., & Zhuang, X. (2007). Internalization and trafficking of cell surface proteoglycans and proteoglycan-binding ligands. *Traffic, 8*(4), 389-401. doi: 10.1111/j.1600-0854.2007.00540.x

Perez-Otano, I., & Ehlers, M. D. (2005). Homeostatic plasticity and NMDA receptor trafficking. *Trends Neurosci, 28*(5), 229-238. doi: 10.1016/j.tins.2005.03.004

Plant, L. D., Kemp, P. J., Peers, C., Henderson, Z., & Pearson, H. A. (2002). Hypoxic depolarization of cerebellar granule neurons by specific inhibition of TASK-1. *Stroke, 33*(9), 2324-2328.

Prezeau, L., Carrette, J., Helpap, B., Curry, K., Pin, J. P., & Bockaert, J. (1994). Pharmacological characterization of metabotropic glutamate receptors in several types of brain cells in primary cultures. *Mol Pharmacol, 45*(4), 570-577.

Pust, S., Dyve, A. B., Torgersen, M. L., van Deurs, B., & Sandvig, K. (2010). Interplay between toxin transport and flotillin localization. *PLoS One, 5*(1), e8844. doi: 10.1371/journal.pone.0008844

Putzke, C., Hanley, P. J., Schlichthorl, G., Preisig-Muller, R., Rinne, S., Anetseder, M., . . . Eberhart, L. (2007). Differential effects of volatile and intravenous anesthetics on the activity of human TASK-1. *Am J Physiol Cell Physiol, 293*(4), C1319-1326.

Raiteri, M., Cerrito, F., Cervoni, A. M., & Levi, G. (1979). Dopamine can be released by two mechanisms differentially affected by the dopamine transport inhibitor nomifensine. *J Pharmacol Exp Ther, 208*(2), 195-202.

Rajan, S., Preisig-Muller, R., Wischmeyer, E., Nehring, R., Hanley, P. J., Renigunta, V., . . . Daut, J. (2002). Interaction with 14-3-3 proteins promotes functional expression of the potassium channels TASK-1 and TASK-3. *J Physiol, 545*(Pt 1), 13-26.

Ren, M., Xu, G., Zeng, J., De Lemos-Chiarandini, C., Adesnik, M., & Sabatini, D. D. (1998). Hydrolysis of GTP on rab11 is required for the direct delivery of transferrin from the pericentriolar recycling compartment to the cell surface but not from sorting endosomes. *Proc Natl Acad Sci U S A, 95*(11), 6187-6192.

Renigunta, V., Yuan, H., Zuzarte, M., Rinne, S., Koch, A., Wischmeyer, E., . . . Preisig-Muller, R. (2006). The retention factor p11 confers an endoplasmic reticulum-localization signal to the potassium channel TASK-1. *Traffic, 7*(2), 168-181. doi: 10.1111/j.1600-0854.2005.00375.x

Robertson, D., Haile, V., Perry, S. E., Robertson, R. M., Phillips, J. A., 3rd, & Biaggioni, I. (1991). Dopamine beta-hydroxylase deficiency. A genetic disorder of cardiovascular regulation. *Hypertension, 18*(1), 1-8.

Roussignol, G., Ango, F., Romorini, S., Tu, J. C., Sala, C., Worley, P. F., . . . Fagni, L. (2005). Shank expression is sufficient to induce functional dendritic spine synapses in aspiny neurons. *J Neurosci, 25*(14), 3560-3570. doi: 10.1523/JNEUROSCI.4354-04.2005

Royle, S. J., Bobanovic, L. K., & Murrell-Lagnado, R. D. (2002). Identification of a non-canonical tyrosine-based endocytic motif in an ionotropic receptor. *J Biol Chem, 277*(38), 35378-35385. doi: 10.1074/jbc.M204844200

Sakrikar, D., Mazei-Robison, M. S., Mergy, M. A., Richtand, N. W., Han, Q., Hamilton, P. J., . . . Blakely, R. D. (2012). Attention deficit/hyperactivity disorder-derived coding variation in the dopamine transporter disrupts microdomain targeting and trafficking regulation. *J Neurosci, 32*(16), 5385-5397. doi: 10.1523/JNEUROSCI.6033-11.2012

Sano, Y., Inamura, K., Miyake, A., Mochizuki, S., Kitada, C., Yokoi, H., . . . Furuichi, K. (2003). A novel two-pore domain K+ channel, TRESK, is localized in the spinal cord. *J Biol Chem, 278*(30), 27406-27412. doi: 10.1074/jbc.M206810200

Saunders, C., Ferrer, J. V., Shi, L., Chen, J., Merrill, G., Lamb, M. E., . . . Galli, A. (2000). Amphetamine-induced loss of human dopamine transporter activity: an internalization-dependent and cocaine-sensitive mechanism. *Proc Natl Acad Sci U S A, 97*(12), 6850-6855. doi: 10.1073/pnas.110035297

Schafer, W., Stroh, A., Berghofer, S., Seiler, J., Vey, M., Kruse, M. L., . . . Garten, W. (1995). Two independent targeting signals in the cytoplasmic domain determine

trans-Golgi network localization and endosomal trafficking of the proprotein convertase furin. *EMBO J, 14*(11), 2424-2435.

Schiekel, J., Lindner, M., Hetzel, A., Wemhoner, K., Renigunta, V., Schlichthorl, G., . . . Daut, J. (2013). The inhibition of the potassium channel TASK-1 in rat cardiac muscle by endothelin-1 is mediated by phospholipase C. *Cardiovasc Res, 97*(1), 97-105. doi: 10.1093/cvr/cvs285

Scholz, R., Berberich, S., Rathgeber, L., Kolleker, A., Kohr, G., & Kornau, H. C. (2010). AMPA receptor signaling through BRAG2 and Arf6 critical for long-term synaptic depression. *Neuron, 66*(5), 768-780. doi: 10.1016/j.neuron.2010.05.003

Schultz, W. (2013). Updating dopamine reward signals. *Curr Opin Neurobiol, 23*(2), 229-238. doi: 10.1016/j.conb.2012.11.012

Schweri, M. M., Skolnick, P., Rafferty, M. F., Rice, K. C., Janowsky, A. J., & Paul, S. M. (1985). [3H]Threo-(+/-)-methylphenidate binding to 3,4-dihydroxyphenylethylamine uptake sites in corpus striatum: correlation with the stimulant properties of ritalinic acid esters. *J Neurochem, 45*(4), 1062-1070.

Sekiyama, N., Hayashi, Y., Nakanishi, S., Jane, D. E., Tse, H. W., Birse, E. F., & Watkins, J. C. (1996). Structure-activity relationships of new agonists and antagonists of different metabotropic glutamate receptor subtypes. *Br J Pharmacol, 117*(7), 1493-1503.

Snyder, S. H., & Coyle, J. T. (1969). Regional differences in H3-norepinephrine and H3-dopamine uptake into rat brain homogenates. *J Pharmacol Exp Ther, 165*(1), 78-86.

Sorkina, T., Doolen, S., Galperin, E., Zahniser, N. R., & Sorkin, A. (2003). Oligomerization of dopamine transporters visualized in living cells by fluorescence resonance energy transfer microscopy. *J Biol Chem, 278*(30), 28274-28283. doi: 10.1074/jbc.M210652200

Sorkina, T., Hoover, B. R., Zahniser, N. R., & Sorkin, A. (2005). Constitutive and protein kinase C-induced internalization of the dopamine transporter is mediated by a clathrin-dependent mechanism. *Traffic, 6*(2), 157-170. doi: 10.1111/j.1600-0854.2005.00259.x

Sorkina, T., Richards, T. L., Rao, A., Zahniser, N. R., & Sorkin, A. (2009). Negative regulation of dopamine transporter endocytosis by membrane-proximal N-terminal residues. *J Neurosci, 29*(5), 1361-1374. doi: 10.1523/JNEUROSCI.3250-08.2009

Straub, R. E., Jiang, Y., MacLean, C. J., Ma, Y., Webb, B. T., Myakishev, M. V., . . . Kendler, K. S. (2002). Genetic variation in the 6p22.3 gene DTNBP1, the human ortholog of the mouse dysbindin gene, is associated with schizophrenia. *Am J Hum Genet, 71*(2), 337-348. doi: 10.1086/341750

Swiatecka-Urban, A., Duhaime, M., Coutermarsh, B., Karlson, K. H., Collawn, J., Milewski, M., . . . Stanton, B. A. (2002). PDZ domain interaction controls the endocytic

recycling of the cystic fibrosis transmembrane conductance regulator. *J Biol Chem, 277*(42), 40099-40105. doi: 10.1074/jbc.M206964200

Tagawa, A., Mezzacasa, A., Hayer, A., Longatti, A., Pelkmans, L., & Helenius, A. (2005). Assembly and trafficking of caveolar domains in the cell: caveolae as stable, cargo-triggered, vesicular transporters. *J Cell Biol, 170*(5), 769-779. doi: 10.1083/jcb.200506103

Talley, E. M., & Bayliss, D. A. (2002). Modulation of TASK-1 (Kcnk3) and TASK-3 (Kcnk9) potassium channels: volatile anesthetics and neurotransmitters share a molecular site of action. *J Biol Chem, 277*(20), 17733-17742.

Talley, E. M., Lei, Q., Sirois, J. E., & Bayliss, D. A. (2000). TASK-1, a two-pore domain K+ channel, is modulated by multiple neurotransmitters in motoneurons. *Neuron, 25*(2), 399-410.

Talley, E. M., Sirois, J. E., Lei, Q., & Bayliss, D. A. (2003). Two-pore-Domain (KCNK) potassium channels: dynamic roles in neuronal function. *Neuroscientist, 9*(1), 46-56.

Talley, E. M., Solorzano, G., Lei, Q., Kim, D., & Bayliss, D. A. (2001). Cns distribution of members of the two-pore-domain (KCNK) potassium channel family. *J Neurosci, 21*(19), 7491-7505.

Tan, P. K., Waites, C., Liu, Y., Krantz, D. E., & Edwards, R. H. (1998). A leucine-based motif mediates the endocytosis of vesicular monoamine and acetylcholine transporters. *J Biol Chem, 273*(28), 17351-17360.

Tang, B., Li, Y., Nagaraj, C., Morty, R. E., Gabor, S., Stacher, E., . . . Olschewski, A. (2009). Endothelin-1 inhibits background two-pore domain channel TASK-1 in primary human pulmonary artery smooth muscle cells. *Am J Respir Cell Mol Biol, 41*(4), 476-483. doi: 10.1165/rcmb.2008-0412OC

Thomsen, M., Han, D. D., Gu, H. H., & Caine, S. B. (2009). Lack of cocaine self-administration in mice expressing a cocaine-insensitive dopamine transporter. *J Pharmacol Exp Ther, 331*(1), 204-211. doi: 10.1124/jpet.109.156265

Toyoda, H., Saito, M., Okazawa, M., Hirao, K., Sato, H., Abe, H., . . . Kang, Y. (2010). Protein kinase G dynamically modulates TASK1-mediated leak K+ currents in cholinergic neurons of the basal forebrain. *J Neurosci, 30*(16), 5677-5689. doi: 10.1523/JNEUROSCI.5407-09.2010

Trapp, S., Aller, M. I., Wisden, W., & Gourine, A. V. (2008). A role for TASK-1 (KCNK3) channels in the chemosensory control of breathing. *J Neurosci, 28*(35), 8844-8850.

Tzivion, G., Luo, Z. J., & Avruch, J. (2000). Calyculin A-induced vimentin phosphorylation sequesters 14-3-3 and displaces other 14-3-3 partners in vivo. *J Biol Chem, 275*(38), 29772-29778. doi: 10.1074/jbc.M001207200

Veale, E. L., Kennard, L. E., Sutton, G. L., MacKenzie, G., Sandu, C., & Mathie, A. (2007). G(alpha)q-mediated regulation of TASK3 two-pore domain potassium channels: the role of protein kinase C. *Mol Pharmacol, 71*(6), 1666-1675.

Verhey, K. J., Yeh, J. I., & Birnbaum, M. J. (1995). Distinct signals in the GLUT4 glucose transporter for internalization and for targeting to an insulin-responsive compartment. *J Cell Biol, 130*(5), 1071-1079.

Veyrat-Durebex, C., Pomerleau, L., Langlois, D., & Gaudreau, P. (2005). Internalization and trafficking of the human and rat growth hormone-releasing hormone receptor. *J Cell Physiol, 203*(2), 335-344. doi: 10.1002/jcp.20233

Vickery, R. G., & von Zastrow, M. (1999). Distinct dynamin-dependent and -independent mechanisms target structurally homologous dopamine receptors to different endocytic membranes. *J Cell Biol, 144*(1), 31-43.

Vina-Vilaseca, A., & Sorkin, A. (2010). Lysine 63-linked polyubiquitination of the dopamine transporter requires WW3 and WW4 domains of Nedd4-2 and UBE2D ubiquitin-conjugating enzymes. *J Biol Chem, 285*(10), 7645-7656. doi: 10.1074/jbc.M109.058990

von Zastrow, M. (2010). Regulation of opioid receptors by endocytic membrane traffic: mechanisms and translational implications. *Drug Alcohol Depend, 108*(3), 166-171. doi: 10.1016/j.drugalcdep.2010.02.014

Wan, Q., Xiong, Z. G., Man, H. Y., Ackerley, C. A., Braunton, J., Lu, W. Y., . . . Wang, Y. T. (1997). Recruitment of functional GABA(A) receptors to postsynaptic domains by insulin. *Nature, 388*(6643), 686-690. doi: 10.1038/41792

Wang, Q., & Limbird, L. E. (2007). Regulation of alpha2AR trafficking and signaling by interacting proteins. *Biochem Pharmacol, 73*(8), 1135-1145. doi: 10.1016/j.bcp.2006.12.024

Whitby, L. G., Axelrod, J., & Weil-Malherbe, H. (1961). The fate of H3-norepinephrine in animals. *J Pharmacol Exp Ther, 132*, 193-201.

Yaffe, M. B., Rittinger, K., Volinia, S., Caron, P. R., Aitken, A., Leffers, H., . . . Cantley, L. C. (1997). The structural basis for 14-3-3:phosphopeptide binding specificity. *Cell, 91*(7), 961-971.

Zhang, J. H., Ge, L., Qi, W., Zhang, L., Miao, H. H., Li, B. L., . . . Song, B. L. (2011). The N-terminal domain of NPC1L1 protein binds cholesterol and plays essential roles in cholesterol uptake. *J Biol Chem, 286*(28), 25088-25097. doi: 10.1074/jbc.M111.244475

Zhao, B., Wong, A. Y., Murshid, A., Bowie, D., Presley, J. F., & Bedford, F. K. (2008). Identification of a novel di-leucine motif mediating K(+)/Cl(-) cotransporter KCC2 constitutive endocytosis. *Cell Signal, 20*(10), 1769-1779. doi: 10.1016/j.cellsig.2008.06.011

Zuzarte, M., Heusser, K., Renigunta, V., Schlichthorl, G., Rinne, S., Wischmeyer, E., . . . Preisig-Muller, R. (2009). Intracellular traffic of the K+ channels TASK-1 and TASK-3: role of N- and C-terminal sorting signals and interaction with 14-3-3 proteins. *J Physiol, 587*(Pt 5), 929-952. doi: 10.1113/jphysiol.2008.164756